PETROGRAPHIC AND FLUID INCLUSION STUDIES ON THE METALORE-GOLDEN HIGHWAY DEPOSIT, THUNDER BAY DISTRICT, ONTARIO

by

Barbara Sylvia Kowalski ©

Submitted in partial fulfilment
of the requirements for a degree of

MASTERS OF SCIENCE

Faculty of Arts and Science
Lakehead University
Thunder Bay, Ontario, Canada

November, 1993

ISBN 0-315-97053-7

ABSTRACT

The gold-bearing Metalore shear zone and Golden Highway quartz-carbonate vein in the Beardmore-Geraldton Archean Greenstone Belt occur along the Paint Lake splay faults at the contact between metavolcanic rocks and metaconglomerates intruded by pre-ore diorite. The Metalore and Golden Highway deposits were emplaced during a late tectonic event. They consist primarily of quartz, clinochlore, ankerite, potassium feldspars, sericite, pyrite, argentite and chalcopyrite with native gold. The minerals have been deformed and are cut by at least three healed fractures by fluid inclusions. Gold typically occurs in recrystallized quartz. Microthermometric and Raman spectroscopy techniques were used to study fluid inclusions in quartz, calcite, ankerite, chlorites and potassium feldspars.

Six types of fluid inclusions were found to occur in three separate generations of hydrothermal fluid activity in the Metalore and Golden Highway. The three generations of hydrothermal fluids represented by fluid inclusions are: (1) pre-ore, low-salinity (<2wt.%) NaCl-$CaCl_2$ aqueous inclusions with small amounts of daughter mineral and H_2O-CO_2 inclusions with 10 and 40 mole percent CO_2 occurring in the Golden Highway and Metalore respectively; (2) syn-ore, $MgCl_2$- H_2O-CO_2 aqueous and vapour rich inclusions with small amounts of daughter minerals with 50 and 80 mole percent in the Golden Highway and Metalore, respectively; (3) post-ore, CO_2-H_2O liquid-vapour and CO_2-rich liquid-vapour inclusion

with variable CO_2 contents ranging from 10 to 50 mole percent CO_2. Homogenization temperatures of pre-ore H_2O-CO_2 inclusions during are 220°-230°C and 356°C; syn-ore 266°C; and post-ore 21°C to 66°C.

The aqueous and CO_2-rich inclusions are interpreted to have been trapped as two immiscible phases in three separate generations. Precipitation of gold may have been induced by pressure, temperature fluctuations and chemical changes from CO_2 effervescence. Metamorphic fluids are the likely source for the onset of precious-metal deposition from reduced sulphur complexes along the Metalore splay fault and precious- and base-metal deposition from both reduced sulphur and chloride complexes along the Golden Highway splay fault.

Table of Contents

List of Figures

List of Tables

Acknowledgments

I thank Metalore Resources Ltd., for the field and analytical support. I am grateful to Dr. Kissin for his patience, guidance and comments, which improved this research. I thank A. Hammond for the polished sections for petrographic and microthermometric work. I thank J. Pastersis for the Raman Spectroscopy work from Washington University, St. Louis.

I'm grateful to my husband Eugene for his endless patience and support.

Chapter 1

1.1 INTRODUCTION

The Archean Beardmore-Geraldton granitoid-greenstone belt produced gold from quartz-carbonate veins and quartz-carbonate veins with banded iron formations. These deposits are associated with felsic porphyritic intrusive rocks and/or occur along anastomosing splay faults from the regional faults in the greenstone belt.

This study examines a gold deposit in the greenstone belt known as the Metalore Contact Zone (Metalore) and an auriferous quartz-carbonate vein known as the Golden Highway Zone (Golden Highway). The Metalore is situated at a contact between meta-andesitic and polymictic metaconglomeratic rocks. An intrusive metadiorite occurs in the meta-andesitic rocks near the metavolcanic-metasediment contact. The Metalore occurs along a splay fault from the regional Paint Lake Fault in the greenstone belt. The Golden Highway occurs west from the Metalore along the contact between meta-andesitic and metadioritic rocks. A branching splay fault from the Metalore splay fault is associated with the vein.

The objective of this thesis is to determine the physicochemical conditions of gold mineralization of the Metalore and Golden Highway. Parameters including (1) timing of mineralization, (2) ore fluid composition, pressure, temperature, and (3) fluid advection, were assessed in examining the mineralogy and fluid inclusions in the Metalore and Golden Highway.

A summary of the regional and local lithology, structural setting (Chapter 1), mineralogy (Chapter 2) and fluid inclusion analysis (Chapters 3 & 4) of the Metalore and Golden Highway Zones provides direct evidence of the composition of the ore fluid and the physicochemical conditions of ore deposition. The conclusions drawn give insight in the application of fluid inclusion analysis and its significance to precious metal exploration (Chapter 5).

1.2 LOCATION AND HISTORY

The Beardmore-Geraldton gold camp is located along Trans Canada Highway #11, 177 km northeast of the city of Thunder Bay, northwestern Ontario. The first discovery of gold in the Beardmore-Geraldton camp was in 1916, at the town of Jellicoe. The area was most active between the years of 1934 and 1939, during which 18 gold mines were located and developed over a 85 kilometre length from Beardmore to Geraldton. During and shortly after the World War II period of 1939 to 1945, most of the mines were closed. The greenstone belt produced 4.12 million ounces of gold and is ranked as one of the top five production camps within the Canadian Shield (Mason and McConnell, 1983). Sporadic exploration work was carried out until 1986, when an upswing in the price of gold and the gold discovery made by Metalore Resources Ltd. (Kowalski, 1987) caused a surge of mining exploration in the area. The author was the company geologist for six of the eleven years exploring in the belt.

1.3 Property Location and Previous Work

The Metalore and Golden Highway gold discoveries, formerly known as the Brookbank and Cherbourg Gold Mines Ltd. occurrences, respectively, are located on the Windigokan Road within 8 km of Trans-Canada Highway 11, approximately 20 km northeast of the town of Beardmore, (Figure 1-1).

The exploration work on the property described below is located in the assessment files of the office of the Ministry of Northern Development and Mines in Thunder Bay, Ontario.

The initial work on the property, was completed by Connell Mining and Exploration Company Ltd. in 1934. Low and erratic gold values were encountered from their surface test pits and shallow diamond drill holes.

In 1944, Noranda Mines Ltd. completed shallow diamond drill holes,intersecting gold values across economic widths.

In 1950, the property was sold to Brookbank Sturgeon Mines Ltd., and in 1975, it was optioned to Lynx Canada Ltd.. Geophysical surveys were completed by Lynx, followed by limited diamond drilling.

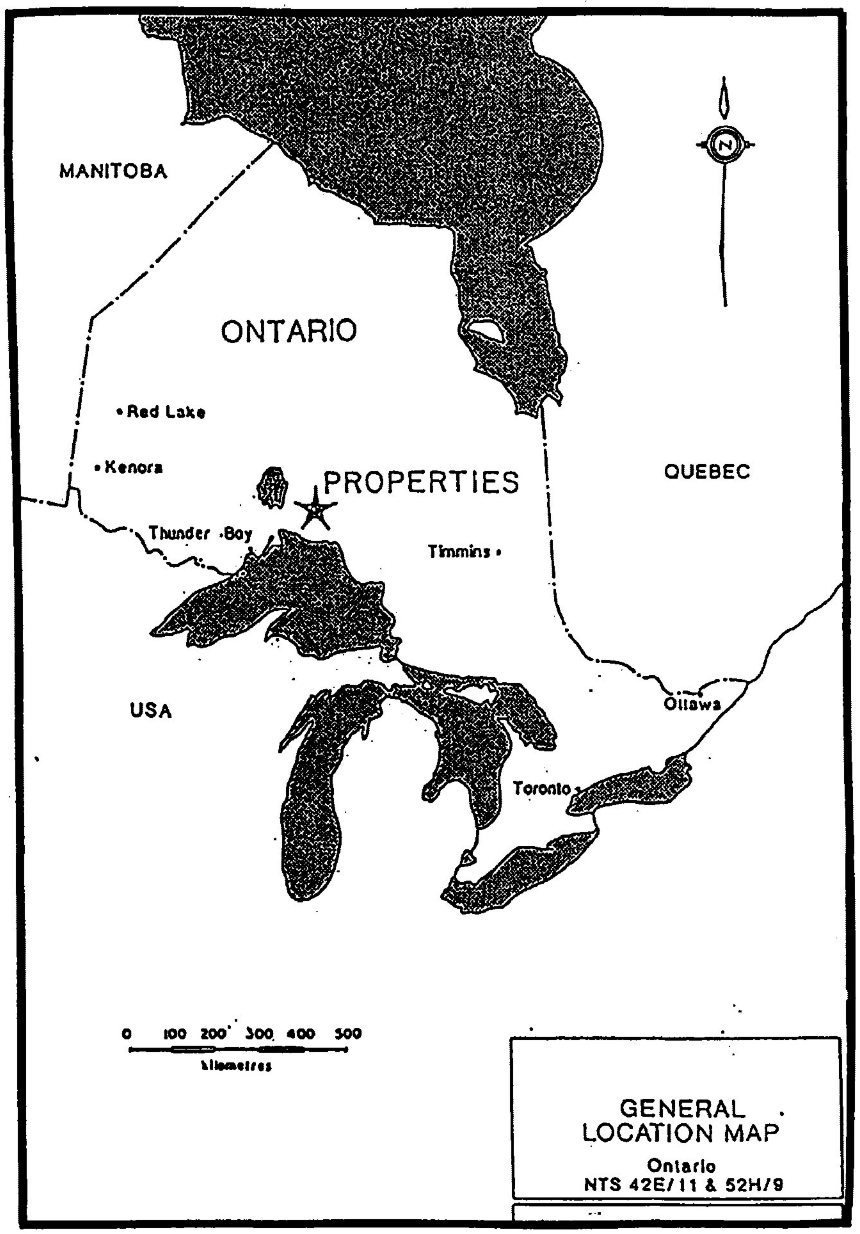

Figure 1-1: Location map of the Metalore and Golden Highway Zones in northwestern Ontario.

The property was returned to Brookbank Sturgeon Mines Ltd. (later known as Ontex Resources Ltd.), who subsequently optioned it to Metalore Resources Ltd. in 1981. Metalore completed sufficient diamond drill holes on the property, encountering gold over economic widths, to establish an auriferous body. Metalore and Ontex optioned the property to Hudson Bay Mining and Smelting from 1986 to 1988, then to Placer Dome Inc. from 1988 to 1992, but the options expired because of an ongoing lawsuit between the owners.

1.4 Regional Geology

The Beardmore-Geraldton region is underlain by a series of rock assemblages of early to late Precambrian in age, located within the Wabigoon and Quetico Subprovinces. The Wabigoon Subprovince lithologies are metamorphosed metavolcanic-metasedimentary rocks with felsic batholiths, stocks and sills, and lenticular mafic intrusions. The prefix "meta" will be deleted in subsequent discussion for brevity. Keweenawan north-striking diabase dykes and west-dipping sills intrude all rock types. Greenschist facies metamorphism pervades all pre-Keweenawan lithologies.

A transitional lithofacies change occurs between the Wabigoon Subprovince and the Quetico Subprovince (Mackasey 1976). The Quetico assemblage located to the south of the

Wabigoon, is underlain predominantly by sedimentary rocks and their high-grade gneissic and migmatitic equivalents.

In the Beardmore-Geraldton area, (Figure 1-2), greenschist facies metamorphism prevails within the three volcanic-sedimentary belts, which have undergone a complex structural history of large- and small- scale folding and subsequent east-trending regional faulting. The sequences within these belts are described below by MacKasey (1976) as the southern, central and northern volcanic-sedimentary sequences. The southern volcanic-sedimentary sequence consists of subaqueous mafic to intermediate volcanic rocks and clastic sedimentary rocks intercalated with chert-magnetite banded iron formation. The volcanic rocks are typically pillowed flows with massive and amygdaloidal lavas, with lesser tuffaceous and volcanic breccia components. The clastic sedimentary rocks consist of feldspathic sandstone and thinly bedded greywacke sandstone interlayered with laminated siltstone and argillite units. Ferruginous sedimentary rocks and/or lean iron formation consist of thin beds of argillite, siltstone, chert, and jasper with variable proportions of fine-grained laminated magnetite and hematite. The central volcanic-sedimentary sequence is separated into intermediate to mafic volcanic and clastic sedimentary rocks.

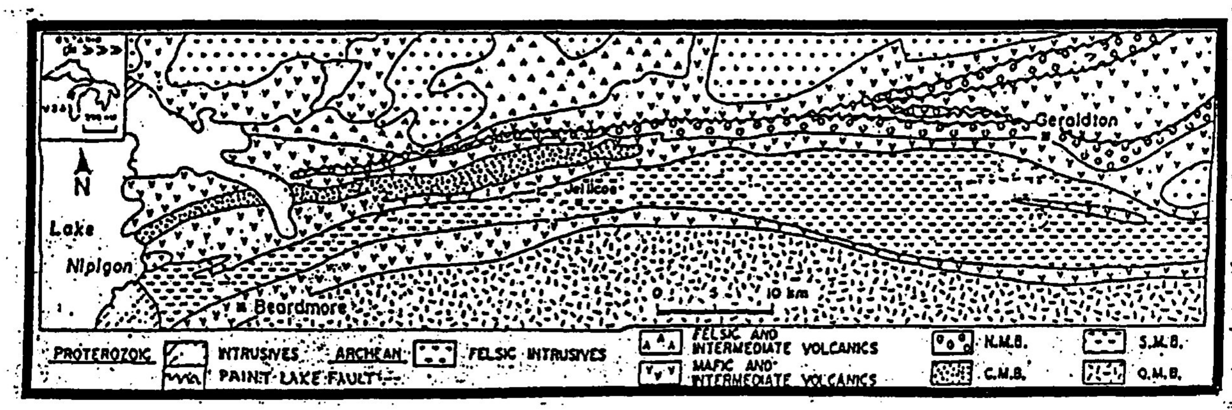

Figure 1-2: Regional geology and location of the Metalore and Golden Highway properties within the Beardmore-Geraldton greenstone belt. N.M.B.- Northern metavolcanic-metasedimentary belt; C.M.B. - Central metavolcanic-metasedimentary belt; S.M.B. - Southern metavolcanic-metasedimentary belt (from Barrett and Fralick, 1989).

Dacitic to basaltic pillow lavas, amygdaloidal flows, flow breccia, tuff sequences with intercalated tuffaceous and feldspar porphyritic dacitic flows constitute the volcanic rocks. The sedimentary rocks are variably intercalated with polymictic conglomerate, sandstone, siltstone and argillite units.

The northern volcanic-sedimentary sequence typically is composed of dacitic volcanic and polymictic conglomerate rocks. The polymictic conglomerate basal zone contains pebbles through boulders of quartz, feldspathic, granitic, and jasper compositions and a matrix of coarse sand. A central interval consisting of a mixture of medium to coarse sand grades into a thin, upper unit of sands and silts.

Mafic and felsic rocks intrude all three stratigraphic sequences. The mafic intrusive rocks consists of quartz diorite and gabbroic lenses which are interbedded with the mafic volcanic rocks. Felsic intrusive rocks occur as trondjhemtitic stocks and narrow feldspar and quartz porphyry dykes. Diabase and feldspar-quartz porphyry lenses, along with north and northeast-striking diabase dykes, and a large, west dipping diabase sheet occur as late intrusive rocks (Laird, 1937).

1.5 Regional Structural Geology

Tectonic processes produced local isoclinal folding along an east-west axis with westerly plunges. These processes removed the original sedimentary structures inducing parallel laminations (Barrett and Fralick, 1989). Prominent east-trending regional faults transect the belt. Dextral movement along the regional faults is apparent from the displacement of diabase dykes occurring along the faults. The Metalore and Golden Highway occur in the northern volcanic-sedimentary belt along splay faults from the regional Paint Lake Fault. During this study other anastomosing splay faults were examined in the belt and were determined to vary locally in strike, dip and dextral and sinistral movements.

1.6 Regional Economic Geology

Gold in the greenstone belt occurs in quartz-carbonate veins located in ductile shear zones and fracture networks. The Metalore Zone, however, is the first auriferous body in the northern volcanic-sedimentary belt that occurs along the contact between the polymictic conglomerate and volcanic rocks. The volcanic rocks exhibit brittle deformation as contrasted to ductile deformation in the conglomerates.

1.7 Metalore and Golden Highway Geology

The Metalore zone occurs within a parallel sequence of east-trending pillowed, brecciated mafic volcanic rocks intruded by a diorite and overlain by polymictic conglomerate. The Metalore fault is shown in Figure 1-3 as the conglomerate with variable sericite schist rocks, the mafic volcanic and the alteration zone rocks. The Metalore fault strikes N70W and is one of many anastomosing splay faults from the regional Paint Lake Fault. An alteration zone characterized by chloritization, carbonatization, feldspathization, silicification and sulphidization is present at the contact between mafic volcanics and conglomerates. Gold within the Metalore and Golden Highway zones is associated with silicification and pyrite.

The Golden Highway quartz-carbonate vein occurs along a contact between pillowed volcanics and a diorite. A sliver of conglomerate is parallel with the vein. The vein pinches and swells from 15 centimetres to several metres in width. It is situated 900 metres to the west of the Metalore along an interpreted subsidiary fault, called the Golden Highway fault, striking N30E away from the Metalore fault. The Golden Highway vein mentioned above are described in detail below on the basis of field observations.

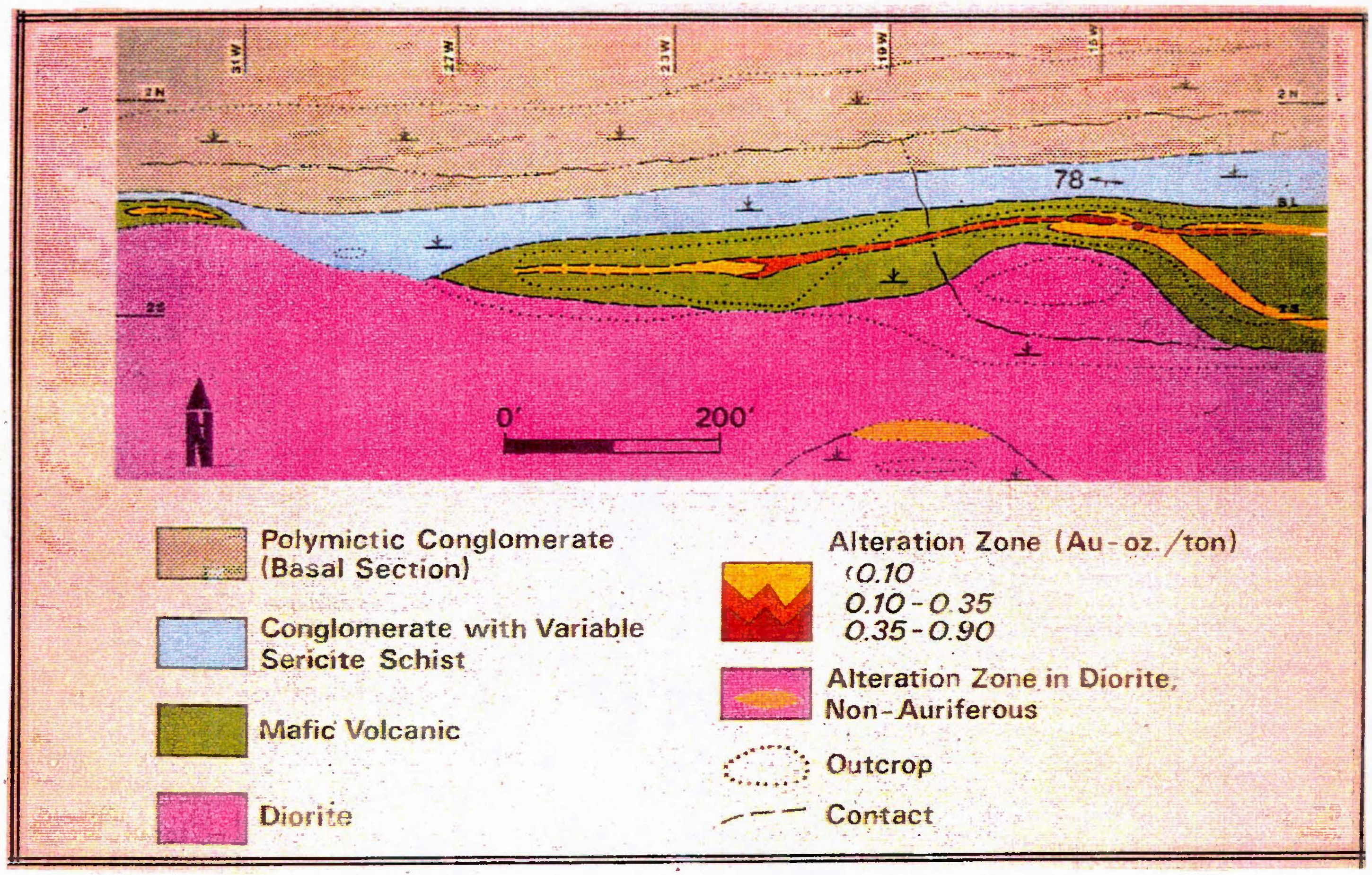

Figure 1-3: The surface geology, alteration halo and gold distribution of the Metalore Zone.

The undeformed, unaltered and deformed and altered volcanic, diorite and conglomerate rocks and their structural setting in the Metalore deposit and Golden Highway mafic volcanic rocks have been overprinted by extensive regional metamorphism (Blackburn et al., 1991); however, the mineralogy of the rocks suggests an andesitic composition. The volcanic rocks occur in pillowed and massive forms. Primary features such as pillows have been flattened and sheared and are parallel to foliation that strikes N80E and dips 78°S throughout the rocks. These rocks show chill margins at the contact with an intrusive dioritic or gabbroic rock. During the petrographic examination portion of this study the dioritic or gabbroic rock could not be positively identified due to overprinting of the greenschist metamorphism, therefore, this rock type will be referred to as a diorite. The diorite intrudes the pillowed volcanics and occasionally protrudes through to the conglomerates. In outcrop and at depth, the diorite has leucoxene crystals 2mm in length occurring adjacent to and surrounding small laths of labradorite and secondary andesine.

The polymictic conglomerate forms the basal section of the sedimentary sequence. In order of decreasing abundance clasts consist of granite, schistose greenstone, diorite or gabbro, gneiss, porphyry, felsite, red jasper, black chert and quartz. The matrix typically is dark green, coarse- to fine-grained sand to silt consisting of quartz and chlorite. The pebbles and boulders are typically well-rounded and closely packed with little interstitial material close to the contact with the mafic volcanic. Farther north from the contact the pebbles and boulders are few in number. The clasts are disorganized showing no grading, stratification or imbrication. The basal conglomerate unit has a minimum thickness of 2 metres and is overlain by a pebbly sandstone conglomerate. Grain size reduction occurs within the Metalore zone in these discrete feldspathic sandstone layers, which have been typically altered to a sericite schist. Primary features, such as imbrication, have been destroyed because of subsequent compaction, folding and faulting in the Metalore zone.

Evidence for major isoclinal folds in the polymictic conglomerate unit are few. MacKasey (1976) suggested that the sediments are overturned to the south and form the north limb of a syncline. A few pillow structures with facing directions to the north in the overturned sequence were observed in this study. Bedding-cleavage relationships are few owing to deformation in the rocks; however, facing directions were determined to be to the north.

The foliation trends in an easterly direction, which parallels the regional structural unit in the volcanic-sedimentary rocks. Flattened pillows define the schistosity, which strikes east and dips 78°S.

No minor folds were found on surface, however, oriented samples taken from surface indicated microscopic-scale folding occurring as kink folds and S- and Z-folds.

Three types of lineations were determined on the property: (1) traces of bedding along cleavage planes (N75E); (2) axes of crenulation (N5E); and (3) lineations produced by the flattening of pillows.

Plunge orientations determined from lineations in the Metalore is 77°SW and Golden Highway is 78°SW.

Ductile deformation occurs along the Metalore and Golden Highway zones, however, local brittle deformation occurs in outcrop and at depth within the drill core. Brecciation and small-scale, cross-cutting, quartz-carbonate filled fractures trend from oldest to youngest, N50E, N50W, and east.

The Metalore splay fault was identified from air photographs and on the surface as a deep, narrow erosional trough with a prominent easterly trend. The faulting at depth is indicated by intense deformation and alteration processes. Cross-faults, striking in a northeasterly and northwesterly direction on the property displace the east striking orebody in several locations.

Minor faulting is inferred on surface by the development of displacements of minor quartz veins of a few centimetres to several metres. The displacements indicate both dextral and sinistral movements.

2.0 Chapter 2

2.1 Alteration and Mineralogy of the Metalore and Golden Highway Zones

Distinctive chemical and mineralogical anomalies de-scribed below were observed and used to target gold in the Metalore and Golden Highway zones (Figure 2-1). Conclusions drawn from these observations were used to determine the physical and chemical parameters that existed during the ore-forming processes.

2.2 Mineralogy of Metalore Alteration Zone

The transport of hydrothermal fluids in different lithologies may alter the mineralogy, chemistry and texture of rocks (Poulsen, 1986). These changes occur as a result of fluctuations in fluid temperature, pressure and composition (Colvine et al., 1988). The compositions of fluid and rock buffer each other as they approach equilibrium (Walther and Wood, 1986) and are dependent upon the degree of intensity of fluid/rock interaction. Through complex metasomatic processes, a distinctive array of minerals prevail in the altered diorite, mafic volcanic and polymictic conglomerate from surface to depth on the Metalore zone.

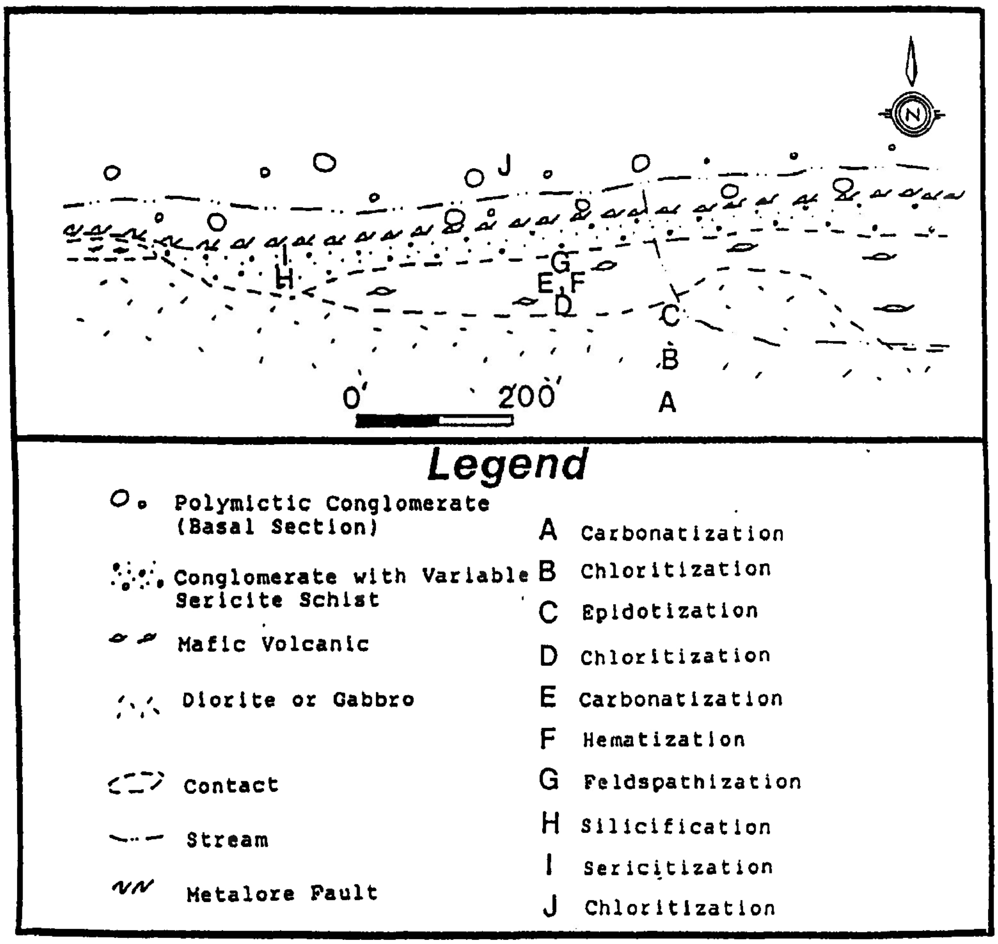

Figure 2-1: Schematic diagram of alteration patterns in outcrop of the Metalore Zone.

Outcrop and drill core descriptions of the three rock types were provided in Chapter 1. Petrographic descriptions of the three rock types reflect regional greenschist facies metamorphism, and their altered equivalents in the Metalore and Golden Highway Zones are presented in the following sections. The mineralogy and modal percentages are summarized for each rock type in Tables 1 to 6. Detailed descriptions of all the core specimens are provided in Appendix 1 and the locations of the diamond drill holes are shown in a long section of the Metalore Contact Zone in Figure 2-2.

There are two representative petrographic descriptions of the dioritic rocks given below, the first of the regionally metamorphosed and the second of the local alteration occurring within the rocks.

The average modal composition of six polished thin sections is provided in Table 2-1. The rock is medium-grained (1-5 mm), dominated by plagioclase feldspar, labradorite bytownite, clinopyroxene, augite, with minor hornblende, sphene and ilmenite. Plagioclase is partly altered to epidote and sericite, clinopyroxene to chlorite and/or actinolite and calcite, hornblende to actinolite, and sphene and/or ilmenite to leucoxenes. The rock is cut by veins with plagioclase and quartz surrounded by a broad alteration halo of epidote-calcite-actinolite-quartz.

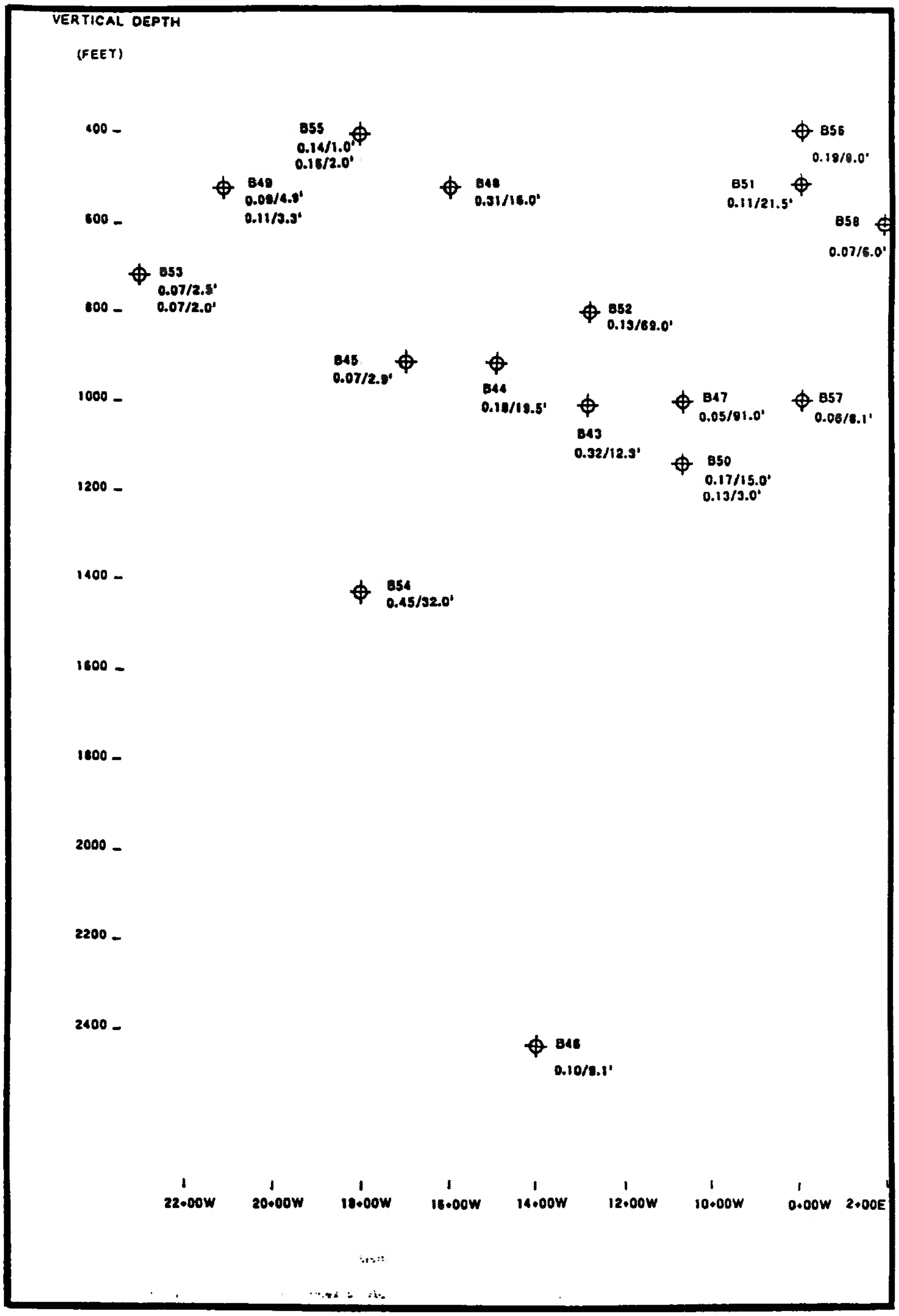

Figure 2-2: Metalore Contact Zone long section, looking north, B43 indicates the diamond drill hole number and 0.32/12.3' represents 0.32 ounces of Au per ton across 12.3 feet.

Table 2-1: Mineralogy and modal percentages of the regionally metamorphosed diorite.

Mineral	Modal Percent
Plagioclase	45.0-50.0
Clinopyroxene	25.0-30.0
Hornblende	0.5
Sphene and Ilmenite	2.0-2.5
Pyrite	0.3
Chalcopyrite	trace
Galena	trace
Hematite	trace
Chlorite	1.5-2.0
Epidote	1.0-10.0
Veinlets of plagioclase+quartz	1.0-1.5
Actinolite	1.2
Calcite	1.5-2.0

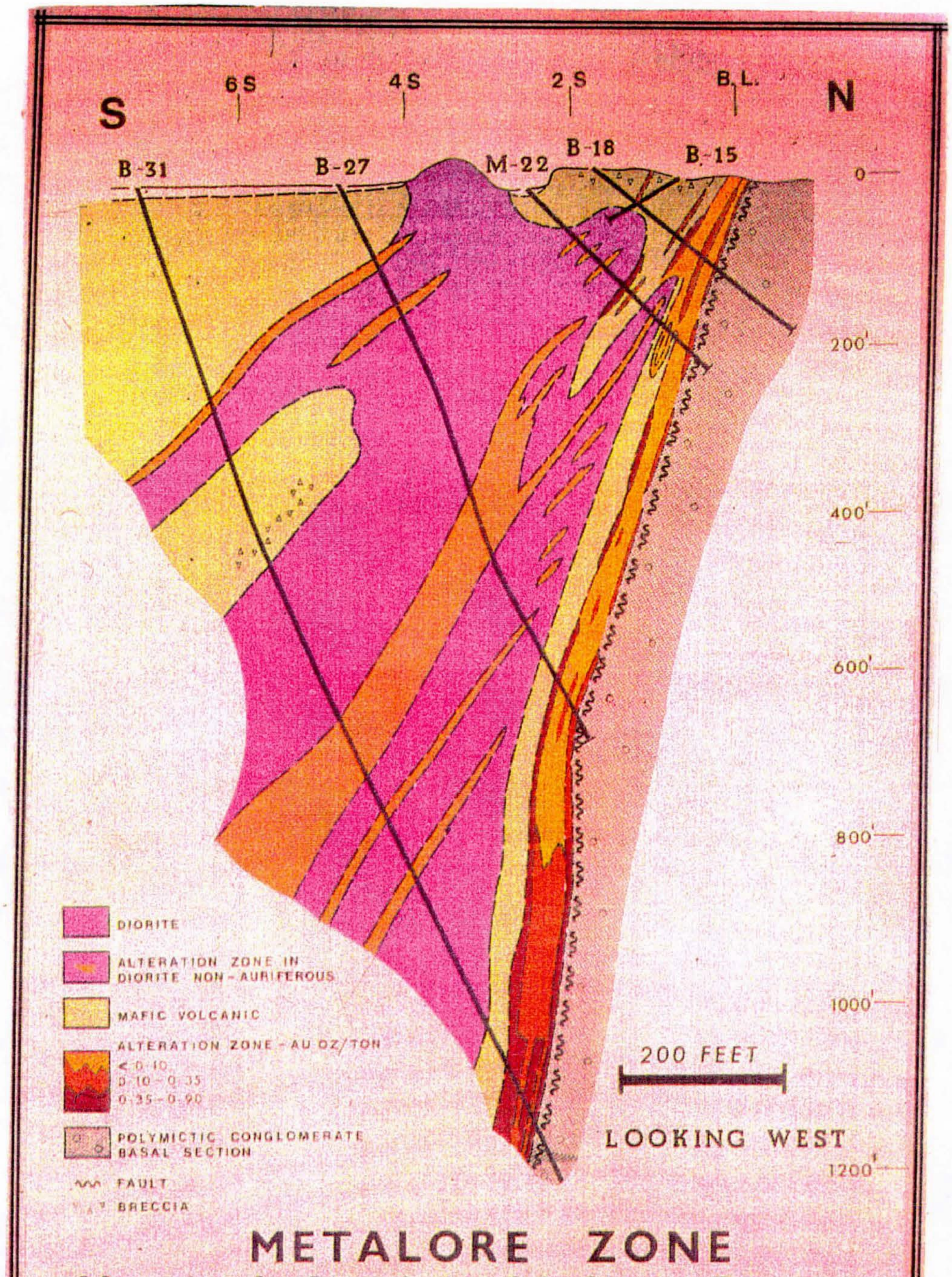

Figure 2-3: Vertical section of the Metalore zone showing the alteration and ore zone at depth, whereas, thin, erratic lenses of the alteration occur toward surface. Also shown is the barren alteration zone in the dioritic rocks. The black lines depict diamond drill holes with their drill hole numbers at surface.

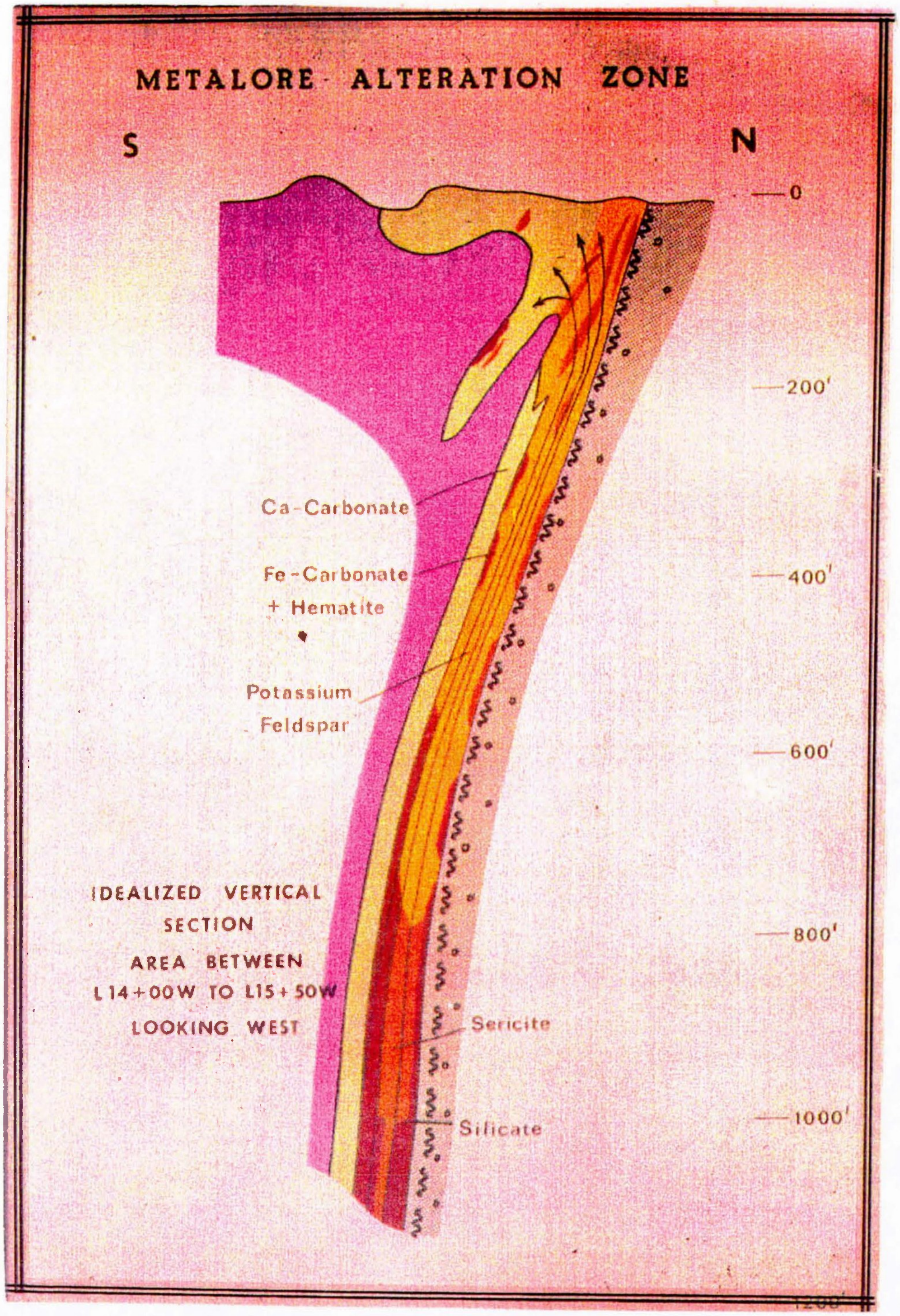

Figure 2-4: Schematic vertical section showing the minerals occurring with depth in the Metalore zone. The colour code is the same as Figure 2-3. The arrows indicate the direction of a portion of hydrothermal fluids rising toward surface.

Plagioclase feldspars of labradorite to bytownite composition form anhedral grains and aggregates averaging 0.3-0.8 mm in diameter, with a few subhedral grains up to 1mm across. The feldspars are altered to fine-grained epidote (<1mm) and locally slightly to moderately altered to disseminations of fine-grained sericite flakes. Augite forms subhedral to euhedral grains averaging 0.5-1.2 mm in size, with a few elongated prismatic grains 1.5 mm long. Augite is irregularly altered in patches and along grain borders and fractures to fine-grained chamosite or to fine-grained actinolite, with or without minor calcite. Hornblende forms scattered anhedral grains up to 0.3 mm in length; it is replaced by pseudomorphic actinolite.

Sphene and ilmenite forms irregular patches averaging 0.2-0.4 mm in size, with a few up to 0.7 mm across. The minerals are completely replaced by leucoxene, however, it could not be determined whether sphene or ilmenite or both have been replaced. Relict structure in the pseudomorphs suggests that the parent was probably ilmenite.

Pyrite forms scattered, anhedral grains and aggregates up to 0.6 mm in diameter. Chalcopyrite generally is associated with pyrite along its border grains. Chalcopyrite grains average 0.01-0.02 mm in diameter. Chalcopyrite and pyrrhotite form scattered inclusions averaging 0.01 mm in diameter in pyrite. Chalcopyrite also forms irregular aggregates of similar size in a few epidote grains. Galena occurs as clusters of fine-grains (0.01 mm) either alone or along the border of coarser-grained pyrite. Associated with galena are tiny patches of fine-grained (5-10 μm) hematite. Hematite extremely fine grain size, with strong red internal reflection forms scattered patches up to 0.05 mm in length.

The alteration that occurs in the intrusive unit is non-auriferous and may not be associated with the emplacement of the Metalore deposit. The alteration in the intrusive is characterized by ankerite (55%), small anhedral grains of quartz (20%), specularite veinlets and disseminations (10%) and pyrite and chalcopyrite (3%); other minerals are listed in Table 2-1.

The following is a description of the undeformed and unaltered mafic volcanic rocks. The mafic volcanic rock contains scattered, irregular patches up to 1mm in size of fine-grained chlorite and minor to very abundant fine-grained subhedral epidote. It is typically cut by 1mm wide cross-cutting quartz veinlets showing a wide range of mineralogies and textures. The central portion of these veinlets consists of fine-grained, anhedral, interlocking plagioclase with lesser quartz towards the centre. Plagioclase is moderately altered to sericite. Bordering this is a zone of intense alteration dominated by fine-grained epidote. In sections this becomes coarser-grained, with patches of interstitial calcite or quartz. In the coarser-grained zones, epidote is generally subhedral to euhedral in outline.

The mafic volcanic rock has fine-grained veinlets forming layers comprising of plagioclase, quartz and chlorite, with the latter commonly concentrated in wispy seams parallel to foliation. A few layers contain moderately abundant sericite intergrown with chlorite. Magnetite forms disseminated grains with anhedral to subhedral, equant outlines and averaging 0.03-0.05 mm across. Few grains are partly rimmed by secondary hematite. Pyrite forms disseminated, anhedral grains up to 0.3mm in size. Chalcopyrite forms scattered patches averaging 0.01-0.02mm across.

Some layers contain minor to moderately abundant ankerite as disseminated grains averaging 0.02-0.03mm in diameter. As the ankerite content increases, the layers grade into ankerite-rich layers of similar to slightly coarser grain size. Magnetite is absent from the layers. The layers show a moderate to strong shear folding, with axial planes parallel to foliation. Hematite occurs in lenses of fine-grained platy aggregates, mainly associated with ankerite-rich layers. Leucoxene forms patches up to 0.8mm in diameter with ankerite layers. Chamosite forms elongated patches of fine-grains in parallel orientation; these are up to 2mm in length and generally are subparallel to within 20 degrees to the main foliation. They probably were formed during a later tensional deformation by migration of iron and magnesium rich fluids into tensional fractures.

The rocks are cut by irregular and in part discontinuous veins and veinlets dominated by fine-grained ankerite. Quartz forms interstitial grains and clusters of grains, commonly showing a preferred orientation subparallel to foliation and with a texture suggestive of recrystallization. Plagioclase is concentrated in a few patches as anhedral grains up to 0.5mm in diameter. It is slightly altered to sericite. Pyrite forms scattered porphyroblasts up to 1mm in diameter; some contain minor to moderately abundant silicate inclusions. Chalcopyrite occurs along borders of pyrite and alone as anhedral grains averaging 0.03-0.1mm across. Anhydrite forms ragged porphyroblasts from 0.3-0.8mm in diameter, mainly intergrown with finer-grained ankerite. Calcite is a minor constituent in the veinlets. The matrix of the conglomerate is dominated by quartz with disseminated ankerite, plagioclase (labradorite) and muscovite-sericite-chlorite concentrated in wispy seams parallel to foliation.

Quartz shows evidence of strong cataclastic deformation and partial recrystallization. Typical mineral distribution of the matrix of the conglomerate is outlined in Table 2-3.

The clasts were not examined under thin section, however, they were identified in hand specimen and were established to be pebble, cobble and the occasional boulder sizes.

Compositions of the clasts in order of decreasing abundance are, granite, schistose greenstone, diorite, gneiss, porphyry, felsite, red jasper, black chert and quartz.

Late-stage quartz veining is similar to the description given in the regionally metamorphosed mafic volcanic section above.

Table 2-2: Mineralogy and modal percentages of the regionally metamorphosed mafic volcanic rocks.

Mineral	Modal Percent
Plagioclase-Quartz-Chlorite-Sericite-Magnetite layers	55-60
Ankerite	15-29.3
Quartz	2.0-3.0
Pyrite	1.5-2.0
Plagioclase	1.5-2.0
Anhydrite	0.5
Chalcopyrite	trace
Chlorite-rich lenses	2.0-3.0
Magnetite	0.2
Leucoxene	trace
Hematite	trace
Sericite	trace

Table 2-3: Mineralogy of the matrix of the regionally metamorphosed polymictic conglomerate.

Mineral	Modal Percent
Quartz	53.5
Ankerite	15.0
Chlorite	15.0
Muscovite-sericite	10.0
Andesine and labradorite	2.0-3.0
Sphene	1.0-2.0
Hematite	1.0
Pyrite	0.5
Chalcopyrite	trace

2.3 Mineral Zonation of the Metalore Deposit

The auriferous alteration zone is characterized by a halo reflected in the mafic volcanic rocks (surface to 280 metres vertical) and in the matrix of the conglomerate (below 280 metres vertical). The auriferous zone is abruptly cut by a 2mm to 20 centimetre thick quartz-tourmaline breccia. The zonation is shown in Figures 2-1 and 2-4 (at surface and depth respectively) and is shown in a series of Figures 2-5 to 2-16. A brief description of typical altered auriferous mafic volcanic and conglomeratic units are summarized below.

The mafic volcanic rock contains irregular relic patches up to 3mm across of porphyritic latite, which was strongly granulated and recrystallized during cataclastic deformation, and later replaced by ankerite and lesser quartz. A few carbonaceous and hematite-rich seams occur throughout. Minor native gold occurs with pyrite. The rock progressively acquires the alteration suite of minerals calcite-quartz-chamosite/clinochlore. The composition of the chlorites were analyzed with a scanning electron microscope and subsequently identified from Bailey (1987) and Laird (1987). Pyrite occurs in two main stages in the principal alteration stage and late quartz-carbonate vein stage. Fragments up to 1mm in diameter consist of fine-grained latite, overprinted by prismatic to equant plagioclase grains up to 0.15 mm in length, with an irregular, unoriented interlocking texture. Larger patches up to 1 cm in size contain minor to moderately abundant, ragged, elongate, oriented plagioclase phenocrysts averaging 0.1-0.2mm in length surrounded by a fine-grained interlocking aggregate dominated by plagioclase with minor to moderately abundant hematite and opaque minerals. A few lenses up to 0.5mm wide are sericite-rich, with moderately abundant leucoxene and hematite. The rock is replaced by a fine-grained aggregate of ankerite with subordinate quartz, pyrite and hematite. A few patches up to 2mm across are hosted by very fine-grained quartz.

The peripheral alteration consists of very fine-grained calcite, with scattered flakes and aggregates of chlorite and patches of quartz, with lesser ankerite, pyrite, and hematite. Ankerite commonly forms subhedral, disseminated grains in quartz-rich patches or in the groundmass of less altered latite. Later, coarser-grained patches contain calcite with lesser quartz, chlorite, pyrite and hematite and still less anhydrite and chalcopyrite. Patches average 0.2-0.5 mm in diameter, with some pyrite grains up to 1mm in diameter. Pyrite commonly contains minor to moderately abundant silicate inclusions and scattered inclusions of chalcopyrite. Pyrite grains contain inclusions with patches of pale yellow native gold 0.02 mm across adjacent to slightly larger patches of chalcopyrite. Other pyrite grains exhibit equant argentite inclusions 0.015mm diameter. Chalcopyrite is common in interstitial zones between pyrite grains and also forms irregular patches up to 0.2mm in diameter near the main cluster of pyrite in late veins.

Anhydrite forms scattered grains up to 0.4mm in diameter intergrown with quartz generally adjacent to ankerite patches. Quartz shows recrystallized textures in pressure shadows of some coarser pyrite grains and adjacent to some ankerite patches. Late veins contain patches of platy specular hematite up to 1.5mm in diameter with plates up to 0.3mm long. These are associated with fine-grained ankerite and much less very fine-grained quartz. Other calcite-pyrite-quartz veins show chlorite concentrated locally along the their borders.

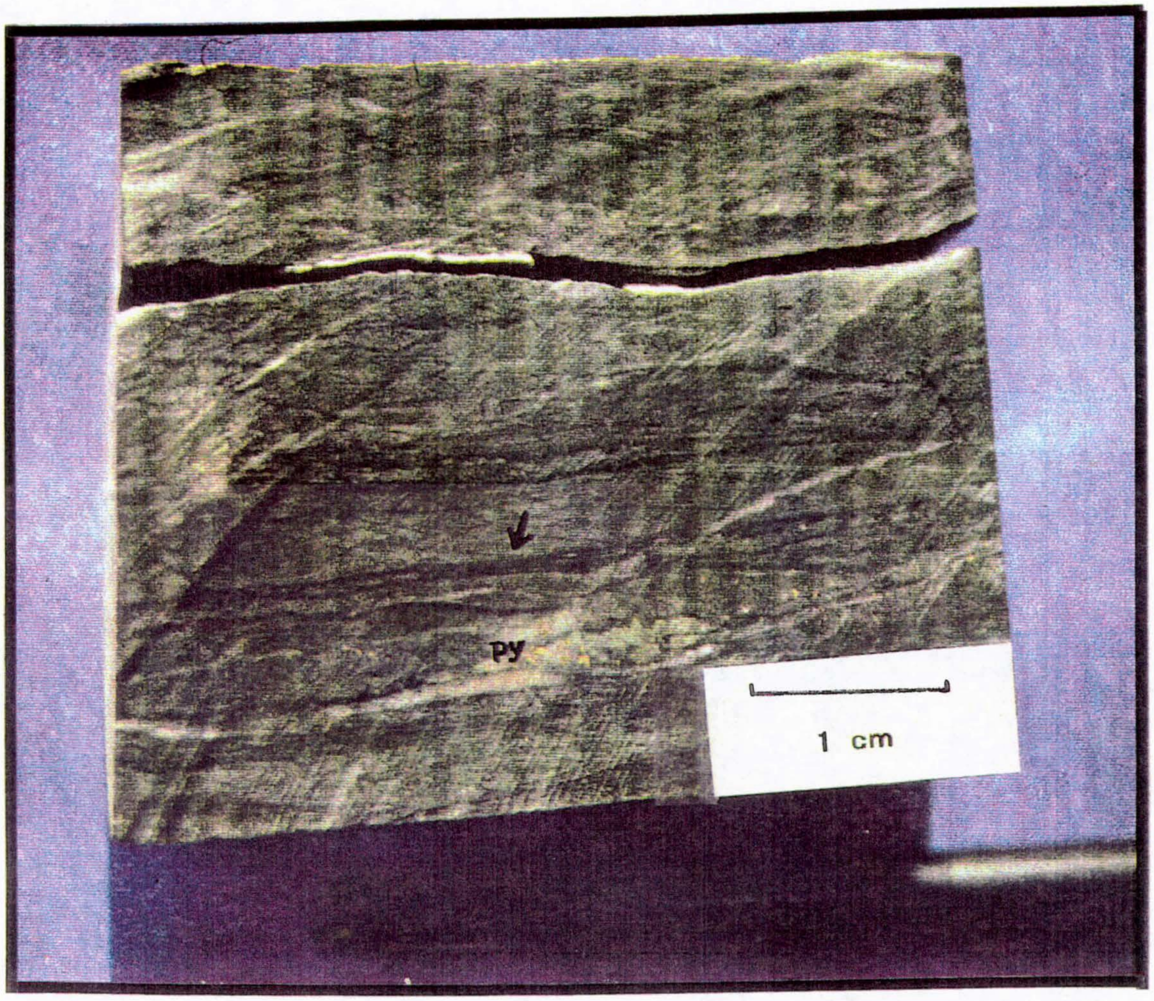

Figure 2-5: Flattened pillow selvages (indicated with an arrow) and the chlorite alteration of the hanging wall of the Metalore zone. Minor pyrite occurs in the sample as indicated by the symbol py. Sample taken from drill hole B-16W2A.

Figure 2-6: Mottled hematite (hem) - ankerite (ank) - quartz (qtz) alteration with evenly distributed fine pyrite (py). Sample taken from drill hole B-16W2A.

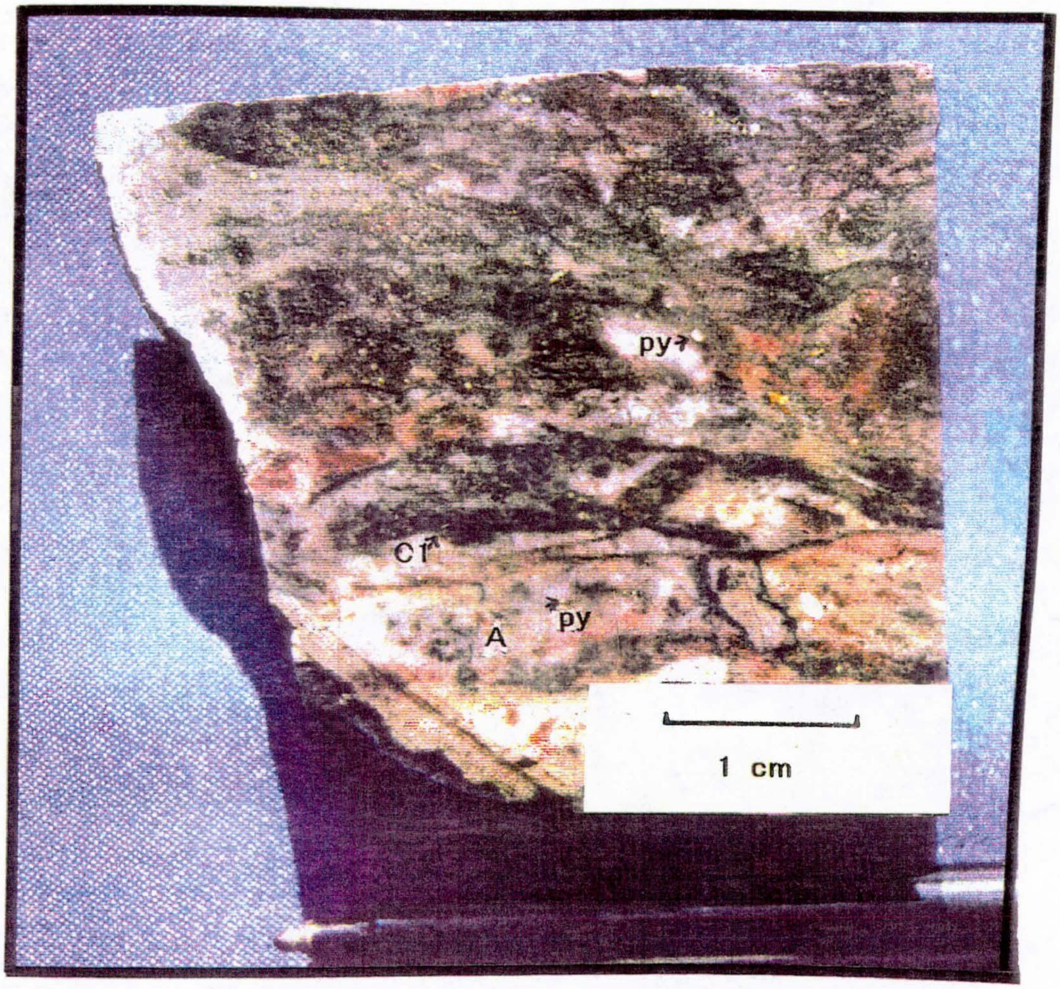

Figure 2-7: Ankerite-quartz-plagioclase feldspar alteration (A). Finely-disseminated pyrite (py) occurs in clinochlore (cl). Sample taken from drill hole B-16W2A.

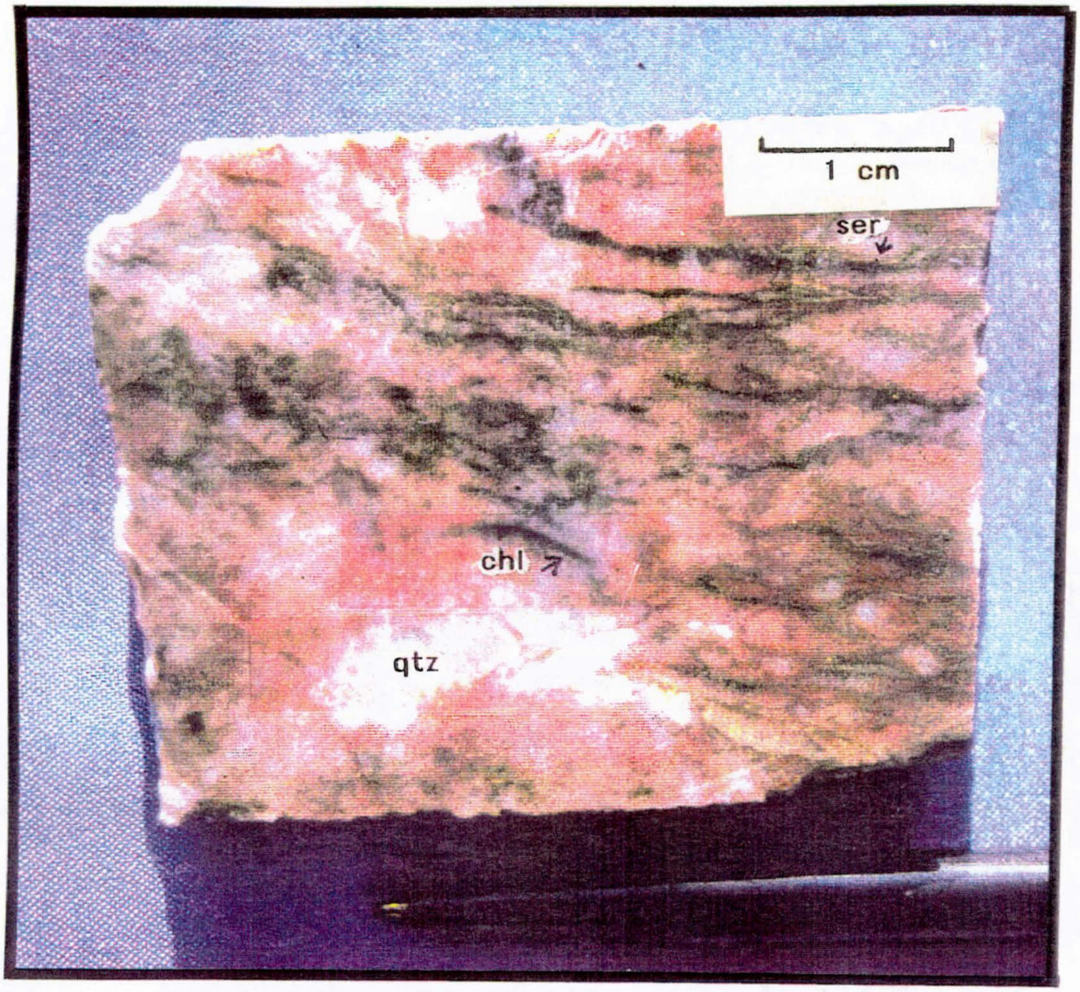

Figure 2-8: The transition between the altered mafic volcanics and altered polymictic conglomerates in the Metalore zone. The pink colouration is attributed to the plagioclase feldspar alteration. Chlorite (chl), quartz (qtz) and sericite (ser) are shown in the photo. Sample taken from drill hole B-16W2A.

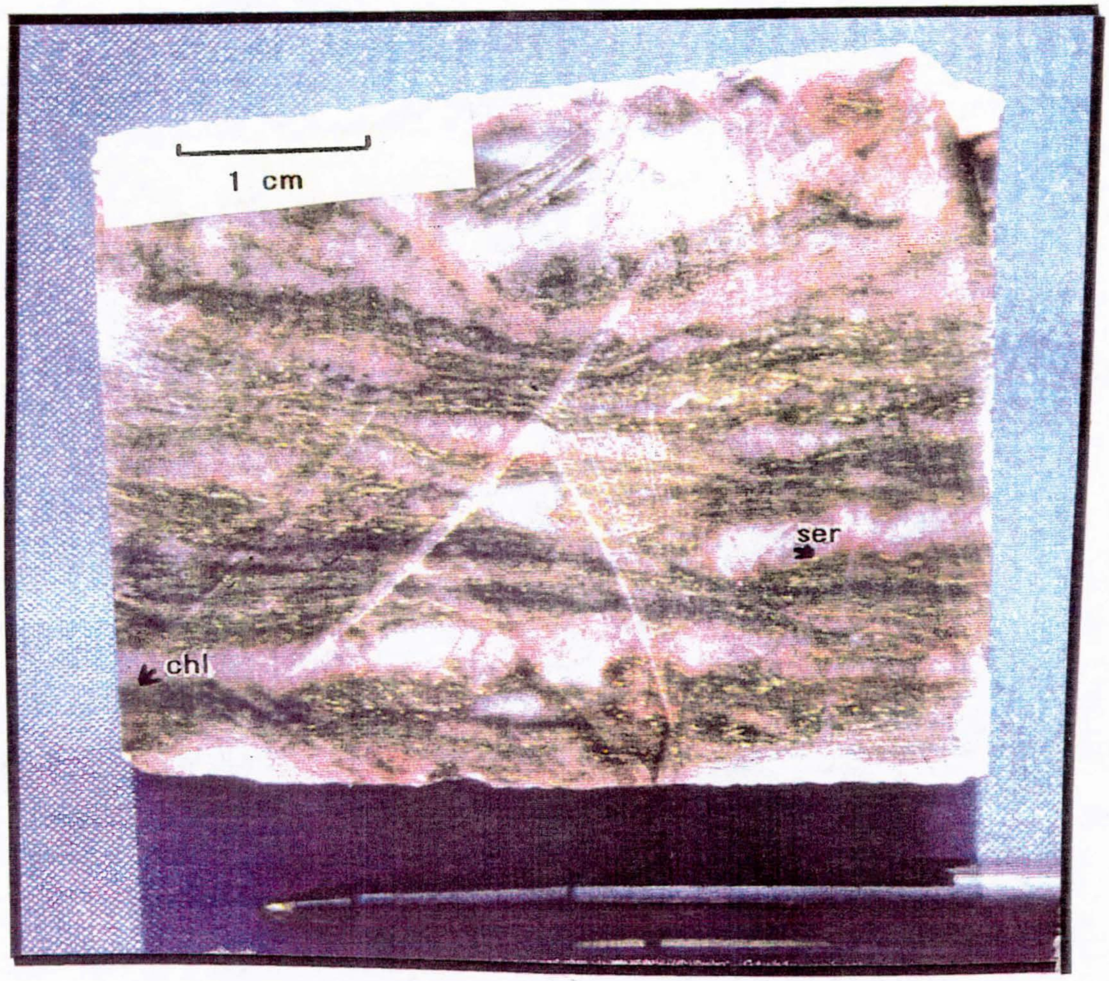

Figure 2-9: Progression of the alteration zone with depth with sericite (ser) and chlorite (chl) occurring throughout the plagioclase feldspar-quartz alteration shown in Figure 2-7. Sample taken from drill hole B-16W2A.

Table 2-4: Alteration suite of minerals occurring in the auriferous mafic volcanic.

Mineral	Modal Percent
Chamosite/Clinochlore	14.2
Sericite	0.5
Ankerite	60.0
Quartz	10.0-12.0
Calcite	7.0
Pyrite	2.0-3.0
Hematite+Specularite	2.0-3.0
Chalcopyrite	0.3
Pyrrhotite	trace
Native gold	trace
Argentite	trace

The conglomerate appears to be finely layered with layers rich in quartz, ankerite, muscovite, sericite and/or plagioclase. Disseminated sulphides include pyrite with much less chalcopyrite, sphalerite, argentite and galena. Native gold and native silver was seen within pyrite grains.

Quartz is concentrated in quartz-rich layers, with lesser ankerite and disseminated sulphides. Quartz is very fine- to fine-grained, with coarser-grained layers generally showing evidence of strong granulation and moderately strained extinction. A few layers and lenses have a cherty texture of equant, anhedral grains averaging 0.01-0.02 mm in diameter. Ankerite commonly occurs in very fine-grained layers with quartz. Where it is abundant, ankerite generally forms anhedral grains and aggregates. Where it is less common, subhedral to euhedral rhombic crystals are moderately abundant. Muscovite and sericite are concentrated in layers up to 2mm wide. Muscovite is oriented parallel to layering as fine-grains. Hematite occurs as subhedral to euhedral platy grains averaging 0.05mm in length and 0.4mm across. Carbonaceous material occurs in wispy seams up to 0.05mm wide along borders of some muscovite-rich layers and weaving through others.

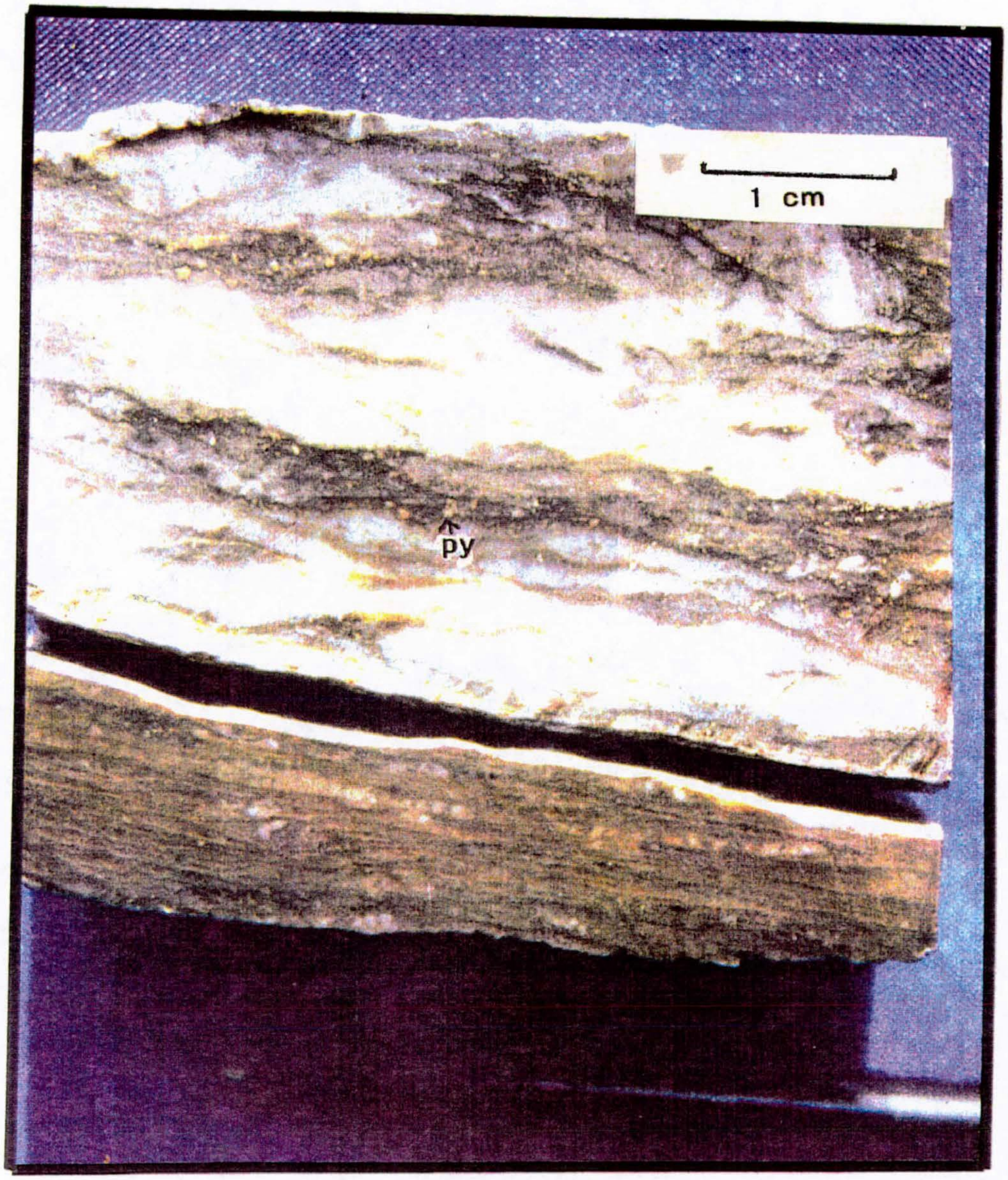

Figure 2-10: Sericite and quartz alteration representing the beginning of the footwall part of the Metalore zone. Pyrite (py) occurs within fine chlorite veinlets as indicated on the photo. Sample taken from drill hole B-16W2A.

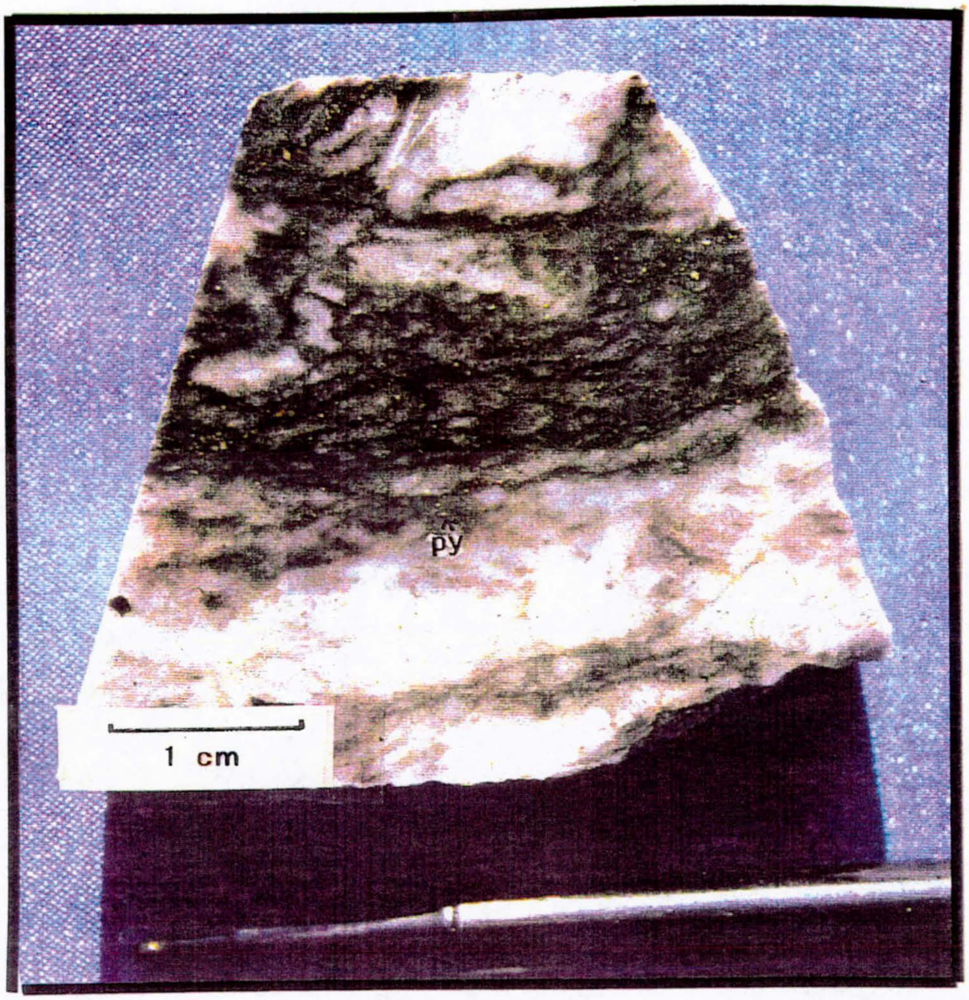

Figure 2-11: Recrystallized quartz, described as silicification in the text, with clinochlore veinlets occur at the footwall of the Metalore zone. Fine disseminations of pyrite (py) are indicated on the photo and are associated with high gold content. Sample taken from drill hole B-16W2.

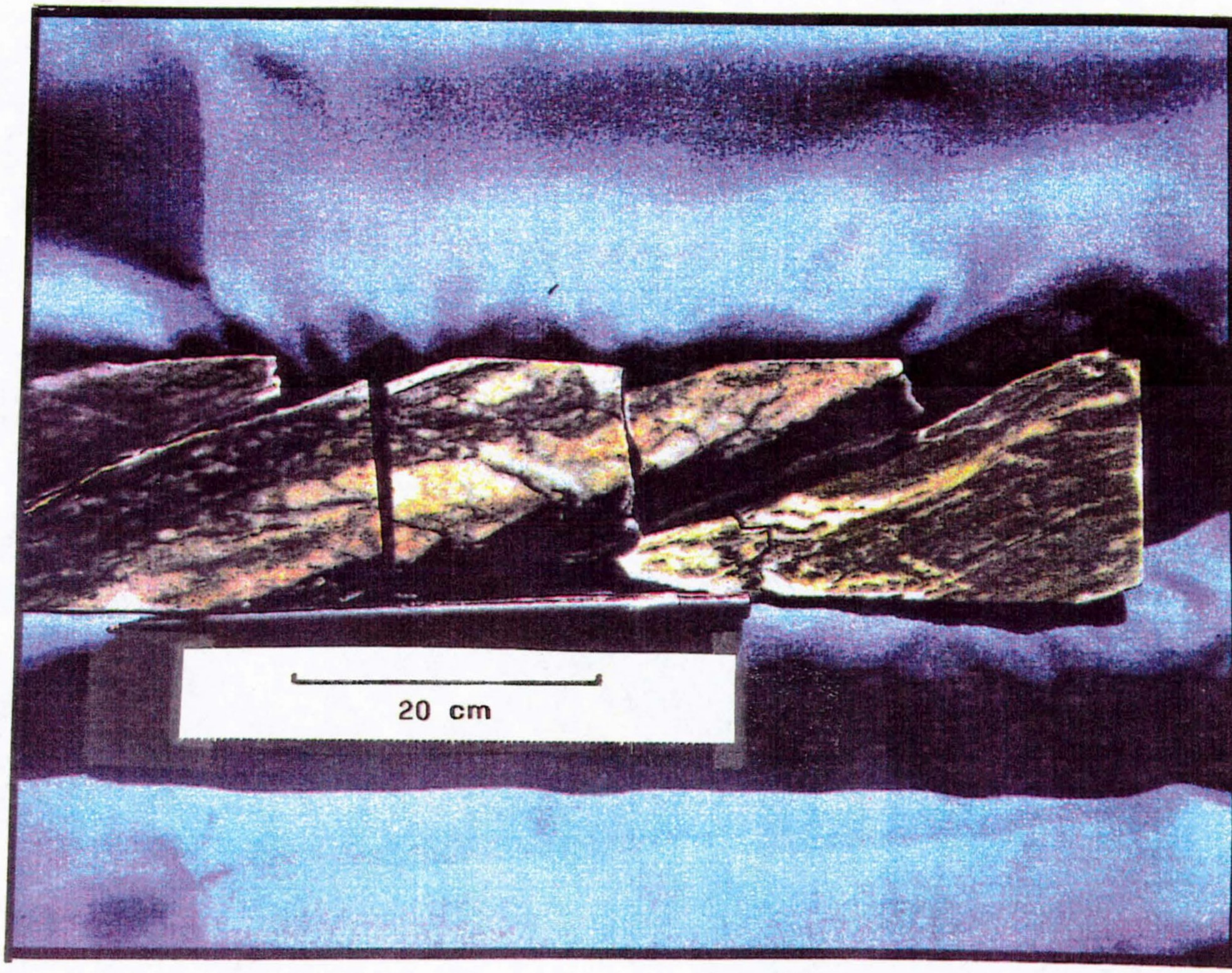

Figure 2-12: Black quartz and tourmaline representing the boundary and the termination of the auriferous alteration zone. Samples taken from drill hole B-16W2A.

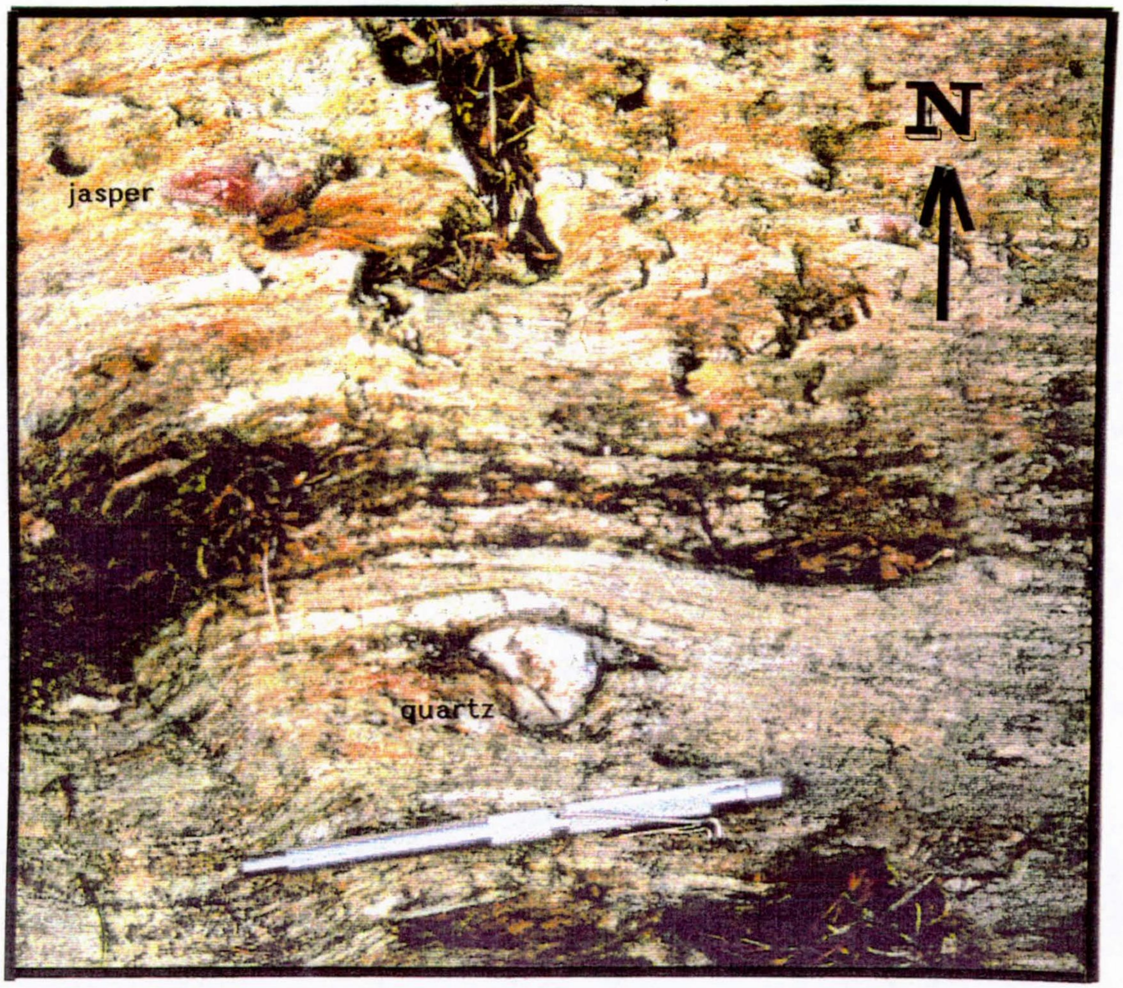

Figure 2-13: Deformed and altered barren polymictic conglomerate occurring at the footwall. Sample taken from drill hole B-16W2A.

Plagioclase forms very few crystal fragments or phenocrysts up to 0.7mm in diameter. More commonly, it forms fine-grained aggregates in layers up to 1mm in width; in some of these it is associated with minor to abundant muscovite.

Pyrite forms disseminated, anhedral to subhedral grains averaging 0.02-0.1mm in diameter. Larger grains commonly have moderately abundant silicate inclusions, and less commonly contains minor inclusions of chalcopyrite (averaging 0.01-0.03mm in diameter). Pyrite grains containing silicate and chalcopyrite inclusions also contain a few native gold inclusions up to 0.015mm in diameter. These have a light yellow colour, suggesting a moderate silver content. Argentite occurs in late, fracture-filling patches and veinlets, with grains up to 0.1mm long and 0.05mm across. Sphalerite is rare to minor, occurring as equant, irregular grains 0.4mm across. It is colourless and contains moderately abundant inclusions of chalcopyrite from 0.003-0.01mm in diameter. Along its borders are few grains of galena up to 0.05mm in diameter.

Gold occurs in the alteration zone of the mafic volcanics and conglomerates in the above discussion. There are four associations of auriferous mineralization observed in the polished sections. Fractured controlled gold within and adjacent to pyrite grains is the dominant association (78%).

Table 2-5: Alteration suite minerals occurring in the auriferous, altered conglomerate.

Mineral	Modal Percent
Quartz	50.2
Muscovite and sericite	17.0-20.0
Ankerite	15.0-17.0
Plagioclase	10.0-12.0
Hematite	0.3
Pyrite	0.3
Carbonaceous opaque	0.2
Chalcopyrite	trace
Argentite	trace
Sphalerite	trace
Galena	trace
Native gold	trace

Other lesser associations include particles of free gold (7%), gold particles encapsulated within pyrite (13%) and gold associated with gangue minerals (<2%). The majority of gold particles observed are in average less than 5 microns in diameter.

A black marker horizon designates the boundary of the alteration and precious metal mineralization of the Metalore Zone. This black horizon consists of brecciated quartz fragments (0.3mm) with associated small laths of tourmaline (0.1mm). It is shown in Figure 2-12 and occurs in other drill holes from 2mm to 60 centimetres true width along several splay faults from the Paint Lake Fault system and is easily recognized in drill core samples.

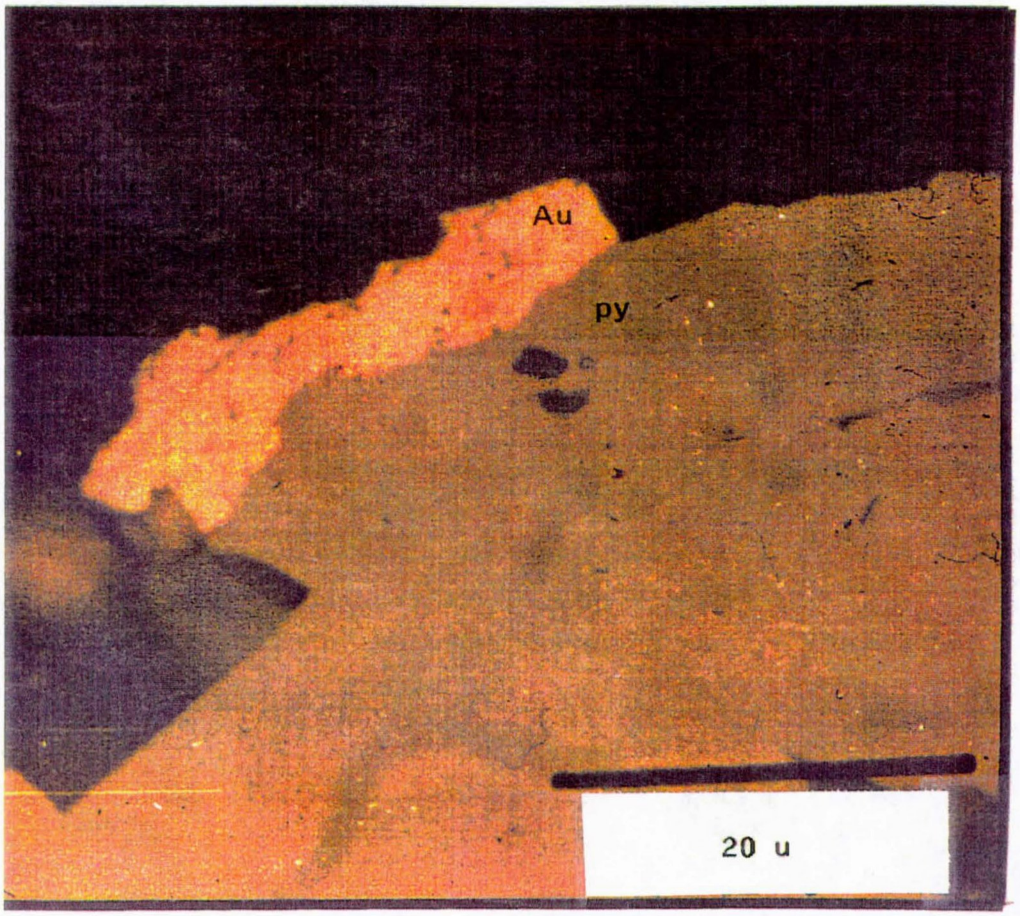

Figure 2-14: Gold adjacent to pyrite in the Metalore zone.
Thin section B-16W-2.

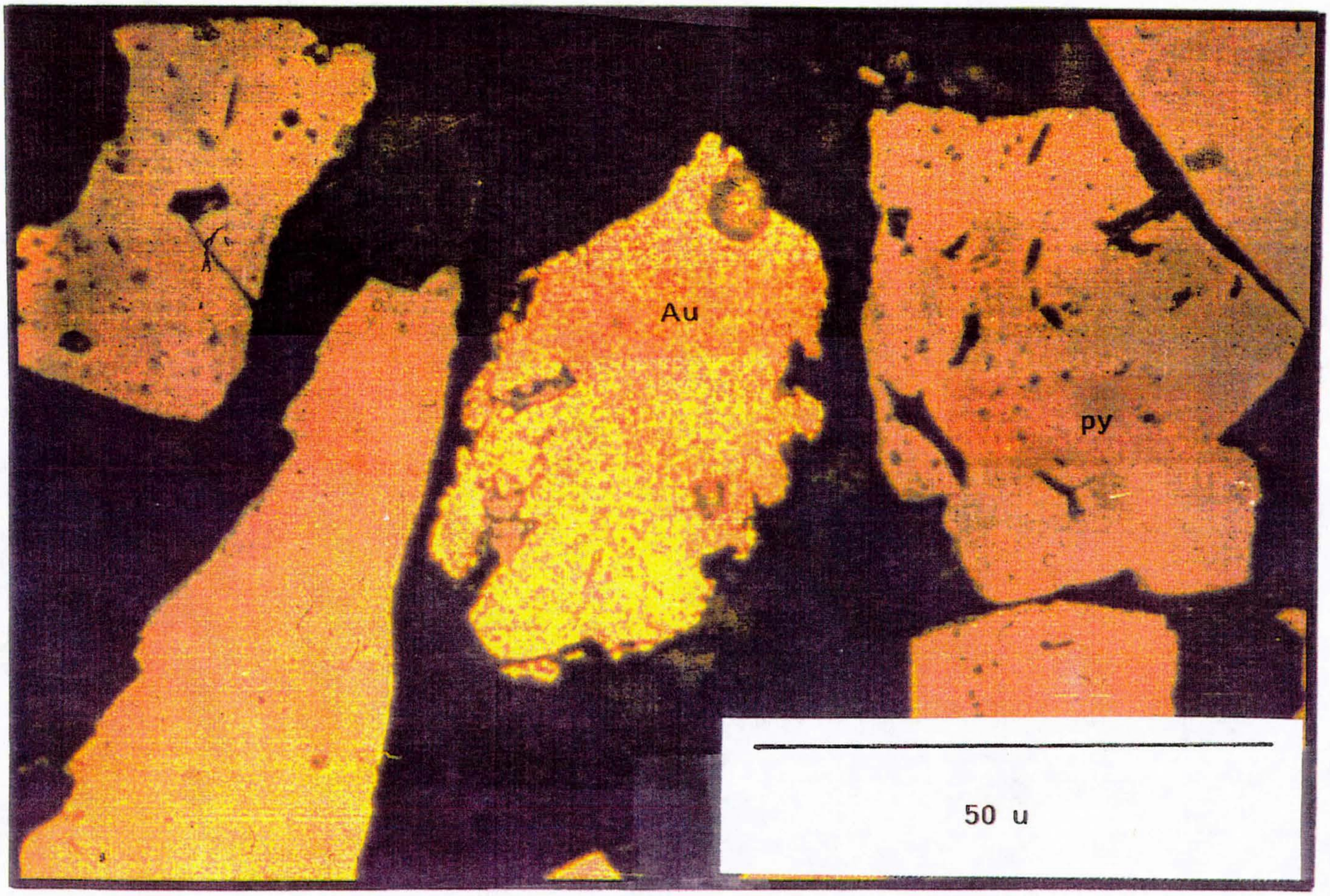

Figure 2-15: Gold amongst gangue minerals. Thin section B-16W-2.

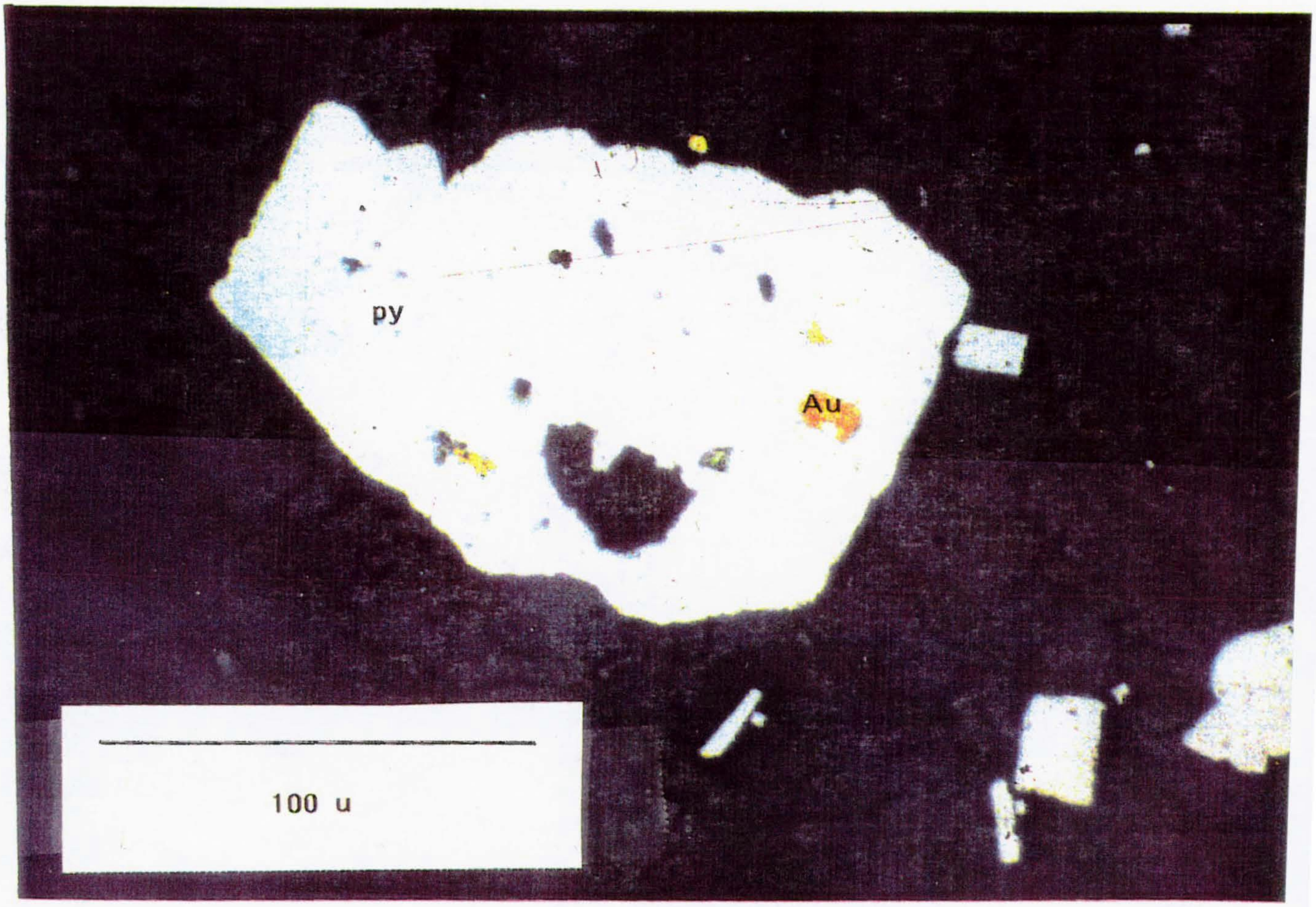

Figure 2-16: Gold encapsulated in pyrite grains in the Metalore zone. Thin section B-16W-2.

2.4 Mineralogy of the Golden Highway Quartz-Carbonate Vein

The Golden Highway vein is situated along a splay from the Metalore fault called the Golden Highway fault, (Figure 1-2). The wallrocks of the vein are deformed and altered mafic volcanics. The mineralogy of the mafic volcanics is enriched with plagioclase-quartz-chlorite layers sericite-magnetite layers and ankerite layers. The vein itself pinches and swells from 10 to 150 centimetres in width. The vein principally consists of quartz and ankerite with minor amounts of calcite, scheelite, and plagioclase feldspars. It is mineralized with pyrite, chalcopyrite, molybdenite, argentite, native copper, silver and gold.

Quartz occurs in layers associated with ankerite and disseminated sulphides. Granulation and strained extinction within the quartz were observed in the fine-grained and coarser-grained layers. Cherty layers and lenses occur as equant quartz. Scheelite occurs as 0.05mm anhedral grains in quartz layers. Ankerite occurs as anhedral grains in the quartz layers. It usually forms as anhedral grains and aggregates, however, euhedral rhombic crystals are less common. Muscovite and sericite occur as fine grains in veinlets parallel to the layering.

Pyrite forms disseminated, anhedral to subhedral grains averaging 0.02-0.1mm in diameter. Silicate and chalcopyrite inclusions occur within few grains. Interstitial to the pyrite are native gold and silver grains. Molybdenite forms subhedral crystals in association with the anhedral 0.1mm grains of chalcopyrite. Native copper occurs as dusty small grains in the silicates, in association with chalcopyrite grains. All other minerals listed in Table 2-6 occur in the same manner as in the altered mafic volcanic described earlier.

Table 2-6: Suite of minerals occurring in the Golden Highway Quartz-Carbonate Vein

Mineral	Modal Percent
Ankerite	40.0-45.0
Quartz	20.0-25.0
Plagioclase	10.0
Latite fragments	3.0-5.0
Sericite and Muscovite	1.0-1.5
Sphene and Ilmenite	0.5
Pyrite	0.5
Chalcopyrite	0.5
Molybdenite	0.3-1.4
Argentite	0.3
Magnetite	0.3
Native copper	trace
Native silver	trace
Native gold	trace
Scheelite	trace
Ankerite-Plagioclase-Quartz	8.0-10.0

Chapter 3

3.1 METHODOLOGY

3.1.1 SAMPLE PREPARATION

Doubly polished thick sections (150 μm in thickness) were prepared utilizing a low temperature procedure. The samples were not heated above 100°C, in order to prevent any alteration of fluid inclusions. A coolant was used during the grinding of the samples to minimize the effects of heating.

3.1.2 MICROTHERMOMETRY

Inclusion work in this study was completed on a modified U.S.G.S. gas-flow heating/freezing stage attached to a Leitz Orthoplan polarizing microscope. Low-temperature data were obtained by flowing nitrogen gas cooled by liquid nitrogen into the sample chamber. Homogenization temperatures were obtained by heating nitrogen gas with a heating coil mounted in the microthermometric stage. This stage has a temperature range between -150 to 600°C, measured with a thermocouple. The thermocouple was calibrated by Sherlock (1989) just prior to this study. The maximum deviation from calibration points in two calibrations was -2.2°C, and most other measurements were within `0.5°C of calibration points. The rate of temperature change during low-temperature determinations was 1-2°C/minute and 1°C/minute during high-temperature determination. The rates were controlled by the combination of cooled and ambient nitrogen gas and the heating of nitrogen gas flow with an electrical heating element.

All low-temperature data determinations were completed prior to gradual warming of the inclusions in order to prevent thermally induced stretching of the fluid inclusions (Lawler and Crawford, 1983; Burruss, 1981).

3.1.3 RAMAN SPECTROSCOPY

INTRODUCTION

Raman spectroscopy is a non-destructive analytical technique that can semiquantitatively identify molecular species, regardless of the physical state of the sample (Long, 1977). The Raman method provides compositional information, such as molar proportions, and can confirm interpretations made using microthermometric analyses.

Reconnaissance Raman spectroscopic analyses were carried out at Washington University, St. Louis, and qualitative analyses of several inclusions were provided. The apparatus used optical microscopes to view the doubly polished plates prepared for microthermometric analyses. There is a coupling optic between the microscope and spectrometer, enabling the laser beam to be focused on a fluid inclusion, or even a phase within an inclusion, and an analysis obtained for the area covered by the beam.

RESULTS

Reconnaissance Raman Spectroscopic analyses for several fluid inclusions detected the presence of H_2O, CO_2 and N_2 in sample number BSK-C-0+95E-2, which was taken from the Golden Highway Zone. The results from the analysis are outlined in Table 3-2. Trace amounts of manganese occurring either in ankerite matrix or as an included daughter phase in a fluid inclusion were detected in sample number BSK-B54-1670, which was taken from the Metalore Contact Zone. The spectral regions and associated (non-aqueous) volatile bands analyzed in the sample were subdivided into two groups. The first group wavenumbers (cm^{-1}) were 1050-2350 with their associated volatile bands being SO_2, CO_2, N_2O, N_2O_4, NO_2, O_2. The second group of wavenumbers were 2200-3400 cm^{-1} with associated volatile bands of CO, N_2, H_2S, CH_4, other olefinic, aliphatic and aromatic hydrocarbons, and NH_3.

There were three phases that occur in fluid inclusions numbered 1 and 2 described in Table 3-1. The two inner phases of the inclusions were analyzed using the Raman method. The inclusions listed in Table 3-1 were also analyzed using microthermometry. The results of the microthermometric analysis of these inclusions are listed in Table 3-2.

Table 3-1: Raman Spectroscopic analysis results of fluid inclusions from sample number BSK-C-0+95E-2.

Inclusion Number	Number of Fluid Phases	Phase
1	3	CO_2
2	3	CO_2
3	1	H_2O
4	1	H_2O
5	2	CO_2, N_2
6	2	CO_2, N_2
7	2	H_2O, N_2

Table 3-2: Microthermometric analysis of fluid inclusions of the Golden Highway sample number BSK-C-0+95E-2. All the data are given in degrees Celsius.

Inclusion	Tf	Stage	Te	Tm	Th	Type	Hom. Phase	Tmcl.
1	-77.9	1	-21.8	-0.4	221.4	3	L	10.5
2	-77.9	1	-21.8	-0.4	221.4	3	L	10.5
3	-77.6	2	-35.3	-0.1	266.2	4A	V	
4	-77.6	2	-35.1	-0.1	266.1	4A	V	
7	-77.6	2	-35.2	-0.1	266.3	4A	V	
5	-77.9	3	-15.9	-1.1	66.6	3	L	
6	-77.9	3	-15.9	-1.1	66.3	3	L	

Abbreviations

Tf -Temperature of freezing

Te -Temperature of eutectic first melting

Tm -Temperature of final melting

Th -Temperature of homogenization

Hom. Phase -Phase of homogenization

Tmcl. -Temperature of melt of clathrate

Chapter 4

4.0 ANALYSIS AND INTERPRETATION OF FLUID INCLUSIONS

4.1 INTRODUCTION

Fluid inclusion investigations involve processes of primary mineral growth in a fluid medium, which, upon crystallization and secondary/pseudosecondary fracturing and healing in the presence of liquid or gaseous fluids, traps small quantities of the encompassing fluids in the host crystal (Roedder, 1984). The fluid inclusions selected in this study are considered to be representative of the fluid at the time of trapping, as discussed in the following section. The inclusions are grouped on the basis of similar inclusion associations, mineral paragenesis and analytical data. The data from the Metalore and Golden Highway Zones are interpreted and discussed in subsequent sections.

4.2 SAMPLE AND FLUID INCLUSION SELECTIONS

Meticulous examination of the outcrops, oriented hand specimens, core samples and petrographic sections of the Metalore and Golden Highway Zones revealed pre-ore, syn-ore and post-ore events. Based on these observations, quartz, chlorite and carbonate occurring in the fluid inclusions were selected from pre-, syn- and post- ore events, designated as stages 1, 2 and 3 respectively. The criteria used to select representative fluid inclusion samples were used during this study and are given by Roedder (1962, 1984) as follows: (i) Inclusions of appropriate size were obtained for suitable optical work; (ii) Primary or pseudosecondary inclusions were distinguished and selected for analysis; (iii) Fractured or cloudy quartz, chlorite and carbonate containing secondary inclusions and demonstrating leakage or necking down were rejected. Other criteria used in this study are summarized in Roedder (1984). Quartz, chlorite and carbonate that were spatially associated with gold and/or iron sulphides were used in this study.

Roedder (1984) explained that primary fluid inclusions were trapped during crystal growth, pseudosecondary inclusions were trapped at the time of fracture healing in a growing crystal and secondary inclusions were trapped after crystal growth and during fracturing healing. Primary or pseudosecondary inclusions are likely to represent syn-mineralization fluids.

A total of 370 measurements of fluid inclusions from the Metalore and Golden Highway Zones were made and are given in Tables 4-1 and 4-2.

Table 4-1: Microthermometric Data Results from the Golden Highway Zone.

Sample #	Tf	Te	Tm	Th	Type	Hom.Phase	Tm clathrate
STAGE 1							
BSK-C-0+43-5	-78.2	-22.0	-0.5	221.3	1	L	10.6
BSK-C-0+43-8	-77.1	-22.5	-0.5	221.7	1	L	
BSK-C-0+43-11	-76.1	-22.4	-0.5	221.3	3	L	10.6
BSK-C-0+43-11	-76.1	-22.4	-0.4	222.0	1	V	10.5
BSK-C-0+43-11	-76.1	-22.3	-0.5	221.8	3	L	10.6
BSK-C-0+43-11	-76.1	-22.2	-0.4	221.8	3	L	10.5
BSK-C-0+43-11	-76.1	-22.4	-0.4	221.6	3	L	10.5
BSK-1	-78.2	-22.3	-0.5	220.3	1	L	10.5
BSK-1	-78.2	-22.3	-0.4	220.9	1	L	10.6
BSK-3	-79.5	-22.2	-0.5	221.1	1	L	10.5
BSK-4	-78.9	-22.1	-0.4	220.3	3	V	10.4
BSK-4	-78.9	-22.1	-0.5	221.7	1	L	
BSK-4	-78.9	-22.0	-0.5	221.9	1	L	
BSK-7	-77.6	-21.9	-0.5	221.3	3	L	10.5
BSK-7	-77.6	-21.7	-0.5	221.4	3	L	10.4
BSK-7	-77.6	-21.4	-0.5	221.4	3	V	
BSK-8	-76.7	-22.6	-0.5	221.9	3	V	10.5
BSK-8	-76.7	-22.9	-0.5	221.5	1	L	10.6
BSK-8	-76.7	-22.4	-0.4	221.8	1	L	10.6
BSK-11	-76.8	-22.1	-0.5	221.3	3	L	10.5
BSK-11	-76.8	-22.4	-0.4	220.9	3	V	10.4
BSK-11	-76.8	-21.0	-0.5	220.6	1	L	10.6
BSK-11	-76.8	-21.8	-0.4	221.8	1	L	10.5
BSK-11	-76.8	-21.1	-0.4	221.7	3	L	10.4
BSK-11	-76.8	-22.1	-0.5	222.0	3	L	
BSK-11	-76.8	-22.4	-0.4	221.4	3	L	
BSK-11	-76.8	-21.0	-0.5	221.3	3	L	
BSK-11	-76.8	-21.8	-0.5	221.9	3	V	
BSK-11	-76.8	-21.1	-0.5	221.4	3	L	
BSK-12	-77.9	-21.3	-0.4	221.3	1	L	
BSK-15	-76.5	-22.0	-0.4	221.9	1	L	
BSK-C-31-1	-88.0	-22.0	-0.5	221.9	3	L	10.6
BSK-C-31-5	-81.2	-22.1	-0.5	221.1	1	L	
BSK-C-31-13	-88.1	-22.2	-0.4	221.3	1	L	10.6
BSK-C-31-14	-88.4	-22.1	-0.5	221.9	3	L	10.5
BSK-C-31-18	-83.8	-22.1	-0.4	221.2	1	L	10.4
BSK-C-0+95E-2	-77.9	-21.8	-0.4	221.4	3	L	10.5
BSK-C-1+60E-2	-82.6	-22.3	-0.4	221.1	1	L	10.6
BSK-C-1+60E-5	-88.4	-22.1	-0.5	221.1	1	L	10.6
BSK-C-1+94E-2	-80.4	-22.1	-0.5	221.3	1	L	10.4
BSK-C-1+94E-3	-81.9	-22.0	-0.5	221.9	1	L	10.4
BSK-C-1+94E-4	-88.3	-21.9	-0.4	222.1	1	L	10.5

Table 4-1: cont'd

Sample #	Tf	Te	Tm	Th	Type	Hom.Phase	Tm clathrate
BSK-5	-77.3	-52.9	-0.5	230.5	3	V	
BSK-5	-77.3	-52.4	-0.4	230.6	3	L	
BSK-5	-77.3	-50.1	-0.5	230.6	3	L	
BSK-5	-77.3	-52.4	-0.5	230.9	1	L	
BSK-13	-76.8	-52.4	-0.5	230.5	1	L	
BSK-13	-76.8	-52.7	-0.5	230.7	1	L	
BSK-14	-76.5	-53.1	-0.5	230.8	3	L	
BSK-19	-77.8	-51.9	-0.4	230.5	3	L	
BSK-C-0+43-6	-77.9	-52.3	-0.5	230.1	1	L	
BSK-C-0+43-7	-76.2	-51.9	-0.4	230.8	1	L	
BSK-C-0+43-7	-76.2	-53.4	-0.5	230.6	3	V	
BSK-C-0+43-7	-76.2	-53.2	-0.4	231.0	1	L	
BSK-C-0+43-7	-76.2	-53.4	-0.5	230.9	1	L	
BSK-C-0+95E-1	-78.4	-52.4	-0.5	230.4	1	L	
BSK-C-0+95E-1	-78.4	-52.1	-0.5	230.7	3	L	
BSK-C-0+95E-3	-77.2	-51.8	-0.5	230.1	3	L	
BSK-C-0+95E-3	-77.2	-51.2	-0.5	230.5	3	V	
BSK-C-0+95E-3	-77.2	-52.1	-0.5	229.8	3	V	
BSK-C-0+95E-4	-77.1	-51.9	-0.4	230.3	3	L	
BSK-C-0+95E-4	-77.1	-51.9	-0.4	230.7	1	L	
BSK-C-1+05E-1	-78.1	-51.9	-0.5	229.7	1	L	
BSK-C-1+05E-3	-79.5	-52.0	-0.5	230.1	3	V	
BSK-C-1+05E-4	-80.1	-52.1	-0.5	230.2	1	L	
BSK-C-1+60E-1	-79.4	-52.2	-0.4	230.7	1	L	
BSK-C-2+78E-3	-82.3	-52.1	-0.5	230.5	1	L	
BSK-C-2+78E-4	-87.9	-52.4	-0.5	230.6	3	L	
BSK-C-2+78E-5	-85.8	-52.1	-0.5	230.1	3	L	
BSK-C-1+94E-5	-79.4	-52.6	-0.5	230.5	3	L	
BSK-C-31-2	-80.9	-52.2	-0.4	230.8	3	L	
BSK-C-31-3	-77.1	-52.1	-0.5	230.6	3	V	
BSK-C-31-8	-78.7	-52.4	-0.4	231.1	1	L	
BSK-C-31-9	-79.2	-52.4	-0.4	230.1	1	L	
BSK-C-31-10	-82.7	-52.1	-0.5	229.8	1	L	
BSK-C-31-15	-77.4	-52.3	-0.5	229.3	1	L	
BSK-C-31-16	-78.9	-52.2	-0.5	229.9	3	V	

Table 4-1: cont'd

Sample #	Tf	Te	Tm	Th	Type	Hom.Phase	Tm clathrate
STAGE 2							
BSK-9	-76.3	-35.7	-0.1	266.7	4A	L	
BSK-10	-76.9	-35.0	-0.1	266.6	4B	L	
BSK-12	-77.9	-35.4	-0.1	266.3	4A	L	10.5
BSK-19	-77.8	-35.8	-0.1	266.5	4A	L	
BSK-19	-77.8	-35.8	-0.1	266.8	4B	L	
BSK-C-0+43-7	-76.2	-36.9	-0.1	266.4	4B	L	
BSK-C-0+43-7	-76.2	-34.4	-0.1	266.8	4A	V	
BSK-C-0+43-7	-76.2	-34.4	-0.1	265.9	4B	L	
BSK-C-0+43-8	-77.1	-34.8	-0.2	266.7	4B	L	10.5
BSK-C-0+43-9	-75.2	-35.8	-0.4	266.5	4B	L	
BSK-C-0+43-9	-75.2	-35.7	-0.4	266.3	4A	V	
BSK-C-0+43-9	-75.2	-35.9	-0.5	266.1	4A	L	
BSK-C-0+95E-1	-78.4	-35.4	-0.1	266.2	4B	L	
BSK-C-0+95E-2	-77.6	-35.1	-0.1	266.1	4A	V	
BSK-C-0+95E-2	-77.6	-35.2	-0.1	266.3	4A	V	
BSK-C-0+95E-2	-77.6	-35.3	-0.1	266.2	4A	V	
BSK-C-0+95E-5	-76.9	-35.8	-0.1	266.4	4A	L	
BSK-C-0+95E-5	-76.9	-35.8	-0.1	266.1	4B	V	
BSK-C-0+95E-5	-76.9	-35.8	-0.1	265.8	4A	L	
BSK-C-0+95E-5	-76.9	-35.8	-0.1	265.9	4A	L	
BSK-C-1+05E-2	-78.2	-35.8	-0.1	265.7	4A	L	
BSK-C-1+05E-5	-80.3	-35.7	-0.1	266.4	4B	L	
BSK-C-1+05E-6	-80.4	-35.9	-0.1	266.8	4B	L	
BSK-C-1+60E-3	-85.7	-35.6	-0.1	266.3	4B	L	
BSK-C-1+60E-4	-81.3	-35.4	-0.1	266.5	4A	L	
BSK-C-1+94E-1	-78.3	-35.5	-0.1	266.4	4A	L	
BSK-C-2+78E-1	-84.6	-35.4	-0.1	266.4	4A	L	
BSK-C-2+78E-2	-77.6	-35.9	-0.1	266.1	4B	L	
BSK-C-2+78E-6	-86.9	-35.3	-0.1	267.1	4B	V	
BSK-C-31-6	-83.6	-35.9	-0.1	266.3	4B	L	
BSK-C-31-7	-84.9	-35.7	-0.1	266.9	4B	L	
BSK-C-31-4	-78.9	-35.8	-0.1	266.6	4A	L	
BSK-C-31-11	-86.3	-35.7	-0.1	266.9	4A	L	
BSK-C-31-12	-87.2	-35.9	-0.1	266.8	4B	L	
BSK-C-31-17	-84.9	-35.8	-0.1	267.1	4B	L	

Table 4-1: cont'd

Sample #	Tf	Te	Tm	Th	Type	Hom.Phase	Tm clathrate
STAGE 3							
BSK-14	-77.2	-55.1	-0.9	55.9	3	V	
BSK-14	-77.2	-55.6	-0.9	38.6	3	L	
BSK-15	-76.5	-54.9	-0.9	44.8	3	L	10.4
BSK-C-0+43-2	-75.9	-56.6	-0.9	32.4	3	L	
BSK-C-0+43-2	-75.6	-56.6	-0.9	32.0	3	L	
BSK-C-0+43-5	-78.2	-56.6	-0.9	32.4	3	L	
BSK-C-0+43-12	-76.2	-56.6	-0.9	32.1	3	L	
BSK-2	-79.8	-56.6	-0.9	32.1	3	V	
BSK-C-0+43-1	-78.1	-14.3	-1.2	44.3	3	L	
BSK-C-0+43-1	-78.1	-15.0	-1.2	66.1	3	L	
BSK-C-0+43-1	-78.1	-15.4	-1.1	68.1	3	L	
BSK-C-0+43-1	-78.1	-15.8	-1.1	68.9	3	V	
BSK-C-0+43-1	-78.1	-14.4	-1.2	66.1	3	L	
BSK-C-0+43-1	-78.1	-14.4	-1.2	69.8	3	L	
BSK-C-0+43-2	-75.9	-15.4	-1.2	21.6	3	L	
BSK-C-0+43-2	-75.6	-15.3	-1.1	42.3	3	L	
BSK-C-0+43-2	-75.6	-15.2	-1.1	40.1	3	V	
BSK-C-0+43-2	-75.9	-15.8	-1.2	21.6	3	L	
BSK-C-0+43-2	-75.9	-15.4	-1.1	21.8	3	L	
BSK-C-0+43-3	-75.0	-15.6	-1.1	58.8	3	L	
BSK-C-0+43-3	-75.0	-14.5	-1.2	23.6	3	V	
BSK-C-0+43-3	-75.0	-15.1	-1.2	62.9	3	L	
BSK-C-0+43-3	-75.0	-15.9	-1.2	58.1	3	L	
BSK-C-0+43-4	-76.1	-15.2	-1.2	44.8	3	L	
BSK-C-0+43-10	-75.9	-15.8	-1.2	51.9	3	L	
BSK-C-0+43-10	-75.9	-15.8	-1.2	38.9	3	L	
BSK-C-0+43-10	-75.9	-15.9	-1.1	42.5	3	L	
BSK-C-0+43-12	-76.2	-14.1	-1.1	29.2	3	V	
BSK-C-0+43-12	-76.2	-14.9	-1.1	31.2	3	L	
BSK-C-0+43-12	-76.2	-18.6	-1.2	46.3	3	L	
BSK-C-0+95E-2	-77.9	-15.9	-1.1	66.6	3	L	

Table 4-2: Microthermometric Data Results from the Metalore Contact Zone.

Sample #	Tf	Te	Tm	Th	Type	Hom.Phase
STAGE 1						
BSK-B43-1007	-90.1	-22.0	-5.9	220.1	3	V
BSK-B43-1035	-78.2	-22.3	-0.5	221.3	1	L
BSK-B49-507	-90.6	-22.4	-0.9	220.4	3	V
BSK-B49-512	-91.5	-22.8	-1.1	221.3	3	V
BSK-B49-535	-84.1	-22.1	-0.8	231.2	1	L
BSK-B49-552	-84.3	-22.3	-0.7	232.2	3	V
BSK-B49-555	-78.1	-22.5	-0.7	233.8	3	V
BSK-B49-558	-78.4	-22.3	-0.6	234.1	3	V
BSK-B49-561	-82.3	-22.8	-0.7	233.2	3	V
BSK-B49-570	-82.1	-22.3	-0.8	233.1	3	V
BSK-B49-610	-80.3	-22.3	-0.8	233.4	3	V
BSK-B49-613	-80.5	-22.4	-0.8	233.5	3	V
BSK-B49-617	-81.9	-22.6	-0.7	235.3	3	V
BSK-B50-1309	-81.9	-22.4	-0.7	221.9	3	V
BSK-B50-1348	-82.4	-22.4	-0.8	220.3	1	L
BSK-B50-1369	-83.2	-22.4	-0.7	220.5	3	L
BSK-B53-917	-76.4	-22.2	-0.7	220.3	3	V
BSK-B53-920	-73.5	-22.3	-0.6	221.1	3	V
BSK-B53-924	-83.2	-22.1	-0.7	220.1	3	V
BSK-B53-947	-88.5	-22.2	-0.7	222.2	3	V
BSK-B56-677	-89.2	-22.0	-0.1	230.4	1	L
BSK-B56-702	-70.9	-22.4	-0.3	232.5	3	V
BSK-B56-738	-83.0	-22.0	-2.3	230.5	3	V
BSK-B58-792	-72.1	-22.0	-0.1	266.8	3	V
BSK-B58-823	-88.9	-22.4	-0.1	229.3	3	V
BSK-B58-862	-83.2	-22.6	-0.1	225.7	3	V
BSK-B58-867	-65.3	-22.9	-0.2	222.2	3	V
BSK-B58-869	-60.0	-22.9	-0.3	231.1	1	L
BSK-B58-869	-85.2	-22.9	-6.3	230.1	1	V
BSK-B61-1923	-65.3	-22.8	-6.6	229.4	1	V
BSK-B53-905	-78.2	-52.3	-0.4	230.1	3	V
BSK-B53-908	-77.3	-52.6	-0.3	231.2	3	V
BSK-B53-914	-77.5	-52.4	-0.5	230.9	3	V
BSK-B53-917	-76.4	-52.1	-0.4	230.1	3	V
BSK-B53-927	-91.4	-52.3	-0.4	230.6	3	V
BSK-B53-930	-92.3	-52.1	-0.4	235.2	3	V
BSK-B53-933	-84.2	-52.8	-0.5	234.3	3	V
BSK-B56-687	-87.4	-52.5	-0.7	235.4	3	V
BSK-B56-697	-73.2	-52.4	-0.8	234.8	3	V
BSK-B58-818	-80.0	-52.3	-0.6	237.4	3	L
BSK-B58-820	-82.3	-52.6	-0.3	238.1	3	V
BSK-B58-877	-63.9	-52.8	-0.3	235.9	3	V
BSK-B58-882	-73.8	-52.3	-0.4	232.2	3	V
BSK-B61-1920	-74.3	-52.6	-0.4	266.4	3	V
BSK-B61-1923	-69.3	-52.4	-0.4	265.4	3	V
BSK-B43-1010	-78.1	-55.1	-0.9	356.9	3	V
BSK-B43-1013	-77.8	-55.4	-0.8	356.7	3	V
BSK-B43-1017	-77.5	-55.1	-0.9	356.9	3	V
BSK-B43-1023	-77.6	-55.3	-0.8	356.6	1	L
BSK-B43-1055	-77.7	-55.3	-0.7	356.6	1	V
BSK-B43-1058	-77.6	-55.1	-0.4	356.6	3	V
BKS-B43-1060	-77.5	-55.6	-0.7	356.7	3	V
BSK-B43-1062	-77.3	-55.0	-0.5	356.6	3	V
BSK-B46-2450	-76.3	-55.3	-0.6	356.2	3	V
BSK-B46-2453	-76.8	-55.1	-0.7	357.1	1	V
BSK-B46-2456	-76.1	-55.3	-0.8	356.8	1	V
BSK-B46-2469	-76.2	-55.1	-0.3	357.1	1	L
BSK-B46-2481	-76.8	-55.4	-0.8	356.3	1	V
BSK-B46-2484	-78.3	-55.9	-0.7	355.9	1	V
BSK-B46-2490	-76.7	-55.1	-0.7	355.8	3	V
BSK-B46-2493	-76.6	-54.8	-0.9	354.9	3	V
BSK-B46-2496	-76.9	-55.3	-0.8	356.1	3	V
BSK-B46-2499	-77.3	-55.6	-0.7	358.3	3	V
BSK-B46-2502	-77.8	-54.9	-0.8	356.7	3	V

Table 4-2: cont'd

Sample #	Tf	Te	Tm	Th	Type	Hom.Phase
BSK-B46-2505	-78.3	-55.4	-0.6	357.6	1	V
BSK-B46-2508	-77.9	-55.6	-0.8	356.2	1	V
BSK-B46-2511	-78.6	-55.3	-0.7	356.9	3	V
BSK-B46-2512	-79.1	-55.6	-0.8	356.7	3	V
BSK-B49-512	-78.8	-55.2	-0.6	357.6	3	V
BSK-B49-558	-78.4	-55.2	-0.5	358.1	1	V
BSK-B49-579	-78.2	-55.4	-0.4	356.2	1	L
BSK-B49-581	-77.9	-55.7	-0.5	356.1	1	V
BSK-B50-1297	-77.4	-55.4	-0.6	356.8	1	V
BSK-B50-1306	-77.9	-55.6	-0.7	356.8	1	L
BSK-B50-1327	-78.1	-55.3	-0.8	356.4	1	V
BSK-B50-1333	-85.6	-55.9	-0.9	356.5	1	V
BSK-B50-1342	-77.2	-55.3	-0.5	356.7	3	V
BSK-B50-1345	-78.3	-55.6	-0.2	356.3	3	V
BSK-B50-1357	-83.2	-55.3	-0.2	356.4	3	V
BSK-B53-890	-81.3	-55.3	-0.4	356.4	3	V
BSK-B53-893	-83.2	-55.2	-0.5	356.8	3	V
BSK-B53-950(OV)	-83.5	-55.3	-0.4	356.4	1	V
BSK-B53-959	-93.5	-55.4	-0.3	356.8	1	L
BSK-B53-962	-91.9	-55.1	-0.2	358.1	1	V
BSK-B53-967	-88.9	-55.3	-0.3	357.9	1	L
BSK-B58-816	-77.4	-55.1	-0.6	353.5	3	V
BSK-B53-983	-83.5	-55.4	-0.5	357.1	3	L
BSK-B53-986	-88.9	-55.3	-0.4	356.9	3	L
BSK-B53-989	-86.3	-55.1	-0.3	356.3	3	V
BSK-B53-995	-92.3	-55.2	-0.3	356.9	3	V
BSK-B53-997	-85.3	-55.4	-0.4	357.4	3	V
BSK-B54-1677	-75.4	-55.3	-0.4	356.6	3	V
BSK-B54-1680	-76.4	-55.8	-0.4	357.5	3	V
BSK-B56-732	-70.3	-55.1	-0.5	356.8	3	V
BSK-B56-735	-73.1	-55.7	-0.5	357.3	3	V
BSK-B58-838	-75.4	-55.3	-0.6	356.9	3	V
BSK-B58-847	-74.8	-55.9	-0.7	355.4	3	V
BSK-B58-852	-78.9	-55.4	-0.6	354.9	3	V
BSK-B61-1907	-93.2	-55.3	-0.8	359.9	3	V
BSK-B61-1915	-82.2	-55.3	-0.7	361.7	3	V
BSK-B61-1918	-88.4	-55.8	-0.6	359.9	3	V
BSK-B61-1927	-66.7	-55.8	-1.2	364.2	3	V
STAGE 2						
BSK-B43-1020	-76.2	-35.1	-0.5	266.3	4B	V
BSK-B43-1026	-76.3	-35.0	-0.4	266.1	4A	L
BKS-B43-1029	-76.8	-35.2	-0.5	266.4	4A	L
BSK-B43-1032	-76.7	-35.3	-0.4	266.3	4B	L
BSK-B43-1037	-76.6	-35.4	-0.6	266.2	4A	V
BSK-B43-1040	-76.8	-35.7	-0.4	266.3	4B	V
BSK-B43-1043(OV)	-76.5	-35.5	-0.5	266.5	4A	L
BSK-B43-1046	-76.8	-35.1	-0.6	266.6	4A	V
BSK-B43-1049	-76.6	-35.1	-0.6	266.6	4B	V
BSK-B43-1052	-76.5	-35.3	-0.5	266.1	4B	V
BSK-B46-2440	-76.8	-35.8	-0.3	266.3	4B	L
BSK-B46-2443	-76.9	-35.3	-0.6	266.2	4A	L
BSK-B46-2447(OV)	-76.4	-35.8	-0.4	266.9	4A	L
BSK-B46-2447(OVA)	-75.9	-36.1	-0.4	266.2	4A	L

Table 4-2: cont'd

Sample #	Tf	Te	Tm	Th	Type	Hom.Phase
BSK-B46-2459	-77.6	-35.2	-0.2	267.2	4A	V
BSK-B46-2462	-77.4	-35.3	-0.1	266.8	4B	V
BSK-B46-2466	-78.5	-34.9	-0.2	266.7	4B	V
BSK-B46-2472(OV)	-75.5	-34.8	-0.5	266.6	4A	L
BSK-B46-2472(OVA)	-75.9	-34.5	-0.9	267.3	4B	V
BSK-B46-2475	-77.8	-35.8	-0.3	266.4	4B	L
BSK-B46-2478	-77.3	-34.8	-0.3	266.4	4B	L
BSK-B46-2487	-78.5	-35.4	-0.2	266.8	4A	L
BSK-B49-526	-78.3	-35.4	-0.2	266.4	4A	V
BSK-B49-538	-78.4	-35.6	-0.1	267.3	4A	V
BSK-B49-542	-78.2	-35.4	-0.2	267.4	4A	V
BSK-B49-564	-79.4	-35.3	-0.2	266.3	4A	V
BSK-B49-589	-79.6	-35.2	-0.2	266.5	4A	L
BSK-B49-595	-79.3	-35.7	-0.2	268.1	4A	V
BSK-B49-598	-77.7	-35.4	-0.3	268.4	4A	L
BSK-B50-1303	-78.5	-35.5	-0.3	267.8	4A	V
BSK-B50-1312	-79.3	-35.1	-0.2	267.5	4A	V
BSK-B50-1315	-81.3	-35.4	-0.3	267.3	4A	V
BSK-B50-1318	-82.4	-35.6	-0.4	267.1	4B	V
BSK-B50-1324	-77.3	-35.3	-0.3	268.2	4B	L
BSK-B50-1351	-76.5	-35.2	-0.3	268.3	4B	V
BSK-B50-1354	-76.3	-35.4	-0.2	268.6	4B	V
BSK-B50-1363	-93.2	-35.4	-0.2	267.4	4A	V
BSK-B50-1366	-93.4	-35.6	-0.4	267.9	4B	V
BSK-B50-1366	-77.4	-34.1	-1.1	265.3	4A	L
BSK-B53-896	-75.9	-35.4	-0.2	268.3	4B	V
BSK-B53-899	-74.9	-35.2	-0.2	268.1	4B	V
BSK-B53-902	-77.2	-35.8	-0.3	267.9	4B	V
BSK-B53-956	-88.8	-35.4	-0.3	268.3	4B	V
BSK-B53-970	-77.5	-35.4	-0.3	268.9	4B	V
BSK-B53-973	-78.9	-35.2	-0.3	267.4	4A	V
BSK-B53-976	-78.3	-35.4	-0.2	266.9	4A	V
BSK-B54-1632	-94.6	-35.5	-8.3	265.3	4A	L
BSK-B54-1637	-95.2	-35.4	-7.4	266.8	4A	L
BSK-B54-1639	-77.2	-35.2	-0.3	267.9	4A	V
BSK-B54-1644	-78.5	-35.6	-8.1	265.4	4B	L
BSK-B54-1647	-79.3	-35.7	-7.5	266.9	4B	L
BSK-B54-1647	-91.1	-34.9	-8.1	265.1	4A	L
BSK-B54-1650	-87.4	-35.4	-0.3	268.1	4A	V
BSK-B54-1653	-86.5	-35.3	-0.3	267.9	4A	V
BSK-B54-1657	-88.2	-35.5	-0.3	268.4	4B	V
BSK-B54-1660	-91.1	-35.4	-8.3	265.9	4B	L
BSK-B54-1663	-83.2	-35.7	-8.9	265.4	4B	L
BSK-B54-1667	-88.9	-35.6	-0.3	267.2	4A	V
BSK-B54-1670	-91.5	-35.0	-8.8	260.2	4A	V
BSK-B54-1675	-89.7	-35.8	-7.5	266.6	4A	V
BSK-B56-667	-74.3	-35.7	-0.1	266.5	4B	L
BSK-B56-677	-89.2	-35.3	-0.1	266.2	4A	L
BSK-B56-714	-75.3	-35.4	-0.4	266.5	4A	V
BSK-B56-717	-81.2	-34.8	-0.4	265.9	4B	V
BSK-B56-720	-83.2	-33.9	-0.4	266.2	4B	V
BSK-B56-723	-88.1	-34.8	-0.5	265.5	4A	V
BSK-B56-726	-73.2	-35.4	-0.3	266.1	4A	V
BSK-B56-729	-70.1	-35.4	-0.4	267.3	4B	V
BSK-B58-797	-75.9	-35.2	-0.5	266.8	4B	V
BSK-B58-800(OV)	-76.4	-35.8	-0.6	266.2	4A	V

Table 4-2: cont'd

Sample #	Tf	Te	Tm	Th	Type	Hom.Phase
BSK-B58-800(OVA)	-76.4	-35.3	-0.5	266.6	4B	V
BSK-B58-803	-85.4	-35.6	-0.3	266.9	4B	L
BSK-B58-806	-88.3	-35.2	-0.4	267.4	4B	L
BSK-B58-818	-80.0	-35.8	-0.6	265.1	4B	L
BSK-B58-826(OV)	-82.1	-35.4	-0.5	268.2	4A	V
BSK-B58-826(OVA)	-73.2	-35.8	-0.4	266.4	4A	V
BSK-B58-829	-69.3	-35.4	-0.3	269.4	4A	V
BSK-B58-832	-74.3	-35.8	-0.4	267.8	4A	V
BSK-B58-857	-77.8	-35.4	-0.4	268.3	4B	V
BSK-B58-872	-66.3	-35.5	-0.4	269.1	4B	V
BSK-B61-1909	-64.9	-35.5	-0.4	255.9	4B	V
BSK-B61-1912	-66.9	-35.1	-0.5	258.3	4B	V
STAGE 3						
BSK-B46-1043(YV)	-78.5	-56.8	-0.9	32.3	3	V
BSK-B46-2447(YVA)	-78.5	-56.3	-0.9	32.5	3	V
BSK-B46-2447(YV)	-78.9	-56.8	-0.9	32.5	3	L
BSK-B46-2472(YVA)	-78.1	-56.5	-0.9	32.9	3	V
BSK-B46-2472(YV)	-79.7	-56.2	-0.7	32.6	3	V
BSK-B46-2513	-79.7	-56.7	-0.7	32.4	3	V
BSK-B46-2513	-80.4	-56.6	-0.8	32.4	3	V
BSK-B49-520	-83.4	-56.6	-0.7	32.3	3	V
BSK-B49-523	-83.5	-56.3	-0.8	32.8	3	V
BSK-B49-532	-81.5	-56.7	-0.8	32.6	3	V
BSK-B49-545	-83.2	-56.5	-0.8	32.4	3	V
BSK-B49-561	-82.3	-56.6	-0.9	32.5	3	V
BSK-B49-567	-83.2	-56.6	-0.9	32.5	3	V
BSK-B49-573	-83.1	-56.6	-0.8	32.6	3	V
BSK-B49-576	-82.9	-56.8	-0.9	32.4	3	V
BSK-B49-601	-78.1	-56.6	-0.9	32.4	3	V
BSK-B49-604	-80.1	-56.8	-0.8	32.5	3	V
BSK-B49-607	-80.5	-56.3	-0.7	32.4	3	V
BSK-B49-622	-84.1	-56.6	-0.9	32.6	3	V
BSK-B49-623	-84.8	-56.5	-0.8	32.4	3	V
BSK-B50-1312	-65.2	-56.6	-1.3	32.5	3	V
BSK-B50-1321	-84.2	-56.6	-1.0	32.6	3	V
BSK-B50-1330	-85.3	-56.7	-1.2	32.9	3	V
BSK-B50-1336	-83.2	-56.5	-0.8	32.3	3	V
BSK-B50-1360	-90.2	-56.6	-1.4	32.5	3	L
BSK-B53-936	-92.3	-56.6	-1.2	32.4	3	V
BSK-B53-950(YV)	-93.5	-56.5	-1.4	32.6	3	V
BSK-B53-997	-85.3	-56.6	-1.4	32.6	3	V
BSK-B54-1647	-91.1	-56.6	-8.1	32.7	3	L
BSK-B54-1670	-91.5	-56.6	-0.7	32.4	3	V
BSK-B54-1677	-75.4	-56.6	-0.7	32.3	3	V
BSK-B54-1680	-76.4	-56.5	-1.1	32.7	3	V
BSK-B56-742	-79.8	-56.6	-1.8	32.7	3	V
BSK-B58-800(YVA)	-76.4	-56.6	-4.3	32.8	3	V
BSK-B58-800(YV)	-76.4	-56.5	-1.5	32.2	3	V
BSK-B58-818	-80.0	-56.6	-0.6	32.8	3	V
BSK-B58-826(YV)	-74.9	-56.6	-4.3	32.9	3	V
BSK-B58-887	-91.3	-56.6	-8.3	32.8	3	L
BSK-B58-892	-88.5	-56.6	-6.8	32.5	3	L
BSK-B43-1043(YV)	-78.2	-56.7	-0.9	32.5	3	L

Abbreviations used in Tables 4-1 and 4-2:
All the temperatures in these tables are given in degrees celsius

Tf - Temperature of freezing
Te - Temperature of eutectic
Tm - Temperature of final melting
Th - Temperature of homogenization
Hom.Phase- Phase of homogenization
OV - Oldest Vein
OVA - Younger vein than OV
YVA - Younger vein than OVA
YV - Youngest vein
BSK-1 - Represents first sample taken on line 0+00 on Golden Highway grid
BSK-C-0+43-5
- Represents the fifth sample taken on line 0+43W on the Golden Highway grid
BSK-B43-1007
- B43 represents diamond drill hole number on the Metalore Zone
- 1007 represent the footage in diamond drill hole B43 that the sample was collected

4.3 FLUID INCLUSION PHASE COMPOSITIONS

Based on microscopic observations of fluid inclusion phase assemblages at room temperature, six types were recognized. The six types of fluid inclusions are H_2O_{liquid} (Type 1); H_2O_{liquid} + S (Type 2); H_2O_{liquid} + $CO_{2\,\text{liquid + vapour}}$ (Type 3); H_2O_{liquid} + $CO_{2\,\text{liquid + vapour}}$ (Type 4A); H_2O_{liquid}+ $CO_{2\,\text{liquid + vapour}}$ + S (Type 4B); and $CO_{2\,\text{liquid + vapour}}$(Type 5), where S indicates a daughter mineral. It is possible that small amounts of $CO_{2\,\text{liquid}}$ too small to detect optically occur in Types 1, 2 and 3 inclusions, also the appearance of clathrates suggest the presence of $CO_{2\,\text{vapour}}$ in Types 3, 4A, 4B and 5 inclusions. Raman spectroscopy verified the presence of H_2O, CO_2 and N_2 phases in a number of inclusions studied. These six types of fluid inclusions were trapped in three stages of mineralization (Stage 1, 2 and 3) and are recognized by their textural relationships with respect to other fluid inclusion assemblages and types of host minerals: quartz, calcite, alkali feldspar, ankerite, chamosite and clinochlore.

STAGE 1

Mottled quartz-carbonate veins and veinlets occur among hematite-ankerite-alkali feldspar-chamosite aggregates and veinlets. Fine-grained pyrite and chalcopyrite are interspersed throughout the rock. The veins and veinlets contain little to no gold. The Stage 1 event is considered to be pre-ore, since it is cross-cut by the auriferous event (Stage 2). Microthermometric measurements of fluid inclusions in quartz, calcite and ankerite from Stage 1 were taken from veinlets in the Golden Highway and from inclusions hosted by quartz, calcite, ankerite, alkali feldspar and chamosite in aggregates and veinlets, in the Metalore. The primary and pseudosecondary fluid inclusions are uniformly round and 2-5μm in diameter and occur as isolated inclusions away from other inclusions and within internal growth zones of crystals. The fluid inclusion phase assemblages that commonly occur in this stage are H_2O-rich $_{liquid}$ (Type 1) and H_2O-rich $_{liquid}$ with an inner CO_2-rich $_{vapour}$ phase (Type 3). The mole proportions of the CO_2 phase present in the inclusions average 10 volume percent in the Golden Highway and up to 40 volume percent in the Metalore.

Secondary fluid inclusions occur in planar arrays on the healed fractures that are cut by crystal boundaries. The inclusions are H_2O-rich $_{liquid}$ and some may contain a daughter mineral that is too small to identify.

STAGE 2

Grey quartz hosting the pyrite and gold occur as automorphic crystals. Tabular and columnar clinochlore crystals up to 5mm in length occur as veinlets amongst the quartz.

The primary and pseudosecondary fluid inclusions in the quartz and clinochlore are uniformly round, 2-4μm in diameter and either H_2O-rich $_{liquid}$ with two inner phases of CO_2-rich $_{liquid}$ and CO_2-rich $_{vapour}$ (Type 4A) or H_2O-rich $_{liquid}$ with two inner phases of CO_2-rich $_{liquid}$ + CO_2-rich $_{vapour}$+ S (Type 4B). The volume proportion of CO_2 vapour phase in the fluid inclusions was optically estimated at 50 volume percent in the Golden Highway and up to 80 volume percent in the Metalore.

Secondary fluid inclusions are similar to those in Stage 1, but there are more CO_2-rich (Type 5) inclusions occurring in both the Golden Highway and Metalore.

STAGE 3

Four post-ore white to pink quartz-calcite veinlets cross-cut and overprint the auriferous zone (Stage 2), described previously. Primary and pseudosecondary inclusions in the quartz and automorphic calcite crystals are H_2O-rich $_{liquid}$(Type 1), H_2O-rich $_{liquid}$+ S (Type 2), H_2O-rich $_{liquid}$ with an inner phase of CO_2-rich $_{vapour}$ (Type 3) or CO_2-rich $_{vapour}$ (Type 5). The Type 5 fluid inclusions are more abundant in the Metalore than in the Golden Highway. The vapour phase present in the inclusions is 10-20 volume percent in the Golden Highway and 20-50 volume percent in the Metalore. The secondary fluid inclusions are similar to those in Stage 1.

4.4 FLUID INCLUSION BEHAVIOUR DURING FREEZING AND HEATING

Observations and measurements of fluid inclusions are described below according to one, two or three phase compositions, followed by a discussion of the results of the eutectic, final melting and homogenization temperature data shown in Figures 4-1 through to 4-5.

One Phase Fluid Inclusions - Pre-Ore Event

The inclusions that were most frequently observed and measured were H_2O_{liquid} (Type 1) and $H_2O_{liquid} + S$.

Rapid cooling of Type 1 inclusions to -76°C or lower commonly produced no visible changes in the inclusions compared with their appearance at room temperature. According to Roedder (1984), this behaviour is common in low saline, near-surface aqueous fluids, trapped at near-surface temperatures. It is assumed that the inclusions froze instantaneously to small (less than 2 μm in diameter) single crystals of ice of refractive index near that of water. On warming over a narrow temperature range, melting was observed by a rapid increase in bubble size to its original volume (2-5 μm in diameter).

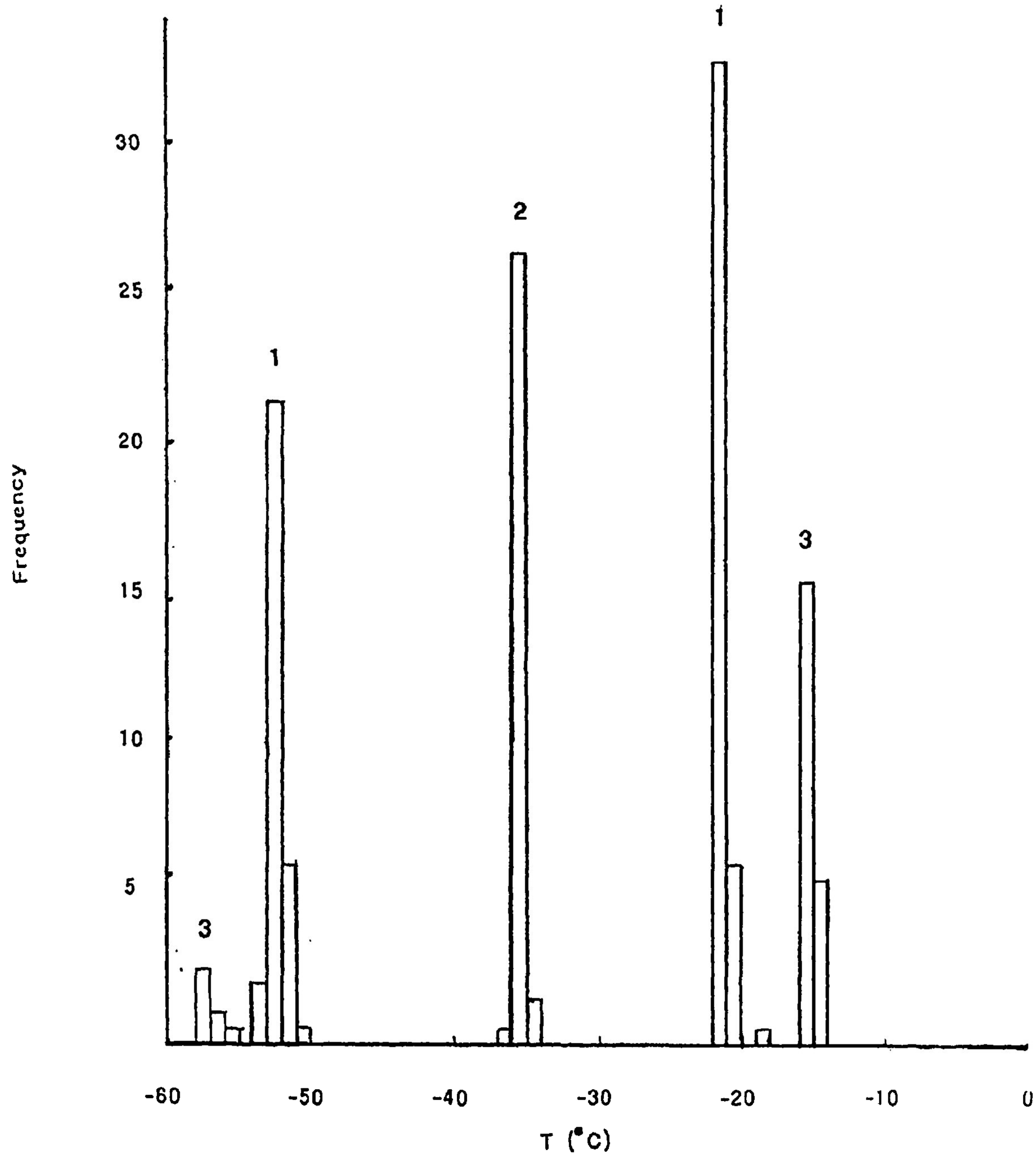

Figure 4-1: Eutectic temperature data from Golden Highway Stages 1, 2 and 3.

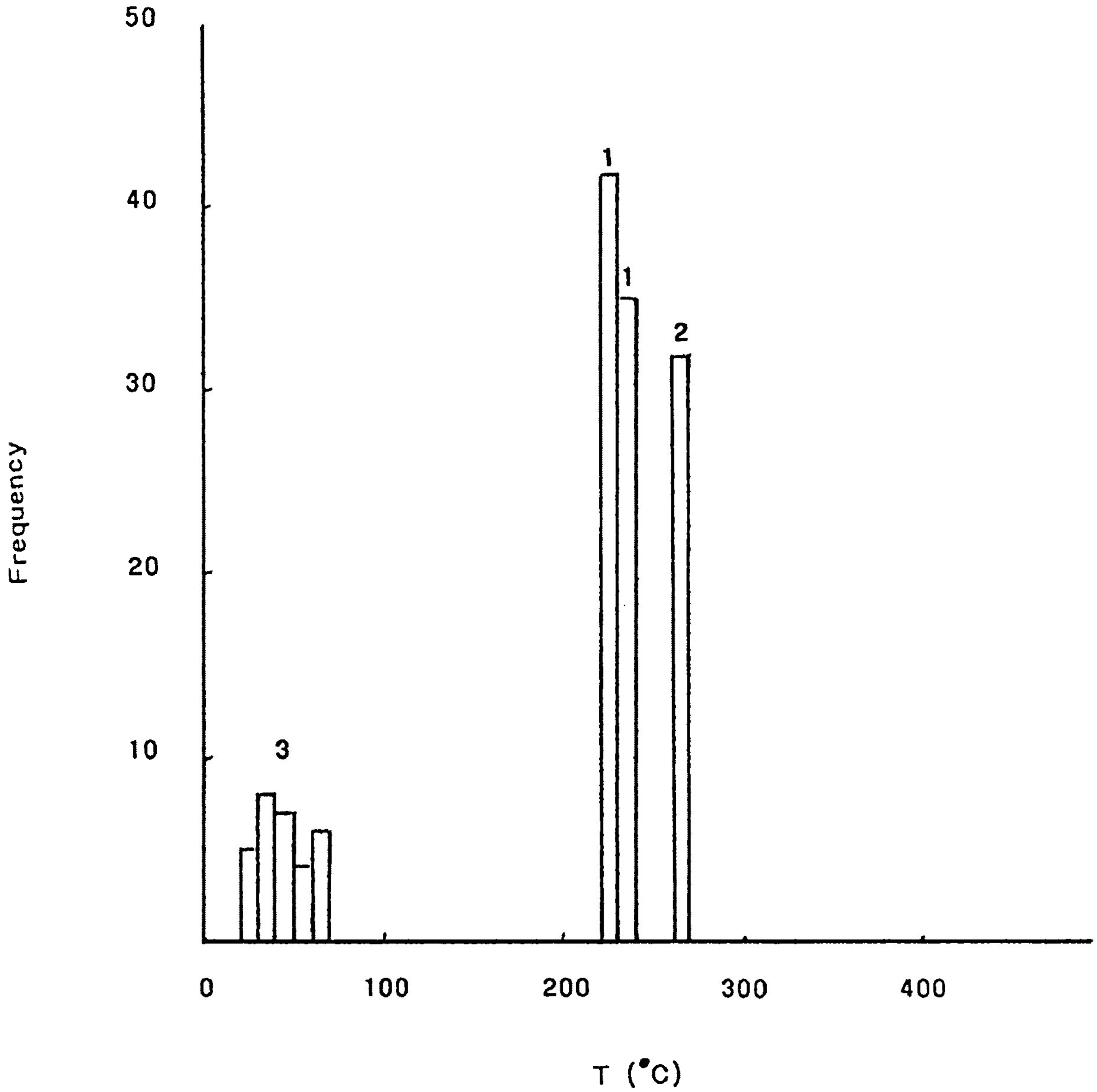

Figure 4-2: Homogenization temperature data from Golden Highway Stages 1, 2 and 3.

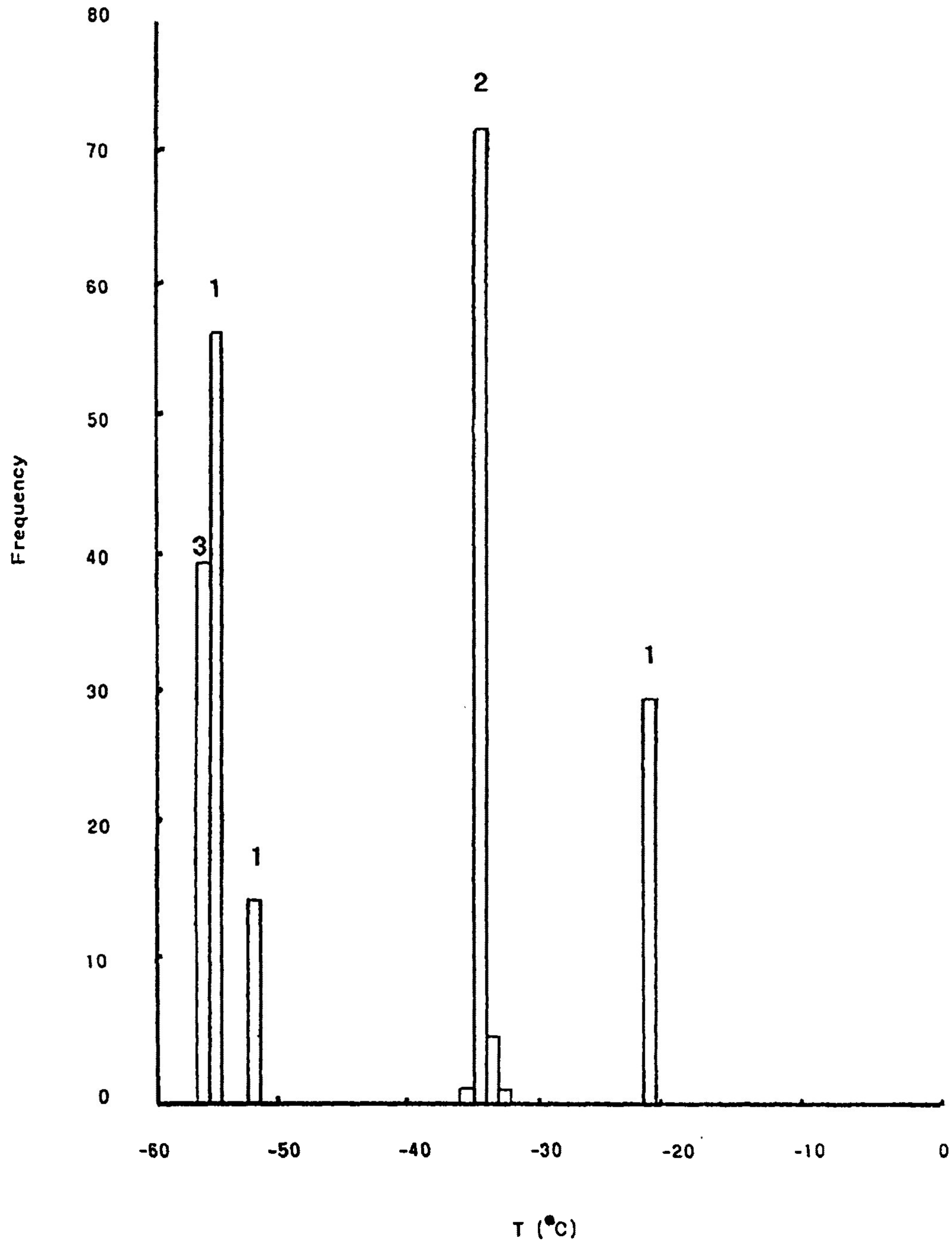

Figure 4-3: Eutectic temperature data from Metalore Stages 1, 2 and 3.

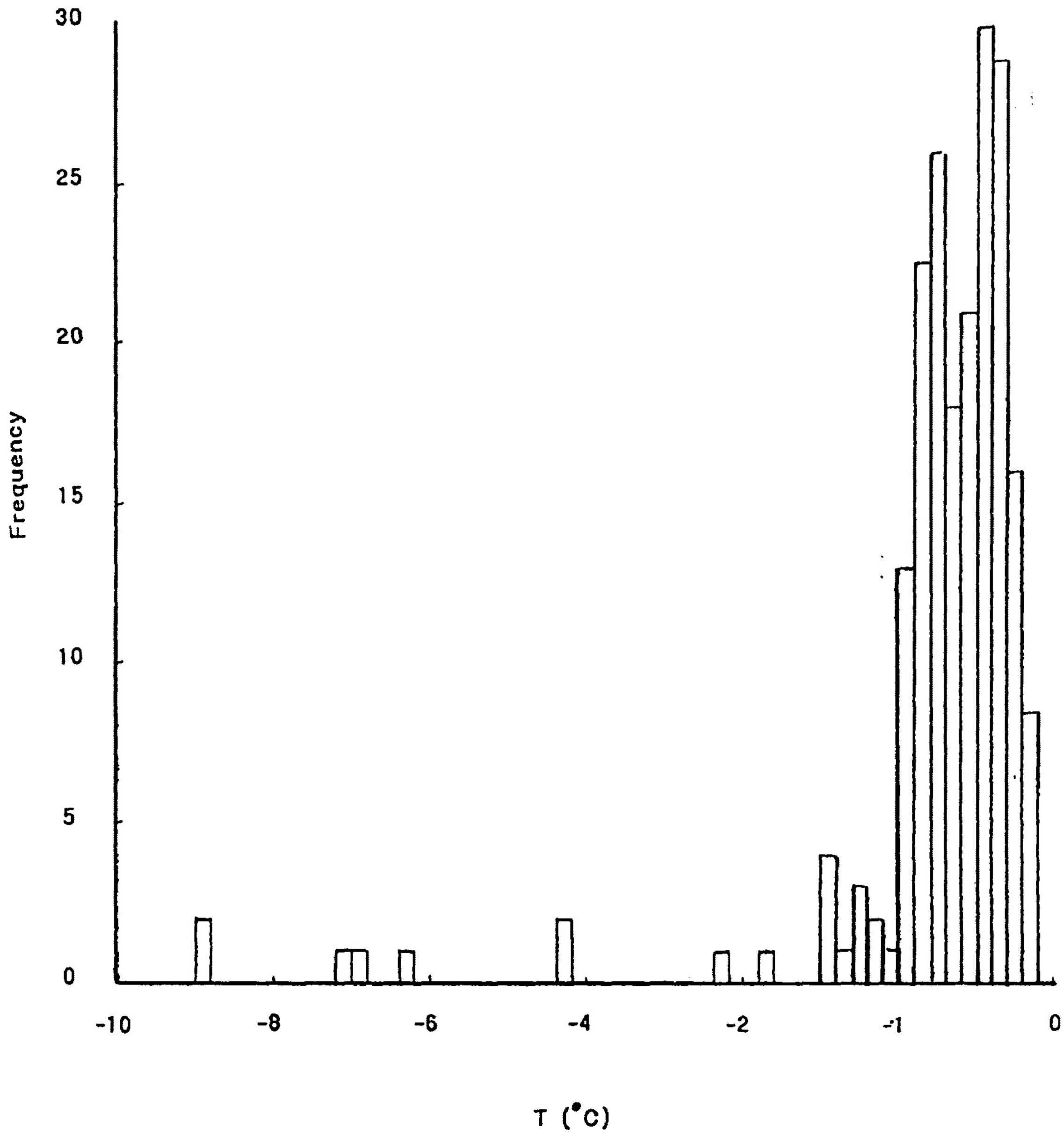

Figure 4-4: Final melting temperature data from Metalore Stages 1, 2 and 3. There are no apparent groups of data for each stage of mineralization.

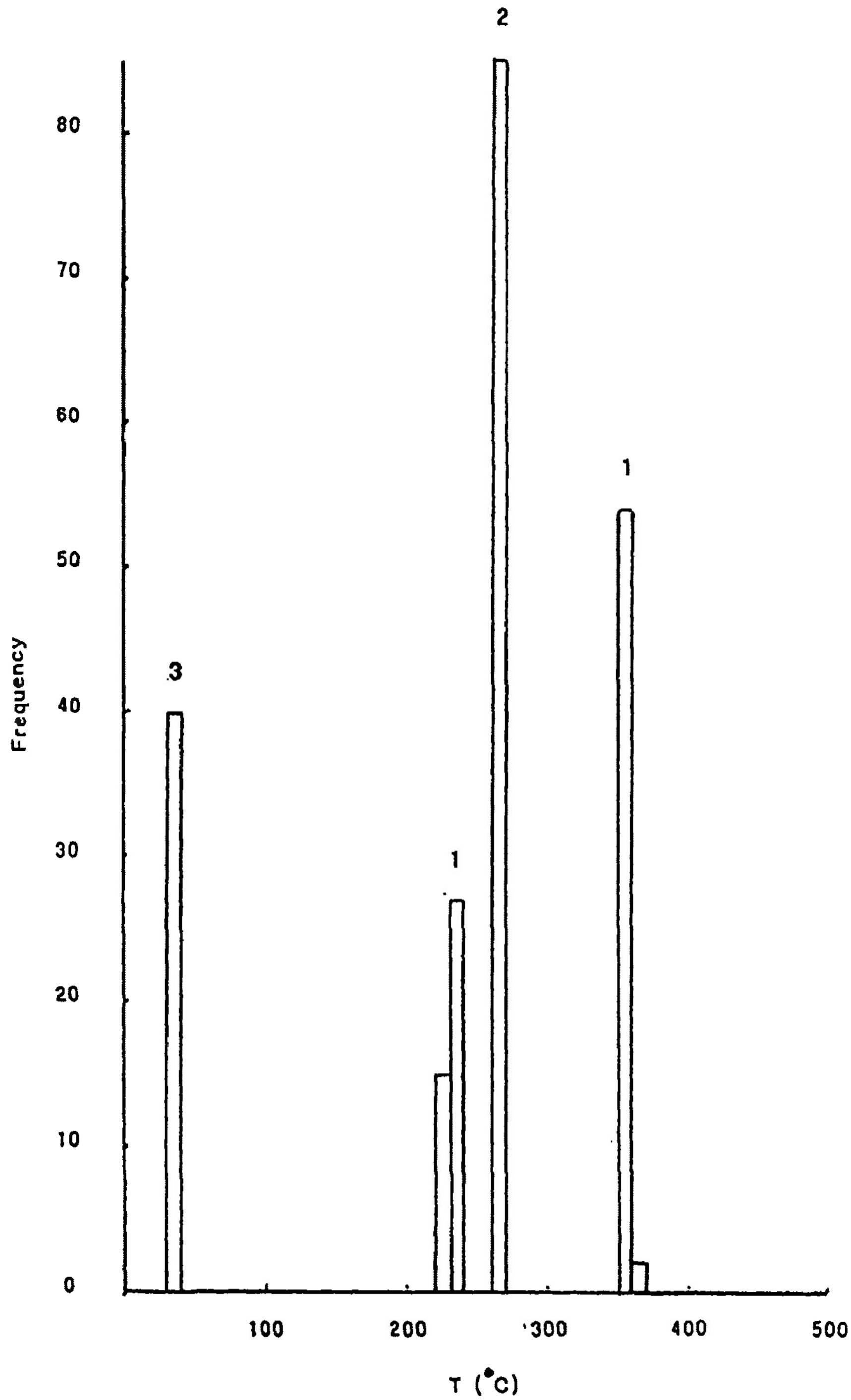

Figure 4-5: Homogenization temperature data from Metalore Stages 1, 2 and 3.

During supercooling of Type 5 inclusions from the Golden Highway, from -74 to -93°C, the liquid were separated from the fluid and condensed on the inclusions walls. During cooling of the fluid inclusions in the Metalore, a gas bubble (2-3 μm in diameter) separated on cooling and grew rapidly (3-5 μm in diameter) with further cooling. Roedder (1984) suggested that CO_2 inclusions behave differently according to whether their densities are greater or less than the critical density of CO_2. During my analysis of the fluid inclusions a second bubble nucleated from either the liquid or vapour phase. Roedder (1984) explained that this occurs in the presence of an additional component. Raman analyses during the study detected the presence of N_2, which may account for the additional component.

Two Phase Fluid Inclusions - Pre- and Post-Ore Events

The inclusions commonly consist of an outer phase of H_2O_{liquid} containing an inner phase bubble of H_2O_{vapour}. The bubble in the H_2O-rich inclusions contracted during rapid cooling and froze between -25 and -60°C. On warming of the frozen inclusions the ice coarsened and was accompanied by an increase of bubble size until they regained their original volume.

Clathrate hydrates were recognized optically as ice-like phases in inclusions. Seitz and Pasteris (1990) describe clathrate hydrates as being ice-like compounds (CO_2-H_2O) consisting of water lattice with cage sites. Gas molecules are partitioned into the cages in varying amounts depending upon the bulk composition, temperature, and density of the system. If the differential partitioning of gases is not considered in microthermometric analysis, errors may result in the determination of gas compositions and bulk density of an inclusion and complications in the interpretation of the microthermometric data. Seitz and Pasteris' (1990) study of clathrate hydrates on a molecular scale have determined that those clathrates melting at approximately 10°C have CO_2 preferentially partitioned into them. Although the melting temperature data of the clathrates measured at 10°C in this study were not corrected, it is assumed that the general composition of the clathrates relative to the bulk fluid is CO_2*5.75H_2O (Roedder, 1963).

Eutectic and homogenization temperatures of the inclusions were recorded and are outlined in the following discussion of the data. Some of the inclusions were heated approximately 15°C above homogenization temperatures, and decrepitation of the inclusions were often observed.

Three Phase Fluid Inclusions - Syn-Ore Event

The outer phase of these inclusions is commonly H_2O-rich with two inner phases that are CO_2-rich in both vapour and liquid. During rapid cooling the inclusions contracted and froze between -64.9 to -94.6°C. On warming of the frozen inclusions, the ice coarsened and was accompanied by an increase in bubble size (approximately 1-2 μm in diameter) until the original volume of the bubble was established (2-4 μm in diameter). These observations were frequently encountered in the Golden Highway inclusions. During warming of the inclusions, the inner phases of CO_2 showed a central vapour phase with a rim of a new liquid phase. Further observations during warming showed an additional smaller vapour bubble being formed inside the original bubble. These observations occurred frequently in the Metalore inclusions. The behaviour of the outer H_2O-rich fluids is similar to that described in the one- and two-phase inclusions. The above observations of fluid inclusion phase behaviour is reflected as distinct groups of microthermometric data.

The eutectic temperature is an estimate of the salt composition in the fluid inclusion representing the eutectic point of the brine trapped in the inclusion during the crystallization of the host mineral (Roedder, 1984). The eutectic temperature was determined at the point indicated by melting and the appearance of the first liquid in the frozen inclusion. The complete eutectic data are provided in Tables 4-1 and 4-2. The data represent different chemical systems of fluid inclusions from different stages in the Golden Highway vein and the Metalore shear. The eutectic temperature in Stage 1 pre-ore event of two vein sets in both the Metalore and Golden Highway discussed earlier have temperature ranges of -22.9 to -21.0°C and -53.4 to -50.1°C. These temperatures represent the eutectics of aqueous NaCl and $CaCl_2$ systems, respectively (Roedder, 1984). The eutectic temperatures between -55.9 to -54.8°C could possibly represent aqueous $FeCl_3$ in the Metalore inclusions. During the mineralizing event, Stage 2, the temperature data occurred between -35.8 and -33.9°C. These data represent fluids of $MgCl_2$ composition occurring some time after the initial vein-forming event of Stage 1. Some fluid inclusions in quartz veinlets (designated as OV and OVA in Tables 4-1 and 4-2) reflect this $MgCl_2$-rich solution composition but are cross-cut by younger veins and veinlets of Stage 3 (designated YV and YVA in Tables 4-1 and 4-2). Stage 3 veins and veinlets indicate temperature ranges between -56.8 to -56.3°C, representing the triple point of the pure CO_2 system at -56°C. Divergent data from the known chemical systems outlined above were obtained from the Golden Highway inclusions. Temperature ranges between -18.6 to -14.1°C were measured from inclusions that probably represent a component of N_2 gases, determined by Raman spectroscopy. Other gases could have been present in the inclusions as minor components but are below the Raman detection limits.

The final melting temperature, as defined by Roedder (1984), is an estimate of the salinity of solution at the time of crystallization. No clusters of final melting temperature data were found but a broad range of temperatures were determined to occur in the inclusions from -8.9 to -0.1°C. The data reflect low salinity conditions during all stages of the mineralizing events. Using the equation developed by Potter (1977) the average salinity of Stage 1 fluids was determined to be 1.77 weight percent NaCl from the Golden Highway data and an average of 1.76 weight percent NaCl from the Metalore data.

The homogenization temperatures of the primary and pseudosecondary fluid inclusions were determined in conjunction with freezing temperature determinations. The majority of the fluid inclusions in the Golden Highway Zone (84%) homogenized to liquid phase, whereas 79% of the inclusions on the Metalore Contact Zone homogenized to vapour phase. The homogenization temperature data correlate with the eutectic data defined as groups representing pre-,syn- and post-ore events. Stage 1 of fluid inclusion temperature ranges from 220.1 to 222.1°C and 229.3 to 231.2°C. A small group of homogenization temperatures in the Metalore Zone occur between 232.2 to 238.1°C and between 354.9 to 364.2°C of which the latter could represent the iron-enriched fluid event in the Metalore Contact Zone. Stage 2 inclusion homogenization data occur at temperatures between 258.3 through to 269.4°C. Stage 3 post-ore event homogenization temperature data range from 32.0 to 32.9°C. The last cluster of data ranged from 21.6 to 66.6°C.

Boiling may have been observed during the analyses of two fluid inclusions located within a 25 μm distance in the same microscopic field of view of the Golden Highway inclusions. On warming of these inclusions, one of the inclusions homogenized to vapour whereas the other to liquid. Evidence of boiling is not conclusive for the Metalore; however, a probable explanation could be that of effervescence of CO_2 from the fluids. The homogenization data of the Metalore during the syn-ore event was determined to occur between temperatures from 258.3 through to 269.4°C. These temperatures according to Roedder's diagram shown as Figure 5-1, occur in a two phase H_2O-CO_2 field along or near the line of critical points. Roedder (1984) explains that on the left side of the locus of critical point curve the homogenization temperatures suggest fluids are dense and would preferentially homogenize to liquid. The majority of the Golden Highway fluid inclusions homogenized to liquid as outlined above. On the right side of the locus of critical point curve, at slightly higher mole percent of CO_2, the fluids preferentially homogenize to vapour. The homogenization data from the Metalore clearly indicate a preference of inclusions to homogenize to vapour. Since, the two phase system of H_2O-CO_2 is associated with very low salinities in this study, then the temperature of homogenization equals the temperature of trapping (lithostatic pressure), therefore, no pressure corrections are required. Effervescence during the auriferous event on the Metalore and likely on the Golden Highway occurred at a minimum pressure of 1,200 bars as shown in Figure 4-6, since the maximum temperature was 268°C.

The results of the microthermometric data reflect discrete mineralizing events of different fluid solution compositions that occurred at different time intervals. The oldest event was Stage 1 that represents a NaCl-$CaCl_2$ system that had been cross-cut by Stage 2 event reflecting a $MgCl_2$ system. The youngest event, Stage 3 represent CO_2 and N_2-rich components. The phenomena of effervescence explains the variation of homogenization phases that were determined in the Golden Highway and Metalore inclusions. Effervescence also suggests that the homogenization temperature of the inclusions is the true temperature of trapping of H_2O-CO_2 phases under very low saline conditions and a minimum pressure of 1,200 bars.

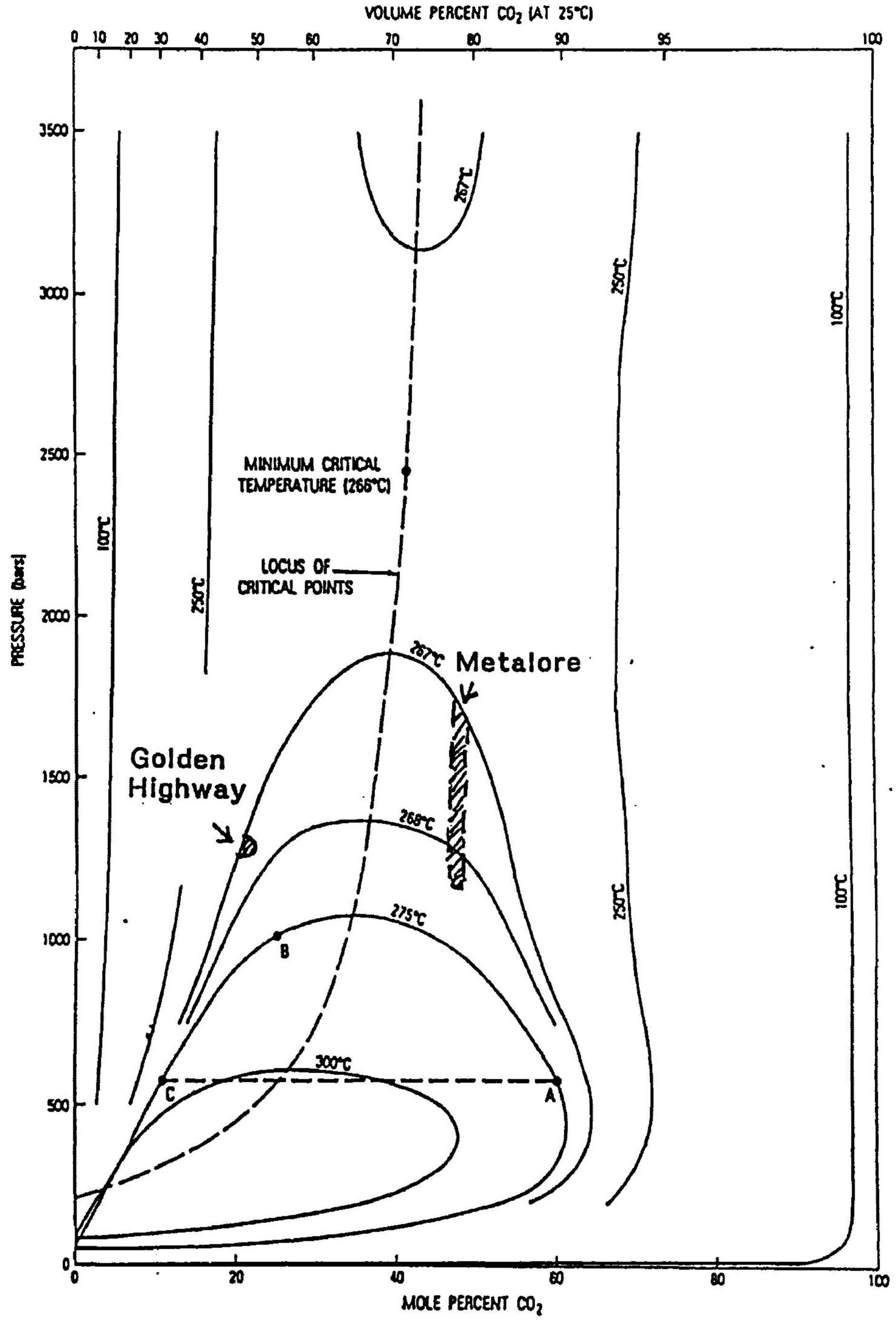

Figure 4-6: P-X plot of isotherms showing compositions of coexisting phases in the system H_2O-CO_2, using data of Todheide and Franck (1963) and Greenwood and Barnes (1966). The upper abscissa shows volume percent CO_2 at 25°C along the CO_2 liquid-vapour curve (64bars), assuming densities of CO_2 liquid, CO_2 vapour, and H_2O liquid of 0.71, 0.24, and 1.0 g/cm^3, respectively (Newitt et al., 1956; Keenan et al., 1969). From Roedder and Bodnar (1980). Homogenization data were plotted with corresponding volume percent CO_2, at 25°C from inclusions of Stage 2 of the Metalore and Golden Highway shown in the shaded areas on the diagram.

CHAPTER 5

Thermochemical Considerations of Ore Deposition

5.1 INTRODUCTION

The characteristic mineral assemblages in the ore and its association with the activity of sulphur are discussed below, followed by a discussion of a proposed fluid source of the Golden Highway and Metalore based on the microthermometric and petrographic data.

5.2 ACTIVITY OF SULPHUR AND TEMPERATURE

The characteristic mineral assemblages in the ores from the Metalore and Golden Highway of the brecciated, ductile and late quartz-carbonate veins of Stages 1, 2 and 3 respectively are:

Stage 1 event Metalore: hematite, pyrite, magnetite, rutile, ilmenite, pyrrhotite.

Stage 1 event Golden Highway: pyrite, pyrrhotite, bornite, chalcopyrite.

Stage 2 event Metalore: pyrite, argentite, silver, gold.

Stage 2 event Golden Highway: pyrite, argentite, silver, gold, bornite, chalcopyrite, molybdenite.

Stage 3 event Metalore and Golden Highway: bornite, pyrite, chalcopyrite (barren of gold and silver).

The estimated temperature and activity changes of sulphur aS_2 for the hydrothermal fluids at the Metalore and

Golden Highway are shown in Figure 5-1. The phase relations in the systems Ag-S, Fe-S, Cu-Fe-S, Fe-O-S, Fe-O-Ti and the equation ΔG (cal)= -4.57561 T log aS_2 (Barton and Skinner, 1979) were used for the calculations, where 4.57561= 2.303R (the gas constant) and T= Temperature in Kelvins. The homogenization temperatures were incorporated into the above equation. Figure 5-1 shows a decrease in the temperature and activity of the sulphur during the pre-ore event, Stage 1, that represents the peripheral alteration region in the Metalore gold-bearing zone. The temperature and log aS_2 values of the Metalore and Golden Highway Stages 1, 2 and 3 are summarized in Table 5-1.

The data of Stage 2 suggest removal of sulphur from solution by sulphidation of wallrocks as the mechanism for the deposition of gold. Gold would preferentially complex over base metals with reduced sulphur ligands at low salinities (NaCl <2wt% ; Weir and Kerrick, 1987) and near neutral pH conditions forming $Au_2(HS)_2S_2$ thio-complex (Seward, 1973). Seward (1973) explained that gold is transported preferentially as thio-complexes in hydrothermal solutions at temperatures of <300°C, whereas silver and lead are preferentially transported as chloride complexes.

Table 5-1: Homogenization temperatures and activity values for the Metalore and Golden Highway Stage 1, 2 and 3 events.

	Temp. (°C)	log aS_2	Controlling Equilibria
Metalore Stage 1	356	-7.2 & -9.0	hem+py,mt, py+mt+rt, ilm
	230 & 220	-14.5 & -15.5	py, po and arg, Ag
Golden Highway Stage 1	230 to 220	-11.0	bn+py,cp
		-14.5 &-15.5	py,po and arg,Ag
Metalore Stage 2	266	-14.0	py,po and arg,Ag
Golden Highway Stage 2	266	-8.1	bn+py,cp
		-11.0	py,po and arg,Ag
Metalore Stage 3	32	-20	bn+py,cp
Golden Highway Stage 3	22 to 66	-20	bn+py,cp

Note to Table 5-1: The abbreviations are (hem) hematite, (py) pyrite, (mt) magnetite, (rt) rutile, (ilm) ilmenite, (po) pyrrhotite, (arg) argentite, Ag (native silver). Secondary stage (bn) bornite and (cp) chalcopyrite also occur in the samples of the Golden Highway and the third stage of the Metalore.

Silver and gold also occur in the Golden Highway vein in conjunction with chalcopyrite, galena and molybdenite suggesting that chloride complexes (Seward 1984, 1986) were involved in the transport for silver, lead and probably copper and molybdenite.

5.3 DISCUSSION OF FLUIDS AND SOURCE

The mineralizing gold reservoir in the Metalore is composed of a complex system of metal cations. Kerrich and Fyfe (1981) described a similar hydrothermal gold ore deposit bearing a complex array of metal cations in an alteration zone. They explained that the alteration zone near a system of gold-bearing quartz carbonate veins contains CO_2, K, Si and Fe, and is depleted in Na with respect to the host rocks. They further explained that gold-bearing veins are enriched with Ca and Mg with respect to the peripheral alteration area of the host rocks. They suggested that in a gold-bearing greenschist facies environment Ca-Fe-Mg-silicates should be out of equilibrium with upward moving metamorphic fluids in a shear zone, resulting in precipitation of carbonates until most of all the CO_2 is removed from the solution.

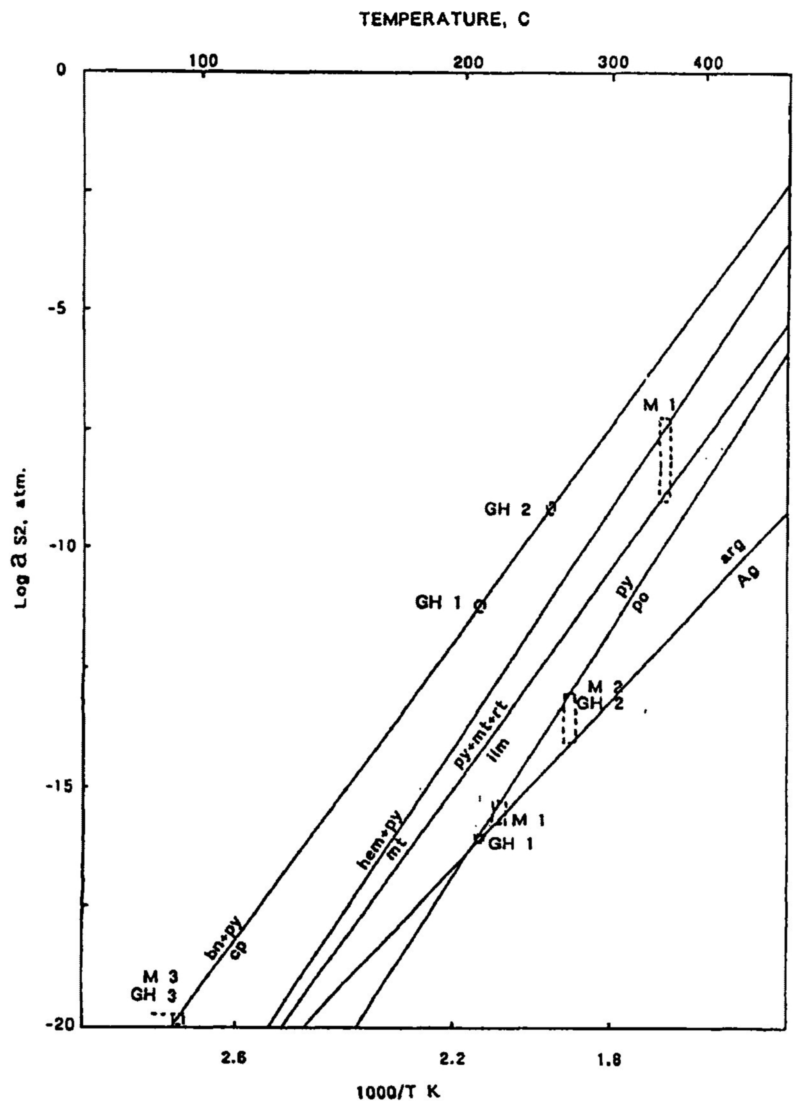

Figure 5-1: Mineral paragenesis, homogenization temperatures and activities for sulphur in the Metalore (M) and Golden Highway (GH) during Stages 1,2 and 3 indicated by M1, M2, M3 and GH1, GH2 and GH3 respectively. The minerals occurring in these stages are hematite (hem), pyrite (py), magnetite (mt), rutile (rt), ilmenite (ilm), argentite (arg), pyrrhotite (po), bornite (bn) and chalcopyrite (cp).

This gold-bearing environment is analogous to the Metalore and Golden Highway wherein elements such as Ca, Mg, Fe, K, combined with CO_2, are the major constituents associated with hydrothermal fluids in the peripheral alteration of the wallrocks. Ankerite, clinochlore and sericite precipitated from the cooling fluids and are the principal minerals that occur in association with silica and gold in Stage 2 of this study. Extensive carbonate-muscovite replacement was observed in the Metalore in cross-cutting relationship with the gold-bearing event. Kerrich and Fyfe (1981) explained that a prerequisite required for extensive carbonate-muscovite replacement is the presence of CO_2 and K in the fluids during prograde metamorphism.

The ore-bearing fluid was determined in this study to have occurred at low salinity <2 wt.% NaCl conditions containing 50 and 80 mole percent CO_2 in the Golden Highway and Metalore, respectively, at low homogenization temperatures of 266°C. These low homogenization temperatures of aqueous inclusions result in CO_2 effervescence from a CO_2-saturated aqueous fluid the fluid is in a region of CO_2-H_2O immiscibility. Pressure and temperature fluctuations at the time of entrapment have a large effect on immiscibility as shown in Figure 5-1. The minimum pressure interpreted from the mole percent CO_2 and homogenization temperature data in this study was 1,200 bars. This figure is in agreement with other analogous studies that have indicated fluids occurring under low saline and pressure conditions (Robert and Kelly, 1987; Leach, Goldfarb and Light, 1986; Clarke and Titley, 1986; DeRonde, 1988a; Kerrick and Fryer, 1979; Read and Meinert, 1986; So and Shelton, 1987; Roedder and Bodnar, 1980). The Metalore and Golden Highway data obtained from the core and petrographic descriptions and the microthermometric study results suggest that metamorphic fluids are the likely fluid source for ore deposition.

Meteroic, connate magmatic and mantle fluids are unlikely fluid sources. Oxygen isotopic studies have indicated meteoric waters mixed of connate origin fluids are typically recorded in modern geothermal systems occurring at higher pressures (1-3kbar) therefore at greater depths (Santosh, 1986; Shelton, Su and Chang, 1988; Thompson, Trippel and Dwelley, 1985; Vikre, 1985; Vlassopoulous and Wood, 1990; Beaty, 1987). Magmatic fluids are an unlikely source since the hypabyssal magmatic fluids must be derived from voluminous granitoid batholith and/or porphyry intrusions in the granitoid-greenstone terrain (Burrows and Spooner, 1987; Coveney, 1981; Konnerup-Madsen, 1979; Wilson and Kyser, 1988). The Metalore and Golden Highway are not spatially associated with this type of intrusion, therefore ruling out magmatic fluid source. Mantle fluids cannot be completely ruled out but are unlikely since the process involves mantle degassing from large tectonic zones in high metamorphic grade terrains (Ahmad, Solomon and Walshe, 1987; Bowers and Helgeson, 1983). Graphite and pyrite unaccompanied by gold are deposited in the regional Paint Lake fault. Carbon in the Metalore and Golden Highway occurs in trace amounts, and therefore, is not a significant part of the gold-bearing process. Instead, gold mineralization is confined to the smaller anastomosing from Paint Lake fault splays such as the Metalore and Golden Highway faults, suggesting that crustal rather than mantle circulation was important for gold deposition. Other studies have indicated similar results for other precious-metal deposits (Colvine, et. al., 1988; Ludden and Hubert, 1986; Macdonald, 1986; Sibson, Robert and Poulsen, 1988; Skinner and Clark, 1991; Smith, Cloke and Kesler, 1984; Smith and Kesler, 1985; Walsh and Kesler, 1988; Devaney and Williams, 1988; Hutchinson and Grauch, 1988; Keays, Ramsay and Groves, 1988). The Metalore and Golden Highway occur in low greenschist facies rocks, and their minerals containing the fluid inclusions are not carbon or methane bearing, therefore supporting a crustal origin for gold deposition.

5.4 CONCLUSIONS

There are a number of studies of fluid inclusion analysis of hydrothermal ore deposits in Archean greenstone terrains (Bursnal, 1989). Multiple generations and compositions of fluid inclusions have been found in precious metal-bearing systems e.g. Studemeister and Kilias, 1987; Touray and Guilhaumou, 1984; Teixweira et al., 1990; Kerrick and Jacobs, 1981; Jacobs and Kerrick, 1981; Hurai, 1992; Hollister and Crawford, 1981; DeRonde, 1988b, Brown, 1989; Brown and Lamb, 1986; Van der Kerhof, 1990. The results from this study have indicated three generations of mineralizing fluids within the alteration zone of the Metalore zone and the quartz-carbonate vein of the Golden Highway were introduced separately at different times and trapped in various sets of fractures. The inclusions selected from the first event were from quartz and carbonate deposition with hematite, chamosite and pyrite. The second event is accompanied by ankerite, clinochlore and gold-bearing silica flooding. The third inclusion-forming event, which is barren of gold and silver, predominates in quartz-carbonate and muscovite-sericite veinlets. Divergent fluid incluison data were obtained in this stage and are believed to be due to the presence of CO_2 and N_2 gases.

The three fluid generations on the Metalore occurred after the emplacement of the diorite intrusion along the conglomerate-volcanic contact, where the Metalore splay fault is located. The three fluid generations in the Golden Highway occur as a fracture-filled quartz carbonate vein on a subsidiary splay fault from the Metalore fault. The composite quartz carbonate vein occurs along the contact with the volcanic-diorite contact with a sliver of conglomerate material occurring within the vein itself. The time of emplacement of the Golden Highway probably occurred simultaneously with, or shortly after the emplacement of the Metalore.

In the Metalore, the gold and silver were probably deposited as a result of destabilization of reduced-sulphur complexes, whereas the chloride-completed base-metals on the Golden Highway remained in solution. Therefore, the genetic models proposed may have involved the production of low saline, H_2O-CO_2 fluids along structures such as the splay faults that had acted as conduits for fluids with suitable compositions for the Metalore and Golden Highway deposits.

REFERENCES

Ahmad, M., Solomon, M. Walshe, J.L., 1987. Mineralogical and Geochemical Studies of the Emperor Gold Telluride Deposit, Fiji: Econ. Geol. v. 82, p. 345-379.

Bailey, S.W., 1987. Chlorites: Structures and Crystal Chem istry: Miner. Soc. of Amer., v. 19, p.169-186.

Barrett, T.J., Fralick, P.W., 1989. Turbidites and iron formations, Beardmore-Geraldton, Ontario: Application of a Combined Ramp/Fan Model to Archaean Clastic and Chemical Sedimentation: Sedimentology, v. 36, p. 221-234.

Barton, P.B., Jr., Skinner, B.J., 1979. Sulfide Mineral Stabilities: in Geochemistry of Hydrothermal Ore Deposits:John Wiley & Sons, Inc., p. 278-403.

Beaty, D.W., Naeser, C.W., Lynch, W.C., 1987. The Origin and Significance of the Strata-Bound, Carbonate-Hosted Gold Deposits at Tennessee Pass, Colorado: Econ. Geol. v. 82, p. 2158-2178.

Blackburn,C.E., Johnson, G.W., Ayers, J., Davis, D.W., 1991. The Wabigoon Subprovince; p. 303-381, In Geology of Ontario, edited by P.C. Thurston, H.R. Williams, R.H. Sutcliff, J.M. Stott. Ontario Geological Survey Special Volume 4 Part 1.

Bowers, T.S., Helgeson, H.C., 1983. Calculation of the thermodynamic and geochemical consequences of nonideal mixing in the system H_2O-CO_2-NaCl on phase relations in geologic systems: metamorphic equilibra at high pressures and temperatures: Amer. Min., v. 68, p. 1059-1075.

Brown, P.E., Lamb, W.M., 1986. Mixing of H_2O-CO_2 in fluid inclusions; Geobarometry and Archean gold depsoits: Geochimica et Cosmochim. Acta, v. 50, p. 847-852.

Brown, P.E., 1989. FLINCOR: A microcomputer program for the reduction and investigation of fluid-inclusion data: Amer. Miner., v. 74, p. 1390-1393.

Burrows, D.R., Spooner, E.T.C., 1987. Generation of a Magmatic H2O-CO2 Fluid Enriched Mo, Au, and W within an Archean Sodic Granodiorite Stock, Mink Lake, Northwestern Ontario: Econ. Geol. v. 82, p. 1931-1957.

Burruss, R.C., 1981. Analysis of Fluid Inclusions: Phase Equilibria at Constant Volume: Amer. J. of Sci., v. 281, p. 1104-1126.

Bursnall, J.T., 1989. Mineralization and Shear Zones: Geological Association of Canada Short Course Notes v. 6.

Clarke, M., Titley, S.R., 1988. Hydrothermal Evolution in the Formation of Silver-gold Veins in the Tayoltita Mine, San Dimas District, Mexico: Econ. Geol. v. 83, p. 1830-1840.

Colvine, A.C., Fyon, J.A., Heather, K.B., Marmont, S., Smith, P.M., Troop, D.G., 1988. Archean Lode Gold Deposits in Ontario: Ministry of Northern Development and Mines and the Ontario Geological Survey Misc. Paper 139, p. 1-136.

Coveney, R.M. Jr., 1981. Gold Quartz Veins and Auriferous Granite at the Oriental Mine, Alleghany District, California: Econ. Geol. v. 78, p. 2176-2199.

DeRonde, C.E.J., 1988a. Hydrothermal Alteration, Stable Isotopes, and Fluid Inclusions of the Golden Cross Epithermal Gold-Silver Deposit, Waihi, New Zealand: Econ. Geol., v. 83, p 895-923.

DeRonde, C.E.J., 1988b. Solubility of the buffer assemblage pyrite+pyrrhotite+magnetite in NaCl solutions from 200-350°C: Geochimica et Cosmochim. Acta, v. 42, p. 1427-1437.

Devaney, J.R., Williams, H., 1988. Evolution of an Archean Subprovince Boundary: A Sedimentological and Structural Study of Part of the Wabgoon-Quetico Boundary in Northern Ontario: Can. J. Earth Sci., v. 26, p. 1013-1026.

Drummond, S.E., Ohmoto, H., 1985. Chemical Evolution and Mineral Deposition in Boiling Hydrothermal Systems: Econ. Geol. v. 80, p. 126-147.

Hollister, L.S., Crawford, M.L., 1981. Short Course in Fluid Inclusions: Applications to Petrology: Miner. Assoc. of

Can..

Hurai, V., 1992. Immiscibility in he system H_2O-CO_2-NaCl: Applications to fluid inclusion thermobarometry: Neues Jahrbuch Miner. Abh. v. 165, p. 5-17.

Hutchinson, R.W., Grauch, R.I., 1988. Historical Perspec tives of Genetic Concepts and Case Histories of Famous Discoveries: Econ. Geol. Mon. 8, p. 1-359.

Jacobs, G.K., Kerrick, D.M., 1981. Methane: An Equation of State with Application to the Ternary System H2O-CO2-CH_4: Geochimica et Cosmochim. Acta, v. 45, p. 607-614.

Keays, R.R., Ramsay, W.R.H., Groves, D.I., 1988. The Geology of Gold Deposits: Econ. Geol. Mon. 6, p. 1-667.

Kerrich, R., Fyfe, W.S., 1981. The Gold-Carbonate Assoc- iation:Source of CO_2, and CO_2 Fixation Reactions in Archean Lode Deposits: Chem Geol., v. 33, p. 265-294.

Kerrich, D.M., Fryer, B.J., 1979. Archaean precious-metal hydrothermal systems, Dome Mine, Abitibi Greenstone Belt. II. REE and oxygen isotope relations: Can. J. Earth Sci., v. 16, p.440-458.

Kerrick, D.M., Jacobs, G.K., 1981. A Modified Redlick-Kwong Equation for H_2O, CO_2, and $H2_2O$-CO_2 Mixtures at Elevated Pressures and Temperatures: Amer. Jour. of Sci., v. 281, p. 735-767.

Konnerup-Madsen, J., 1979. Fluid Inclusions in Quartz from Deep-seated Granitic Intrusions, South Norway: Lithos v.

12, p. 12-23.

Kowalski, B., 1987. The Metalore Gold Discovery: Northern Miner Magazine, v. 204 p. 34-38.

Laird, H.C., 1937. The Western Part of the Sturgeon River Area: Ontario Department of Mines, v. 45, Part II, p. 60-117.

Laird, J., 1987. Chlorites: Metamorphic Petrology: Min. Soc. of Amer., v. 19, p.405-447.

Lawler, J.P., Crawford, M.L., 1983. Stretching of Fluid Inclusions Resulting from a Low-Temperature Microthermometric Technique: Econ. Geol. v. 78, p. 527-533.

Leach, D.L., Goldfarb, R.J., Light, T.D., 1986. Fluid In clusion Constraints on the Genesis of the Alaska-Juneau Gold Deposit: Geoexpo/86 Exploration in the North American Cordillera, p. 150-159.

Long, D.A., 1977. Raman Spectroscopy: McGraw-Hill, Inc..

Ludden, J., Hubert, C., 1986. Geologic Evolution of the Late Archean Abitibi Greenstone Belt of Canada: Geol., v. 14, p. 707-711.

Macdonald, A.J., 1986. Gold '86: Geological Association of Canada and Ministry of Northern Development and Mines and Ontario Geological Survey, p. 1-517.

Mackasey, W.O., 1976. Geology of Dorothea, Sandra and Irwin Townships District of Thunder Bay: Ontario Department of Mines, Government Report No. 122, p. 1-83.

Mason, J. K. and McConnell, C.D., 1983. Gold Mineralization in the Beardmore-Geraldton Area; p. 84-97 in The Geology of Gold in Ontario, edited by A.C. Colvine, Ontario Geological Survey, Misc. Paper 110.

Potter, R.W., 1977. Freezing Point Depression of Aqueous Sodium Chloride Solutions: Sci. Comm. U.S.Geol.Surv., p 284-285.

Poulsen, K.H., 1986. Aurferous Shear Zones with Examples from the Western Shield: Econ. Geol. and Geological Society of Canada, p. 86-103.

Read, J.J., Meinert, L.D., 1986. Gold-Bearing Quartz Vein Mineralization at the Big Hurrah Mine, Seward Peninsula, Alaska: Econ. Geol., v. 81, p. 1760-1774.

Robert, F., Kelly, W.C., 1987. Ore-Forming Fluids in Archean Gold-Bearing Quartz Veins at the Sigma Mine, Abitibi Greenstone Belt, Quebec, Canada: Econ. Geol. v. 82, p. 1464-1482.

Roedder, E., 1962. Studies of Fluid Inclusions I:Low Temperature Application of a Dual-Purpose Freezing and Heating Stage: Econ. Geol., v. 57, p. 1045-1061.

Roedder, E., 1963. Studies of Fluid Inclusions II: Freezing Data and Their Interpretation: Econ. Geol. v. 58, p. 162-211.

Roedder, E., 1984. Fluid Inclusions: Min. Soc. of Amer., v. 12, p. 1-644.

Roedder, E., Bodnar, R.J., 1980. Geologic Pressure Determinations from Fluid Inclusion Studies: Ann. Rev. Earth Nucl. Planet. Sci., v. 8, p 263-301.

Santosh, M., 1986. Ore Fluids in the Auriferous Champion Reef of Kolar, South India: Econ. Geol. v. 81, p. 1546-1552.

Seitz, J.C., Pasteris, J.D., 1990. Theoretical and Practical Aspects of Differential Partitioning of Gases by Clath Clathrate Hydrates in Fluids Inclusions: Geochim. et Cosmochim. Acta, v. 54, p. 631-639.

Seward, T.M., 1973. Thio Complexes of Gold and the Transport of Gold in Hydrothermal Ore Solutions: Geochim. et Cosmochim. Acta, v. 37, p. 379-399.

Seward, T.M., 1984. The Formation of Lead(II) Chloride Complexes to 300C: A Spectrophotmetric Study: Geochim. et Cosmochim. Acta, v. 48, p. 121-134.

Seward, T.M., 1986. The Stability of Chloride Complexes of Silver in Hydrothermal Solutions up to 350°C: Geochim. et Cosmochim. Acta, v. 40, p. 1329-1341.

Shelton, K.L., Sup So, C., Chang, J.S., 1988. Gold-Rich Mesothermal Vein Deposits of the Republic of Korea: Geochemical Studies of the Jungwon Gold Area: Econ. Geol., v. 83, p 1221-1237.

Sherlock, R.L., 1989. A Study of the Third Dimension in the Thunder Bay Silver Veins: Fluid Inclusion and Stable Isotope Results. M.Sc. Thesis, Lakehead University.

Sibson, R.H., Robert, F., Poulsen, K.H., 1988. High-angle Reverse Faults, Fluid-pressure Cycling, and Mesothermal Gold-Quartz Deposits: Geology, v. 16, p. 551-555.

Skinner, B.J., Clark, K.F., 1991. A Special Issue on Application of Hydrothermal Alteration Studies to Mineral Exploration: Econ. Geol., v. 86, p. 461-698.

Smith, T.J., Cloke, P.L., Kesler, S.E., 1984. Geochemistry of Fluid Inclusons from the McIntyre-Hollinger Gold Deposit, Timmins, Ontario, Canada: Econ. Geol. 79, p. 1265-1285.

Smith, T.J., Kesler, S.E., 1985. Relation of Fluid Inclusion Geochemistry to Wallrock Alteration and Lithogeochemical Zonation at the Hollinger-McIntyre Gold Deposit, Timmins, Ontario, Canada: CIM Bulletin, v.78, p. 35-45.

Studemeister, P.A., Killias, S., 1987. Alteration Pattern and Fluid Inclusions of Gold-Bearing Quartz Veins in Archean Trondhjemite near Wawa, Ontario, Canada: Econ. Geol. v. 82, p. 429-439.

So, C.S., Shelton, K.L., 1987. Fluid Inclusion and Stable Isotope Studies of Gold-Silver-Bearing Hydrothermal Vein Deposits, Yeoju Mining District, Republic of Korea: Econ. Geol., v. 82, p 1309-1318.

Swanenberg,H.E.C., 1979. Phase Equilibria in Carbonic Sys tems, and Their Application to Freezing Studies of Fluid Inclusions: Contrib. Miner. Petrol., v.68, p. 303-306.

Teixweira, J.B.G., Kishida, A., Marimon, M.P.C., Xavier, R.P., McReath, I., 1990. The Fazenda Brasileiro Gold Deposit, Bahia: Geology, Hydrothermal Alteraion and Fluid Inclusion Studies: Econ. Geol., v. 85, p. 990-1009.

Thompson, T.B., Trippel, A.D., Dwelley, P.C., 1985. Mineral ized Veins and Breccias of the Cripple Creek District, Colorado: Econ. Geol., v. 80, p 1669-1688.

Touray, J.C., Guilhaumou, N., 1984. Characterization of H2S bearing fluid inclusions: Bull. Min. 107, p. 181-188.

Van den Kerkhof, A.M., 1990. Isochoric phase diagrams in the systems CO2-CH4 and CO2-N2: Application to fluid in clusions: Geochim. et Cosmochim. Acta, v. 54, p. 621-629.

Vikre, P.G., 1985. Precious Metal Vein Systems in the Na- tional District Humboldt County, Nevada: Econ. Geol. v. 80, p. 360-393.

Vlassopoulos, D., Wood, S.A., 1990. Gold speciation in natural waters: I. Solubility and Hydrolysis Reactions of Gold in Aqueous Solution: Geochim. et Cosmochim. Acta, v.54, p. 3-12.

Walsh,J. F, Kesler,S.E., 1988. Fluid Inclusion Geochemistry of High Grade, Vein-Hosted Gold Ore at the Pamour Mine, Porcupine Camp, Ontario: Econ. Geol. v. 83, p. 1347-1367.

Walther, J.V., Wood, B.J., 1986. Fluid-Rock Interactions during Metamorphism: Advances in Phys. Geochem. v. 5, p. 1-218.

Weir, R. H., Jr., Kerrick, D.M., 1987. Mineralogic, Fluid Inclusion, and Stable Isotope Studies of Several Gold Mines in the Mother Lode, Tuolumne and Mariposa Counties, California: Econ. Geol. v. 82, p. 328-344.

Wilson, M.R., Kyser, K., 1988. Geochemistry of Porphyry-Hosted Au-Ag Depsits in the Little Rocky Mountains, Montana: Econ. Geol. v. 83, p. 1329-1346.

APPENDIX I

SAMPLE DESCRIPTIONS OF THE METALORE CONTACT ZONE

Explanation of Terms:

There are 16 diamond drill hole sections descriptions of the Metalore Contact Zone below. From each section of the Metalore Contact Zone the majority of the 4-5 inch core sample were taken at approximately 3-4 foot intervals. The locations of the diamond drill holes described below on the Metalore Contact Zone grid are shown in Figure 2-2.

The descriptions for each of the drill holes begins with a deformed mafic volcanic that progressively becomes sheared and altered beyond recognition. At this point, the polymictic conglomerate is highly deformed and altered and is in transitional contact with the volcanic until towards the end of the zone, where recognizable clasts occur.

B43-1007 Diamond drill hole number B43, core sample taken at 1007 feet.

C/A Core axis was the angle measured between the length of the core sample representing 0° and the foliation.

SAMPLE NUMBER	LOCATION	DESCRIPTION
		DIAMOND DRILL HOLE NUMBER B43
B43-1007	L13+30W 5+10S	The mafic volcanic is sheared and brecciated. The foliation was measured to be 25° to C/A. The minerals that occur throughout the rock are chlorite 50%, ankerite 30%, hematite 10%, quartz 6%, sericite 2% pyrite 1% and less than 1% chalcopyrite. Quartz carbonate veins of different ages from the oldest to youngest were measured to be 25, 52 and 85° to C/A. Pyrite follows the 25° to C/A veinlets and the chalcopyrite follows the veinlets oriented at 85° to C/A. This section of the drill hole assayed 0.13 ounces of gold per ton across 88.0 feet.
B43-1010	L13+30W 5+10S	Fine muscovite-sericite-talc veinlets occur along the foliation measured at 5° to C/A. Pyrite disseminations of 1% occur along the foliation in these veinlets. Quartz carbonate

		veinlets of different ages from oldest to youngest were measured to be 5, 25, 50, and 85° to C/A. Fine disseminations of chalcopyrite less than 1% occurs along the veinlets oriented at 85° to C/A.
B43-1013	L13+30W 5+10S	Similar description as for the B43-1007 above; however, two generations of pyrite occur in the sample. The oldest generation of pyrite occurs as disseminated coarse grains 1mm in diameter and are the youngest generation of pyrite occurs as fine grains less than 1mm in size following the muscovite-sericite-talc veinlets oriented at 25° to C/A.
B43-1017 5+10S	L13+30W 5+10S	The minerals that occur in the sample are ankerite 70%, quartz 20%, chlorite 5%, pyrite 3% and hematite 2%. Muscovite-sericite-talc veinlets occur at 10° to C/A and are associated with the oldest generation of pyrite. These veinlets are cross-cut by younger

		muscovite-sericite-talc veinlets occurring at 26° to C/A with fine-grained pyrite. Chlorite veinlets were measured at 10 and 26° to C/A.
B43-1020	L13+30W 5+10S	Over 80% of the sample is chlorite with minor muscovite-sericite-talc,quartz and other gangue minerals listed above. In the muscovite-sericite-talc veinlets pyrite is less than 1mm in diameter, however, in the chlorite veinlets the pyrite is 1-2mm in diameter. Two generations of chlorite veinlets were measured, the oldest at 5° to C/A and the youngest cross-cutting the previous veinlets at 42° to C/A.
B43-1023	L13+30W 5+10S	Potassium feldspars (3%) occur in quartz (26%). Other minerals in the sample are chlorite (10%), ankerite (60%), pyrite (1%), minor sericite. Pyrite occurs in sericite veinlets and in ankerite that comprise the foliation measured at

		27° to C/A. Quartz veinlets oriented at 85° to C/A displace the sericite veinlets. The quartz veinlets are displaced by another series of sericite and chlorite veinlets void of pyrite oriented at 47° to C/A.
B43-1026	L13+30W 5+10S	Grey silicic alteration (93%) in association with 5% potassium feldspars. Chlorite occurs as 2mm brecciated fragments with associated pyrite (2%).
B43-1029	L13+30W 5+10S	Sericite veinlets (5%) occur with 2% pyrite that are associated with grey silicification and 3% ankerite.
B43-1032	L13+30W 5+10S	In the grey silicification (98%), chlorite and sericite veinlets occur with pyrite (2%). A second series of sericite veinlets and potassium feldspars cross-cut the older veinlets and contain no pyrite.
B43-1035	L13+30W 5+10S	Sericite veinlets (30%) occur along the foliation measured at

		23° to C/A. Fine and coarse pyrite grains are associated with the sericite. Less than 1% chlorite veinlets occur throughout the rock.
B43-1037	L13+30W 5+10S	Hairline quartz veinlets occur throughout the sericite described in the previous samples.The quartz veinlets occur along the foliation measured at 47° to C/A. They are associated with coarse grains of pyrite. The second part of the sample is silicified (78%), with associated sericite (15%), pinkish feldspars (2%) and chlorite veinlets (1%) with associated pyrite (3-4%) occurring as fine disseminations.
B43-1040	L13+30W 5+10S	The rock is silicified (70%) with associated pinkish feldspars (20%) occurring throughout the sample. Chlorite veinlets (9%) with as sociated fine grains of pyrite (1%) occur throughout the rock.
B43-1043	L13+30W	Chlorite veinlets (1%) with

	5+10S	(2%) pyrite occur throughout the sericite fragments and veinlets. The oldest pyrite was measured in veinlets oriented at 27° C/A. The youngest pyrite occurs in the chlorite veinlets that cross-cut the previous veinlets measured at 47° C/A.
B43-1046	L13+30W 5+10S	The foliation of the rock is 25° C/A. Fine and coarse grains of pyrite (2%) occur in chlorite veinlets oriented along the foliation. Potassium feldspars (60%) are dispersed throughout the sample. Sericite veinlets are barren from sulphides.
B43-1049	L13+30W 5+10S	The rock is silicified (60%) with sericite veinlets (20%) occurring throughout. In the sericite veinlets (1%) finely disseminated pyrite was observed.
B43-1052	L13+30W 5+10S	Pyrite occurs in chlorite veinlets (10%) and in sericite veinlets (1%) in the silicified rock.
B43-1055	L13+30W	Ankerite and potassium feldspars

	5+10S	comprise (80%) and sericite (20%) of the sample. No sulphides present.
B43-1060	L13+30W 5+10S	The oldest quartz carbonate veinlets were are 70° C/A. Sericite, chlorite veinlets with pyrite measured at 25° C/A crosscuts the previous quartz carbonate veinlets. The sericite-chlorite veinlets are in turn cross-cut by quartz carbonate veinlets oriented at 74° C/A. These veinlets are in turn cross-cut by another series of quartz-carbonate veinlets oriented at 80° C/A, that are cross-cut by yet another group of quartz-carbonate veinlets measured at 350° C/A.
B43-1062	L13+30W 5+10S	Polymictic conglomerate sample the matrix being mostly chlorite with quartz and clasts comprised of jasper, quartz, granite and mafic volcanics.

DIAMOND DRILL HOLE NUMBER B44

B44-940	L15+30W 5+00S	Brecciated mafic volcanic, where brecciated fragments are sericitic and ankeritic in composition. Fine-grained pyrite, (1%), occurs in chlorite veinlets 30° C/A. This section of the Metalore Contact Zone was assayed for gold and returned values of 0.18 ounces of gold per ton across 41.5 feet in one section. A second section assayed 0.71 ounces of gold per ton across 3.1 feet.
B44-943	L15+30W 5+00S	The minerals in this brecciated mafic volcanic are ankerite (40%), magnetite-ilmenite-specularite veinlets (20%), chlorite veinlets (15%), quartz (5%) and pyrite (1%).
B44-946	L15+30W 5+00S	Chlorite in this sample is mottled with hematite, quartz, ankerite and potassium feldspars. The foliation is defined by the chlorite veinlets that are oriented at 38° C/A. Fine-grained

		disseminated pyrite (1%) occurs in the chlorite veinlets.
B44-949	L15+30W 5+00S	The minerals in this brecciated mafic volcanic are sericite (50%) grey quartz (30%), ankerite (20%) and minor chlorite. Pyrite (5%) occurs in the sericite veinlets oriented at 40° C/A.
B44-958	L15+30W 5+00S	The minerals in this sample are similar to those described in the previous sample. They are seri cite (60%), ankerite (30%), chlorite (1%), pyrite (1%) and other gangue minerals.
B44-961	L15+30W 5+00S	The foliation is 40° C/A in the sample. The minerals that occur in the sample are potassium feldspars (40%), ankerite (30%), sericite (5%), quartz-carbonate veinlets (3%), leucoxene (1%), chlorite (1%), pyrite (1%), ilmenite and specularite (1%).
B44-965	L15+30W 5+00S	The minerals in the sample are potassium feldspars (80%), chlorite veinlets (3%), sericite

		(2%) and pyrite (1%). The pyrite occurs in the chlorite-sericite veinlets.
B44-968	L15+30W 5+00S	Brecciated fragments of chlorite (80%) occur in the mafic volcanic. The other minerals in the sample are a mixture of quartz-ankerite-potassium feldspars (10%), ser icite (1%), ilmenite (1%), pyrite (1%) and other gangue minerals.
B44-971	L15+30W 5+00S	The minerals in the sample are quartz-chlorite intermixed (60%), ankerite (10%), sericite (5%), potassium feldspars (5%) and fine-grained pyrite in sericite veinlets (2%).
B44-974	L15+30W 5+00S	The minerals in the sample are ankerite and potassium feldspars (80%). Sericite veinlets that are barren of sulphides comprise 10% of the sample. Sericite veinlets with pyrite (2%), comprise 5% of the sample. Chlorite, ilmenite, specularite and magnetite total 2% and define the foliation oriented

		at 33° C/A.
B44-977, B44-980, B44-983, B44-986.	L15+30W 5+00S	Same description as sample B44 974.

DIAMOND DRILL HOLE NUMBER B45

B45-917	L17+30W 5+00S	The minerals in the sample are chlorite (90%), quartz carbonate veinlets (7%), pyrite (2%) and argentite (1%).
B45-921	L17+30W 5+00S	Similar description as for sample B45-917.
B45-924	L17+30W 5+00S	The minerals in the sample are ankerite (35%), sericite-muscovite (10%), quartz intermixed with chlorite (10%), specularite (1%),- ilmenite 1%. The oldest quartz carbonate veinlets are oriented at 30° C/A and are cross-cut by younger quartz carbonate veinlets 80° C/A.
B45-927	L17+30W 5+00S	The minerals in the sample are chlorite veinlets and fragments,

		2mm in diameter (40%), sericite veinlets (2%), and a quartz-carbonate-feldspar vein with 1% pyrite cuts the sample. Foliation is 33° to C/A.
B45-930	L17+30W 5+00S	Chlorite veinlets (80%) are around sericite fragments (5%). Three generations of quartz-carbonate veinlets are present. They are oriented from oldest to youngest at 5, 40 and 345° to C/A. The sericite veinlets displace the veinlets oriented at 345°. The sample is void free of sulphides.
B45-933	L17+30W 5+00S	The minerals in the sample are ankerite (50%), sericite (4%), chlorite (2%) and pyrite (2%). The pyrite occurs in the chlorite veinlets that define the foliation measured at 35° to C/A.
B45-934	L17+30W 5+00S	Chlorite dominates the sample (99%) with quartz and pyrite composing the remaining 1%.
B45-941	L17+30W 5+00S	Sericite and chlorite veinlets are mottled with quartz, carbonate and

potassium feldspar fragments that are 2mm in diameter.

DIAMOND DRILL HOLE NUMBER B46

B46-2440	L16+00W 5+00S	Chlorite and quartz (80%) occur as veinlets oriented at 20°C/A. Pyrite (2%) occur in these veinlets. Quartz-carbonate-feldspar veinlets (18%) occur in random order throughout. The Metalore Contact Zone core was assayed and returned a grade of 0.09 ounces of gold per ton across 35 feet.
B46-2443	L16+00W 5+00S	The minerals in the sample are sericite veinlets (65%), ankerite (25%), quartz (5%), pyrite (3%), and minor leucoxene.
B46-2447	L16+00W 5+00S	The oldest quartz carbonate veinlets are 0° to C/A and are cross-cut by leucoxene-chlorite-ankerite-sericite-muscovite veinlets at 15° to C/A. Fine grained pyrite (1%) and coarse grained argentite (2%) occur along

		the 15° foliation. A third stage of quartz carbonate veinlets cross cut the veinlets described above at 67° to C/A. The final stage of quartz-carbonate veinlets are oriented at 20° to C/A.
B46-2450	L16+00W 5+00S	Ankerite, potassium feldspars and hematite (53%) are mottled throughout the sample. Other minerals in the sample are sericite (20%), chlorite (25%), less than 1% coarse-grained chalcopyrite, less than 1/2% argentite, and less than 1/2% pyrite.
B46-2453	L16+00W 5+00S	Minerals in the sample are ank erite (40%), accompanied by sericite veinlets (20%), which define the foliation at 35° to C/A. Other minerals in the sample are quartz (20%) and chlorite (19%). Less than 1% pyrite and argentite occur in association with the sericite veinlets.
B46-2456	L16+00W 5+00S	Chlorite, quartz, potassium feldspars and leucoxene comprise

		99% of the sample.Coarse-grained disseminated pyrite constitutes the remainder of the sample.
B46-2459	L16+00W 5+00S	Ankerite (40%),quartz (40%), and chlorite and quartz (16%) are deformed and define the foliation oriented at 15° to C/A. Uniformly disseminated are 3% pyrite and 1% argentite. One quartz vein oriented at 310° to C/A cross-cuts the sulphides.
B46-2462	L16+00W 5+00S	Chlorite (95%) and leucoxene (3%) throughout the sample. Less than 1% fine-grained pyrite follows the foliation oriented at 5° to C/A and is cross-cut by a quartz vein oriented at 310° to C/A.
B46-2466	L16+00W 5+00S	Ankerite (81%), sericite (15%), pyrite (2%) occurs as dissemin-ations throughout the sample. The minerals are deformed and define the foliation defined at 12° to C/A.
B46-2469	L16+00W 5+00S	The minerals in the sample are ankerite and quartz (80%). The

		principal alteration in the sample is silicification. Pyrite (2%) occurs in sericite veinlets (3%) oriented at 8° to C/A.
B46-2472	L16+00W	Four sets of veinlets cross-cut each other in the sample.The first set of veinlets are sericite-chlorite with associated pyrite, 8° to C/A. The second veinlets are quartz-carbonate oriented at 25° to C/A. The third set of veinlets are quartz-carbonate at 80° to C/A. The fourth set of veinlets are chlorite-sericite oriented at 8° to C/A and parallel to foliation. The other minerals in the sample are ankerite+leucoxene (2%) and fine and coarse-grained pyrite (2%). Fuchsite occurs as a minor mineral.
B46-2475	L16+00W 5+00S	A quartz carbonate vein occurs through the sample. On the walls of the vein chlorite, sericite, potassium feldspars, leucoxene and 2% fine-grained pyrite are the

		minerals surrounding the vein.
B46-2478	L16+00W 5+00S	Ankerite and potassium feld spars (97%) occur with minor sericite veinlets. Sericite also occurs as brecciated fragments with associated 1% fine-grained pyrite. Brecciated fragments of grey quartz and chlorite less than 1mm in diameter occur throughout.
B46-2481	L16+00W 5+00S	Massive chlorite (98%) occurs with wispy sericite and fragments of quartz-carbonate. Less than 1% ankerite and 1% fine grains of pyrite occur throughout. The foliation defined by the sericite minerals is at 21° to C/A. This sample is in sharp contact with sample B46-2478.
B46-2484	L16+00W 5+00S	Ankerite, potassium feldspars and quartz comprise 90% of the sample. Sericite (2%) occurs as veinlets and chlorite (1%) occur as veinlets. Pyrite (1%) is finely disseminated throughout the sample.

B46-2487	L16+00W 5+00S	The minerals that comprise the sample are 48% chlorite and quartz, 48% ankerite and potassium feldspars, sericite (3%) and fine-grained pyrite (1%). The pyrite follows the foliation oriented at 20° to C/A.
B46-2490	L16+00W 5+00S	Veinlets of chlorite and quartz (37%) are associated with 37% ankerite veinlets and 25% sericite veinlets. Ilmenite and magnetite occur within the chlorite and quartz. Fine-grains of pyrite and argentite (1%) occur as disseminations throughout the sample.
B46-2493, B46-2496, B46-2499, B46-2502.	L16+00W 5+00S	Same descriptions as sample B46-2490.
B46-2505	L16+00W 5+00S	Ankerite, quartz and potassium feldspars (82%) are associated with 1% fine grains of pyrite disseminated throughout. Ilmenite, magnetite, pyrite and argen-

		tite veins occur as 15% of the sample.
B46-2508	L16+00W 5+00S	Ilmenite, magnetite and argentite occur as veins and fragments less than 1mm in diameter. Ankerite, quartz and potassium feldspars are associated with veinlets of sericite. Pyrite (3%) occurs as fine disseminations throughout the sample.
B46-2511	L16+00W 5+00S	Ankerite, quartz and potassium feldspars occur throughout the sample. Fine grains of pyrite (3%) occur in chlorite veinlets.
B46-2512	L16+00W 5+00S	Chlorite and fragments of grey quartz occur throughout the sample. A 1.25cm wide quartz vein cross-cuts the chlorite and marks the contact with the polymictic conglomerate. Sericite veinlets with associated pyrite occur as minor minerals.
B46-2513	L16+00W 5+00S	Potassium feldspars are altered to sericite are cross-cut by quartz-carbonate veinlets. The foliation

is 10° to C/A.

DIAMOND DRILL HOLE NUMBER B47

B47-954	L11+35W 5+35S	Quartz-carbonate and potassium feldspar veinlets are 300° to C/A. These veinlets are barren of sulphides. A second stage of veinlets that are chloritic in composition are at 15° to C/A and are associated with 5% fine and coarse grains of pyrite. The Metalore Contact Zone was assayed and returned a grade of 0.05 ounces of gold per ton across 91 feet along the core length.
B47-957	L11+35W 5+35S	Chlorite (58%) and ankerite (30%) are veinlets oriented at 5° to C/A. Sericite (10%) veinlets and is associated with 2% coarse-grained pyrite. Two sets of quartz-carbonate veins cross-cut the chlorite and ankerite veinlets at 15° to C/A. The younger quartz-carbonate veinlets cross-cut the sericite veinlets at

		290°to C/A.
B47-960	L11+35W 5+35S	The minerals in the sample are ankerite (80%), chlorite (17%), sericite (2%) and fine and coarse grains of pyrite (1%).
B47-963	L11+35W 5+35S	The minerals in the sample are hematite and ankerite (96%), quartz-carbonate veinlets (3%) with associated 1% fine-grained disseminated pyrite.
B47-970	L11+35W 5+35S	The minerals in the sample are ankerite (90%), sericite veinlets (5%), quartz fragments (2%) and fine grains of pyrite (2%). The sericite veinlets occur along the foliation at 15° to C/A.
B47-973	L11+35W 5+35S	The minerals in the sample are ankerite and potassium feldspars (73%), chlorite (30%) and sericite (3%) and 1% fine grained pyrite disseminated throughout. The veinlets occur along the foliation at 15° to the C/A. Cross-cutting the foliation are ilmenite, magnetite, specularite and argen-

		tite veinlets oriented at 38° to C/A. These late stage veinlets are in turn cross-cut by sericite veinlets at 10°to C/A.
B47-976	L11+35W 5+35S	Ankerite is the major mineral in sample (95%). Chlorite-quartz, ilmenite-specularite-magnetite-argentite veinlets (3%) occur along the foliation at 17° to C/A. Associated with the veinlets are fine grains of pyrite (1%). A second stage of veinlets, comprised of sericite and muscovite are barren of sulphides and are oriented at 5° to C/A.
B47-979	L11+35W 5+35S	The minerals in the sample are ankerite (80%), sericite (10%), chlorite (2%) and fine-grained disseminated pyrite (5%). Quartz, carbonate and potassium feldspars occur as brecciated fragments. The ankerite and other associated minerals occur along the foliation at 13° to C/A. The quartz, carbonate and potassium feldspar brecciated

		fragments occur along veinlets that cross-cut the ankerite and other minerals at 85° to C/A.
B47-985	L11+35W 5+35S	The sample is dominated by 90% ankerite. Fine and coarse grains of pyrite occurr in a 0.5 cm wide quartz carbonate vein that comprises the remainder of the sample.
B47-1041	L11+35W 5+35S	Chlorite dominates the sample (90%) with four generations of quartz, carbonate and sericite veinlets cross-cutting each other. The oldest to youngest veinlets are at 5, 340, 75, and 7° to C/A, respectively.
B47-1044	L11+35W 5+35S	Ankerite with associated 2% fine-grained pyrite occurs with 1mm sericite veinlets. Cross-cutting the veinlets are quartz veinlets oriented at 80° to C/A. A second stage of veinlets is comprised of chlorite and sericite with associated 2% fine-grained pyrite. These veinlets are cross-cut by

		magnetite-ilmenite-specularite-argentite-quartz veinlets oriented at 63° to C/A. The last stage of veinlets is sericite and chlorite veinlets that are barren of sulphides, however, they cross-cut all of the preceding veins.
B47-1050	L11+35W 5+35S	The major mineral in the sample is ankerite cut by sericite veinlets. The other minerals in the sample are potassium feldspars and a mixture of chlorite, quartz, specularite, magnetite, argentite and sericite veinlets. Pyrite occurs as fine disseminations (1%) and also is associated with the sericite veinlets.
B47-1053	L11+35W 5+35S	Ankerite occurs with chlorite and sericite veinlets. Quartz-carbon ate veinlets from from sulphides, are cross-cut by specularite-ilmenite-magnetite veinlets. Less than 1% pyrite and hematite occur in the sample.
B47-1054	L11+35W	Sericite, chlorite and potassium

	5+35S	feldspars free from sulphides are all cross-cut by veinlets of chlorite, specularite oriented at 60° to C/A. A second stage of sericite veinlets cross-cut the chlorite specularite veinlets. These latter sericite veinlets define the foliation and are at 35° to C/A.
B47-1058	L11+35W 5+35S	One half of the sample is ankerite and the other is quartz, carbon ate and feldspar. Cross-cutting the sample are sericite-chlorite veinlets with associated fine grains of pyrite that occur along the foliation at 5° to C/A.
B47-1061	L11+35W 5+35S	Remnant veinlets of chlorite occur as wisps with associated fine grains of pyrite.These are cross-cut by quartz-carbonate-feldspar veinlets. These veinlets are in turn cross-cut by sericite-muscovite veinlets.
B47-1064	L11+35W 5+35S	Same description as for sample 1061; however, chlorite and pyrite

		occur as minor minerals.
B47-1067	L11+35W 5+35S	Fragments of quartz, carbonate, potassium feldspars, pyrite, sericite and chlorite veinlets are oriented at 27° to C/A and are cross-cut by sericite-muscovite veinlets oriented at 15° to C/A. The latter veinlets are barren of sulphides.
B47-1070	L11+35W 5+35S	Quartz, carbonate and potassium feldspars comprise 80% of the sample. The feldspars are par tially altered to sericite with associated fine grains of pyrite. A second generation of sericite veinlets with muscovite cross-cuts the sericite veinlets.
B47-1073	L11+35W 5+35S	The minerals in the sample are quartz, carbonate, potassium feldspars, ankerite and sericite veinlets. Cross-cutting these minerals are sericite-muscovite veinlets oriented between 0 and 5° to C/A. These veinlets are asso ciated with chlorite, specularite,

		ilmenite and magnetite.
B47-1076	L11+35W 5+35S	Similar description as for sample B47-1073 with the sericite-musco vite veinlets cross-cut by chlorite-specularite veinlets at 90° to C/A. Less than 1% fine disseminations of pyrite occur throughout the sample.
B47-1079	L11+35W 5+35S	Similar descriptions as for sample B47-1073 with alterations of feldspars to sericite. Pyrite is finely disseminated throughout. Overprinting these minerals are veinlets of sericite, muscovite and chlorite.
B47-1082	L11+35W 5+35S	Ankerite (90%) occurs with quartz-carbonate-feldspar veinlets that are cross-cut by sericite-musco-vite veinlets. Minor chlorite veinlets and pyrite occur in the sample.
B47-1085	L11+35W 5+35S	Quartz-ankerite-feldspars (90%) occur with sericite veinlets (8%) and less than 1% chlorite veinlets and minor pyrite.

B47-1088	L11+35W 5+35S	Same description as sample B47-1085.
B47-1092	L11+35W 5+35S	Polymictic conglomerate with fragments of sericite, chlorite, quartz, feldspar, jasper and other detrital fragments occur through out the sample. Other detrital fragments that are altered to chlorite occur in the sample.

DIAMOND DRILL HOLE NUMBER B48

B48-529	L16+00W 3+50S	The minerals in the sample are ankerite (65%), quartz (20%), sericite (5%), chlorite (5%) and feldspars (3%). There are two generations of chlorite veinlets, the first oriented at 25° to C/A with associated 2% fine-grained pyrite. The second generation of chlorite veinlets are at 31° to C/A and are barren of sulphides. The drill core section of the Metalore Contact Zone was assayed and returned grades of 0.31 ounces of gold per ton across 16 feet.

B48-546	L16+00W 3+50S	Abrupt change from the sample described above. Chlorite domi nates the sample (80%) with quartz-carbonate-feldspar veinlets cutting the sample. Massive veinlets of specularite and feld spar occur in the sample. Seri-cite veinlets 1mm in width occur with recrystallized black quartz fragments. The sericite veinlets are oriented at 40° to C/A.
B48-549	L16+00W 3+50S	Ankerite (40%) is mottled with sericite-muscovite-chlorite veinlets (30%), and with specu larite veinlets (4%) with associ-ated 1% coarse grains of pyrite.
B48-552	L16+00W 3+50S	Ankerite (60%) is brecciated, and specularite-ilmenite veinlets (15%) are also brecciated. Qu-artzfragments (10%) are recrystallized 10% and are associ-ated with chlorite (4%) and minor pyrite.
B48-555	L16+00W 3+50S	The minerals in the sample are sericite, muscovite, potassium

		feldspar and quartz comprising 80 % of the sample. The min erals occur along the foliation at 43° to C/A. Quartz veinlets (15%) and specularite ilmenite veinlets (3%) occur randomly throughout the sample.
B48-558	L16+00W 3+50S	The sample is similar to sample 555; however, one grey recrystallized quartz vein 2.5 cm wide occurs in the sample. Asso ciated with the vein is chlorite and 5% pyrite.
B48-561	L16+00W 3+50S	The sample is brecciated with fragments of ankerite (80%) chlorite (15%) and quartz (1%). A foliation was defined at 25° to C/A with associated 2% fine-grained pyrite. Specularite and ilmenite veinlets (2%) occur ran-domly throughout the sample.
B48-564 B48-567	L16+00W 3+50S	Same description as B48-561.
B48-570	L16+00W 3+50S	Ankerite and hematite are inter mixed with veinlets of sericite-

		muscovite (90%). The sericite-muscovite veinlets occur along a foliation at 37° to C/A. Late quartz-carbonate veinlets (1%) occur randomly with fine grains of pyrite.
B48-573	L16+00W 3+50S	Same description as B48-570.
B48-576	L16+00W 3+50S	Sericite-muscovite veinlets with associated pyrite follow the foliation at 42° to C/A. Ankerite and black quartz eyes occurs among chlorite-ilmenite-specularite-magnetite veinlets.
B48-579	L16+00W 3+50S	The sample is brecciated with fragments of sericite, muscovite, quartz, carbonate, specularite, ilmenite and magnetite. Pyrite occurs in trace amounts.
B48-581	L16+00W 3+50S	The sample is vuggy owing to the presence of calcite. Less than 1% pyrite occurs in sericite-ankerite veinlets.
B48-584	L16+00W 3+50S	One vuggy quartz-carbonate veinlet is 0.5cm in width and

		follows the foliation at 45°to C/A. The vein is mineralized with 5% fine grains of pyrite.
B48-587	L16+00W 3+50S	Ankerite, hematite and grey quartz occur between veinlets of chlorite that occur along the foliation at 30° to C/A. Pyrite (5%) occurs in the chlorite veinlets.
B48-590	L16+00W 3+50S	Ankerite and hematite are associ ated with veinlets of sericite and muscovite. The foliation is defined by the sericite-muscovite veinlets at 30° to C/A. These veinlets are associated with 1% pyrite. Cross-cutting the veinlets are chlorite-specularite-magnetite veinlets oriented at 320° to C/A with less than 1% as-sociated chalcopyrite.
B48-593	L16+00W 3+50S	Sericite-muscovite-carbonate veinlets occur along the foliation at 40° to C/A. They are associ ated with smoky quartz and chlorite veinlets that have 2% fine-grained pyrite.

B48-596	L16+00W 3+50S	Sericite, muscovite and ankerite occur as massive veins that are deformed along a foliation at 33° to C/A. Associated with these minerals are quartz and leucoxene that occur as fine fragments disseminated throughout the sample. Minor veinlets of chlorite, specularite, ilmenite, magnetite and pyrite occur in the sample.
B48-599 B48-602	L16+00W 3+50S	Same description as B48-596.
B48-605	L16+00W 3+50S	Same description as B48-596 except quartz and carbonate predominate in the sample (85%) with an associated chlorite veinlet with pyrite less than 1mm in width. Otherwise, the sample is devoid of sulphides and chlorite.
B48-608	L16+00W 3+50S	Black quartz is brecciated mottled with white quartz and carbonate.

DIAMOND DRILL HOLE NUMBER B49

B49-507	L21+00W	Chlorite is the major mineral in

	3+23S	sample and is deformed and follows the foliation at 25° to C/A. One 1mm wide quartz veinlet with associated pyrite occurs in the sample. Leucoxene (3%) occurs as disseminations in the sample. Another quartz-carbonate veinlet cross-cuts the foliation at 330° to C/A and is barren of sulphides. The core was assayed through the Metalore Contact Zone and yielded 0.11 ounces of gold per ton across 3.3 feet and another section of the core assayed 0.09 ounces of gold per ton across 4.9 feet.
B49-512	L21+00W 3+23S	The minerals in the sample are ankerite (77%), sericite (20%), minor chlorite veinlets with associated 2% pyrite occurring along the walls of the veinlets. Specularite and ilmenite veinlets 1% occur randomly in the sample.
B49-515	L21+00W 3+23S	The minerals in the sample are quartz and ankerite with sericite-chlorite veinlets with pyrite,

		following the foliation at 35° to C/A. Cross-cutting the foliation are quartz-carbonate veinlets rimmed with specularite oriented at 334° to C/A.
B49-520	L21+00W 3+23S	Textures of sample B49-515 are visible with sericite-muscovite-mariposite veinlets with pyrite following the foliation at 35° to C/A.
B49-523	L21+00W 3+23S	The minerals ankerite, chlorite and sericite are brecciated with hairline veinlets of chlorite and specularite occurring randomly throughout the sample. Pyrite occurs as disseminations (5%) th-roughout the sample.
B49-526	L21+00W 3+23S	The minerals in the sample are ankerite, sericite and chlorite that are barren of sulphides and occur along a foliation at 35° to C/A. One quartz carbonate veinlet 2mm in wide has pyrite along the walls only.
B49-532	L21+00W	Same description as B49-515. The

	3+23S	foliation is 40° to C/A.
B49-535	L21+00W 3+23S	Same description as B49-535 with the foliation at 25° to C/A. Quartz-carbonate veinlets cross-cut the foliation at 355° to C/A.
B49-538	L21+00W 3+23S	The minerals in the sample are quartz (80%), sericite-chlorite veinlets (10%), ankerite (5%) and pyrite (5%) occurring along the foliation at 25° to C/A.
B49-542	L21+00W 3+23S	Same description as B49-538. The foliation was at 25° to C/A.
B49-545	L21+00W 3+23S	Sericite-chlorite veinlets are brecciated and intermixed with quartz, carbonate, and feldspars.
B49-552	L21+00W 3+23S	The minerals sericite and muscovite follow the foliation at 28° to C/A. Ankerite is associated with finely disseminated pyrite. Specularite veinlets cross-cut the foliation at 80° to C/A.
B49-555	L21+00W 3+23S	Same description as B49-552, except that specularite veinlets are oriented at 355° to C/A.
B49-558	L21+00W	Mottled quartz, ankerite, chlorite

	3+23S	and sericite are comprise 98% of the sample. The sample is deformed, and the foliation is 40° to C/A. Pyrite and leucoxene (2%) are finely disseminated throughout the sample.
B49-561	L21+00W 3+23S	The major mineral in the sample is chlorite comprising 80%. The remainder of the minerals are quartz, ankerite and sericite. Pyrite occurs in trace amounts. The foliation is 45° to C/A.
B49-564	L21+00W 3+23S	Ankerite constitutes 85% of the sample with sericite-muscovite veinlets (12%) occurring through out. Leucoxene overprints the ankerite, sericite and muscovite. Pyrite is minor in the sample and occurs in quartz-chlorite veinlets oriented at 30° to C/A.
B49-567	L21+00W 3+23S	Chlorite (60%) is intermixed with minerals as described in sample
B4-564		Leucoxene (3%) is disseminated throughout. The foliation is 30° to C/A.

B49-570	L21+00W 3+23S	Same description as B49-564. The foliation is 30° to C/A. Cross-cutting the foliation is one quartz carbonate vein that is at 350° to C/A.
B49-573 B49-576	L21+00W 3+23S	This sample is barren of sulphides and is similar to sample B49-564.
B49-579	L21+00W 3+23S	The minerals that comprise the sample are ankerite (50%), chlorite and specularite veinlets (49%) and minor quartz.
B49-581	L21+00W 3+23S	The minerals in the sample are ankerite (60%), chlorite and specularite veinlets (20%), seri cite (19%) and pyrite (1%).
B49-585	L21+00W 3+23S	The minerals in the sample are ankerite and muscovite (90%), sericite (7%), chlorite and specularite veinlets (2%) and minor pyrite. The foliation is 35° to C/A.
B49-589	L21+00W 3+23S	The minerals in the sample are ankerite and potassium feldspars (70%), sericite (23%), quartz-car

		bonate veinlets (5%), chlorite-specularite veinlets (1%) and pyrite (1%) in the sericite veinlets. The foliation is 38° to C/A.
B49-595	L21+00W 3+23S	Mottled quartz-carbonate-specularite veinlets with less than 1% fine-grained pyrite disseminated throughout. The foliation is 38° to C/A.
B49-598	L21+00W 3+23S	The foliation is 35° to C/A. The minerals ankerite, sericite, muscovite and chlorite all follow the foliation. Two sets of veinlets cross-cut the foliation. The first are chlorite veinlets that are oriented at 26° to C/A and the second are quartz-carbonate veinlets oriented at 85° to C/A.
B49-601	L21+00W 3+23S	The sample is barren of sulphides. Ankerite, sericite, musco vite and chlorite veinlets follow the foliation at 40° to C/A.
B49-604	L21+00W	Same description as B49-601;

	3+23S	however, the foliation is measured at 22° to C/A.
B49-607	L21+00W	Same description as B4-601;
B49-610	3+23S	the foliation is 30° to C/A.
B49-613	L21+00W 3+23S	Same description as B49-601; however, the foliation was is 34° to C/A.
B49-617	L21+00W 3+23S	Chlorite (60%), quartz-carbonate (20%), muscovite and potassium feldspars (17%), and pyrite (2%) follow the foliation is 30° to C/A.
B49-620	L21+00W 3+23S	Fragments of jasper, sericite, and quartz occur in a matrix of chlorite in the conglomerate. Leucoxene occurs disseminated thr-oughout. The foliation is 25° to C/A.
B49-622	L21+00W 3+23S	Quartz is mottled with ankerite in the sample. Sericite veinlets follow the foliation at 42° to C/A. Pyrite (5%) occurs as fine disseminations throughout the quartz-rich sample.
B49-623	L21+00W	Polymictic conglomerate with

	3+23S	detrital grains of quartz, jasper, and granite 1mm in diameter. Less than 1% pyrite disseminated thr-oughout the sample.

DIAMOND DRILL HOLE NUMBER B50

B50-1297	L11+35W 6+30S	Mafic volcanic rock with chlorite as the major mineral and minor amounts of ankerite, quartz, feld-spars, leucoxene and pyrite. The Metalore Contact Zone was assayed and returned three intersections of gold of 0.06 ounces per ton across 18 feet, 0.13 ounces per ton across 3 feet and 0.17 ounces per ton across 15 feet.
B50-1303	L11+35W 6+30S	The sample is brecciated with fragments of ankerite, chlorite, specularite, magnetite and ilmen ite. The brecciation is cross-cut by hairline quartz-carbonate veinlets, that are in turn, cross-cut by veinlets of pyrite and chalcopyrite.
B50-1306	L11+35W	The sample is foliated with

	6+30S	chlorite veinlets intermixed with ankerite, sericite and less than 1% pyrite.
B50-1309	L11+35W 6+30S	The minerals in the sample are chlorite (86%), translucent quartz (10%), ankerite (2%), sericite (1%) and leucoxene and pyrite (1%) disseminated throughout.
B50-1312	L11+35W 6+30S	The sample is brecciated with fragments of ankerite (85%), chlorite (5%), sericite (3%), quartz (2%) and fine grains of pyrite following the foliation at 30° to C/A. Specularite, magnetite and ilmenite occur randomly throughout the sample.
B50-1315 B50-1318	L11+35W 6+30S	Same description as B50-1312.
B50-1321	L11+35W 6+30S	Abrupt change to a chlorite-rich sample 95% with minor amounts of ankerite, potassium feldspars, quartz and pyrite. The foliation is 18° to C/A.
B50-1324	L11+35W 6+30S	Same description as B50-1312 with textures of B50-1321. One quartz-

		carbonate vein shows crack-seal texture with pyrite occurring along the walls of the vein.
B50-1327	L11+35W 6+30S	The sample is brecciated with ankerite, chlorite and quartz fragments.
B50-1330	L11+35W 6+30S	Same description as for sample B50-1312.
B50-1333 B50-1336	L11+35W 6+30S	Same descriptions as for sample B50-1321.
B50-1342 B50-1345	L11+35W 6+30S	The determined foliation is 13° to C/A. The minerals that follow the foliation are chlorite comprising 80% of the sample, ankerite and quartz (19%) and less than 1% sericite and pyrite.
B50-1348	L11+35W 6+30S	Chlorite is the major mineral (90%) with ankerite (5%) compris ing the remainder of the sample. The foliation is 10° to C/A.
B50-1351	L11+35W 6+30S	Smoky quartz (71%) is intermixed with ankerite and potassium feld-spars (20%). Some of the feld spars have been altered to seri-

		cite (2%). Chlorite occurs as veinlets (5%), and sericite occurs as veinlets with associated with pyrite. The foliation is 24° to C/A.
B50-1354	L11+35W 6+30S	The minerals in the sample are ankerite and potassium feldspars (75%), chlorite (20%), sericite (2%) and associated fine-grained pyrite (2%). Less than 1% quartz in the sample.
B50-1357	L11+35W 6+30S	An abrupt change from previous sample in that muscovite, sericite and ankerite comprise the bulk of the sample. Chlorite occurs as brecciated fragments among the veinlets of sericite, ankerite and muscovite. Less than 1% pyrite generally occurs as disseminations in the sample; however, one local area of 1% fine grains of pyrite occurs in a pocket amidst the ank-erite.
B50-1360	L11+35W 6+30S	Ankerite, potassium feldspars, sericite and muscovite dominate

		the sample with fragments of chlorite and translucent quartz occurring throughout. Fine grains of pyrite are associated with sericite veinlets and are oriented at 6° to C/A. Cross-cutting the sericite are quartz-carbonate veinlets oriented at 327° to C/A.
B50-1363	L11+35W 6+30S	The minerals in the sample are ankerite (57%), chlorite (40%), leucoxene (2%), quartz (1%) and pyrite (1%).
B50-1366	L11+35W 6+30S	Same description as B50-1363 with a hairline black quartz veinlet at the boundary with the polymictic conglomerate.
B50-1369	L11+35W 6+30S	Polymictic conglomerate with detrital fragments of granite, jasper, mafic and quartz and a chloritic matrix.

DIAMOND DRILL HOLE NUMBER B51

B51-507	L0+00W 1+80S	Mafic volcanic rich in chlorite (90%) and ankerite (9%) with 1% quartz occurring through the

		sample. The Metalore Contact Zone core was assayed and returned a grade of 0.11 ounces of gold per ton across 21.5 feet.
B51-510	L0+00W 1+80S	Fragments of ankerite and quartz occur in mafic volcanics The foliation is 26° to C/A.
B51-513	L0+00W 1+80S	Same description as B51-510 with one 2 cm wide quartz carbonate veinlet following the foliation.
B51-517	L0+00W 1+80S	Similar description as sample B50-1312 with 60% ankerite, quartz and less than 1% hematite. The remainder of the sample is a mixture of the minerals described B51-510. The foliation is 10° C/A.
B51-520	L0+00W 1+80S	The minerals in the sample are chlorite (90%), ankerite (6%) and potassium feldspars (4%). The sample foliation is 29° to C/A.
B51-523	L0+00W 1+80S	Similar description as B50-1312.
B51-526	L0+00W 1+80S	The minerals in the sample are chlorite (80%), ankerite (17%),

		sericite (3%) and minor pyrite.
B51-529	L0+00W 1+80S	Same description as B50-1312.
B51-532	L0+00W 1+80S	The sample is brecciated with fragments of ankerite, and the matrix is chlorite-rich.
B51-535	L0+00W 1+80S	The major minerals in this foliated sample are sericite, ankerite and chlorite occurring as veinlets.
B51-537	L0+00W 1+80S	The sample is brecciated with fragments of ankerite and a matrix comprised of chlorite.
B51-540	L0+00W 1+80S	The sample is brecciated with fragments of muscovite,sericite and ankerite that are cross-cut by hairline quartz veinlets.
B51-543	L0+00W	Abrupt change of composition from previous sample. The major minerals in the sample are ankerite (90%), muscovite-sericite (3%) and less than 1% quartz.
B51-546	L0+00W 1+80S	Same description as sample B51-543 except 10% translucent quartz and 3% muscovite-sericite veinlets are

		associated with fine-grained pyrite.
B51-549	L0+00W 1+80S	Smoky recrystallized quartz (45%) occur as fragments and is sur rounded by chlorite and sericite veinlets that are associated with pyrite.
B51-552	L0+00W 1+80S	Same description as for sample B51-549 except a hairline black quartz veinlet crosses the core sample. This black quartz marks the contact with the polymictic conglomerate below.
B51-555	L0+00W 1+80S	Detrital grains and fragments of quartz, granite and mafic volcanic occur in the chlorite-rich matrix of this polymictic conglomerate.

DIAMOND DRILL HOLE NUMBER B52

B52-800	L13+30W 5+10S	The mafic volcanic is dominated by 90% chlorite with minor amounts of ankerite, sericite, feldspar and trace pyrite. The foliation of the rock is 25° to C/A. The

		Metalore Contact Zone core from this diamond drill hole was assayed and returned a section carrying 0.13 ounces of gold per ton across 69 feet.
B52-803	L13+30W 5+10S	Ankerite is the principal mineral comprising 90% of the core sample. Quartz fragments with muscovite-sericite-chlorite veinlets occur among the fragments. Fine grains of pyrite 1% are dissemi nated throughout the sample. The foliation is 20° to C/A.
B52-806	L13+30W 5+10S	The minerals in the sample are chlorite (81%), ankerite-quartz (15%), hematite (2%) and 2% fine-grained pyrite associated with sericite veinlets. The sericite veinlets follow the foliation, which is 21° to C/A.
B52-809	L13+30W 5+10S	Abrupt change of minerals in the sample with chlorite (80%), anker ite (19%) and trace quartz, sericite and pyrite. The foliation is 27° to C/A.

B52-812	L13+30W 5+10S	Similar description as for sample B50-1312 except a 2cm wide quartz-carbonate vein cross-cuts the sulphides at 25° to C/A. The sulphides occur along a foliation oriented at 5° to C/A.
B52-815	L13+30W 5+10S	The minerals in the sample are chlorite (90%), sericite and mari-posite (6%), ankerite and quartz (4%) and trace pyrite. The foliation is 20° to C/A.
B52-818	L13+30W 5+10S	Same description as B50-1312.
B52-821	L13+30W 5+10S	The rock is well foliated with ankerite, chlorite and pyrite following the foliation and they cross-cut the earlier brecciation. Translucent quartz (10%) and fine-grained pyrite (2%) occur as disseminations in the sample.
B52-824	L13+30W 5+10S	Ankerite and chlorite follow the foliation (24°to C/A) and cross-cuts the brecciated zone.
B52-827	L13+30W 5+10S	Ankerite, chlorite and quartz veins follow the foliation deter

		mined to be at 27° to C/A. Pyrite (2%) occurs in the veins and trace amounts occur in the matrix of the rock.
B52-830	L13+30W 5+10S	The description for this sample is the same as B52-827 with the exception of the presence of sericite microveinlets (2%) occurring randomly. Fragments of ankerite with associated pyrite occur as minor minerals.
B52-833	L13+30W	The foliation is 23° to C/A. One quartz-carbonate veinlet crosses the foliation at 340° to C/A.
B52-836	L13+30W 5+10S	Quartz-carbonate veinlets (9%) with trace pyrite occur throughout the chlorite-rich (90%) sample.
B52-839, B52-842 B52-845	L13+30W 5+10S	Same description as B52-836.
B52-847	L13+30W 5+10S	Abrupt change to chert. Quartz is the dominant mineral with minor feldspar, chlorite and pyrite occurring throughout. The sample is brecciated with fragments of

		ankerite.
B52-850	L13+30W 5+10S	Abrupt change to a sericite dominated (94%) sample with veinlets of chlorite, ankerite and quartz (5%) that follow the foliation at 20° to C/A. Pyrite occurs as fine grains and follows the foliation.
B52-853	L13+30W 5+10S	The sample is intermixed with chlorite veinlets (10%) and quartz (40%). Fine grains of pyrite occur throughout the sample (6%). The remainder of the sample is brecciated fragments of ankerite, quartz and minor sericite. The minerals follow the foliation measured at 35° to C/A.
B52-856	L13+30W 5+10S	Abrupt to change to a chlorite dominated (95%) sample with micro-veinlets of ankerite and quartz interspersed throughout the sample.The foliation is 30° to C/A.
B52-859	L13+30W	Abrupt change to grey quartz (84%)

	5+10S	with chlorite veinlets (10%) and associated pyrite (6%) occurring throughout the sample.
B52-862	L13+30W 5+10S	Same description as sample B52-859, except sericite veinlets (4%) follow the foliation at 40° to C/A.
B52-865	L13+30W 5+10S	A microveinlet of black quartz marks the contact with the poly-mictic conglomerate. Detrital fragments of granite, jasper, quartz, mafic volcanic occur among the chlorite dominated matrix.
B52-868	L13+30W 5+10S	Black quartz is intermixed with white quartz and sericite veinlets occurring randomly throughout the sample. The occasional grain of pyrite occurs in the sample.
B52-871	L13+30W 5+10S	Chlorite and quartz dominate the matrix with clast compositions of granite, quartz, jasper and mafic volcanic that follow the foliation at 27° to C/A.

DIAMOND DRILL HOLE NUMBER B53

B53-890	L23+40W 6+00S	Chlorite (90%) is the principal mineral with minor brecciated fragments of ankerite and hematite comprising the remainder of the sample. The Metalore Contact Zone core was assayed and returned grades of 0.07 ounces of gold per ton across 2 feet and 0.07 ounces of gold per ton across 2.5 feet.
B53-893	L23+40W 6+00S	Same description as sample B53-890. The foliation is 27° to C/A.
B53-896	L23+40W 6+00S	The minerals in the sample are chlorite (79%), hematite (10%), quartz (5%), feldspar (3%) and pyrite (3%). The pyrite is associated with a 2cm wide vein comprised of a mixture of ankerite-quartz and feldspar.
B53-899	L23+40W 6+00S	Prominent quartz, ankerite and chlorite veinlets occur in the sample. Pyrite (1%) is associated with the chlorite veinlets.
B53-902	L23+40W 6+00S	The sample is brecciated with fragments of chlorite and quartz.

		Pyrite occurs in a 2.5cm wide, well foliated mixture of sericite, ankerite, feldspar, chlorite and minor hematite that cross-cuts the brecciation.
B53-905	L23+40W 6+00S	Ankerite dominated sample with veinlets of sericite, quartz and feldspar with trace pyrite occurring randomly throughout the sample.
B53-908	L23+40W 6+00S	Same as sample B53-905, except the foliation is at 28° to C/A.
B53-914	L23+40W 6+00S	Same description as B53-905.
B53-917	L23+40W 6+00S	Feldspars are partially altered- to sericite and comprise 96% of the sample. Chlorite, quartz and calcite occur as minor minerals and comprise the remainder of the sample. The foliation is 25° to C/A.
B53-920 B53-924	L23+40W 6+00S	Same description as B53-917.
B53-927	L23+40W 6+00S	Bands of chlorite and sericite (50%) occur along the foliation of

		the sample at 35° to C/A. Brecciated fragments of ankerite and quartz occur among the bands. Minor hematite and pyrite occur dispersed through the sample.
B53-930	L23+40W 6+00S	The minerals in the sample are sericite (50%), ankerite (30%), feldspar (10%), chlorite (5%) and leucoxene (2%). Quartz and ankerite occur as veinlets (3%). The foliation is 40° to C/A.
B53-933	L23+40W	Same description as B53-930.
B53-936	L23+40W 6+00S	Three sets of quartz-ankerite veinlets; the oldest veinlets are oriented at 27° to C/A, which are cross-cut by veinlets oriented at 15° to C/A that are displaced and cross-cut by veinlets oriented at 355° to C/A. The sample is barren of sulphides.
B53-947	L23+40W 6+00S	Abrupt change to sericite, muscovite and feldspar (95%) dominated sample. Leucoxene (4%) occurs as disseminations. Quartz (1%) occurs locally, and the sample is

		barren of sulphides.
B53-950	L23+40W 6+00S	Chlorite (90%) is the principal mineral with three generations of quartz veinlets comprising 10% of the sample. The oldest veinlets are oriented at 30° to C/A that are cross-cut by veinlets oriented at 40° to C/A that are cross-cut by quartz-ankerite veinlets oriented at 80° to C/A.
B53-953	L23+40W 6+00S	Brecciated chlorite and quartz fragments are cross-cut by a ductile event accompanied by quartz, chlorite, ankerite and feldspar. Pyrite (1%) occurs in the ductile event as fine-grained disseminations.
B53-956	L23+40W 6+00S	Ankerite fragments are surrounded by chlorite, sericite and musco vite veinlets. The veinlets follow the foliation oriented at 15° to C/A. The sample is barren of sulphides.
B53-959	L23+40W 6+00S	The minerals that comprise the sample are ankerite (60%),

		chlorite (20%), sericite (10%) and quartz (10%). The minerals follow the foliation defined at 35° to C/A. No sulphides were found in the sample.
B53-962	L23+40W 6+00S	Same description as B53-959.
B53-967	L23+40W 6+00S	The sample is brecciated with fragments of specularite, hema tite, ilmenite, magnetite, chlorite, ankerite, quartz and pyrite.
B53-970	L23+40W 6+00S	Same as B53-967, however, 2% pyrite occur in sericite veinlets (4%).
B53-973	L23+40W 6+00S	The minerals in the sample are ankerite (90%), chlorite (3%), quartz (3%), sericite (3%) and less than 1% fine disseminations of pyrite.
B53-976	L23+40W 6+00S	Abrupt change in composition to sericite dominated sample (90%) with minor minerals muscovite (5%), quartz (3%), chlorite (1%) and pyrite (1%). The pyrite is

		associated with the chlorite veinlets that follow the foliation at 33° to C/A. The sericite veinlets are two different ages.The oldest veinlets occur with the chlorite, and the youngest veinlets displace the chlorite veinlets.
B53-979	L23+40W 6+00S	The minerals in the sample are ankerite (92%), chlorite (2%), feldspar (2%), muscovite (2%) and pyrite (2%).
B53-983	L23+40W 6+00S	Sericite and quartz are intermixed and occur with fragments of ank erite and quartz. The sample is barren of sulphides.
B53-986	L23+40W 6+00S	Same description as sample B53-983 except chlorite veinlets are oriented at 345° to C/A and cross-cut the foliation at 34° to C/A.
B53-989	L23+40W 6+00S	Brecciated sample with fragments of ankerite. Veinlets of specula-rite, ilmenite, magnetite and chlorite surround the fragments. The foliation is 80° to C/A, which

		is displaced by quartz-carbonate veinlets oriented at 10° to C/A.
B53-995	L23+40W 6+00S	The principal minerals in the sample are ankerite (90%), chlorite (5%), quartz (3%) and pyrite (2%).
B53-997	L23+40W 6+00S	The above sample is in contact with this sample of polymictic conglomerate. The matrix of the conglomerate is principally comprised of chlorite with clasts (1-2mm in diameter) of quartz, jasper, granite, feldspar porphyry, mafic volcanics and diorite. A 4cm wide vein of intermixed grey quartz, ankerite and sericite cuts the sample.
B53-1000 B53-1003	L23+40W 6+00S	Same as description for B53-997.

DIAMOND DRILL HOLE NUMBER B54

B54-1632	L18+54W 9+25S	This mafic volcanic sample has quartz-carbonate veinlets 3mm wide cutting the sample. Pyrite

		and chalcopyrite are associated with the veinlets. The Metalore Contact Zone core was assayed and returned 0.45 ounces of gold per ton across 32 feet.
B54-1637	L18+54W 9+25S	The minerals in the sample are chlorite (67%), ankerite (30%), feldspar (2%), hematite (1%) and fine disseminations of pyrite. The foliation is 33° to C/A.
B54-1639	L18+54W 9+25S	Brecciated sample with ankerite fragments (80%), hematite and specularite (10%), chlorite (10%) and less than 1/2% fine dissemination of pyrite and chalcopyrite.
B54-1644	L18+54W 9+25S	Abrupt change of minerals occurs in the sample with quartz (70%), potassium feldspars (10%), ankerite (15%) and chlorite (3%) veinlets and associated pyrite (2%). The chlorite veinlets follow the foliation is 30° to C/A.
B54-1647	L18+54W 9+25S	Grey quartz constitutes 90% of the sample with 1mm wide veinlets of chlorite (8%) and fine dissemina-

		tions of pyrite (2%) occurring as the remainder of the sample.
B54-1650	L18+54W 9+25S	Sericite veinlets that occur in this sample are younger than the grey quartz described in the previous sample. Ankerite, feld-spars and quartz occur among the sericite veinlets. Specularite and argentite occur as minor minerals in the sample.
B54-1653	L18+54W 9+25S	Ankerite (59%), sericite (25%), quartz (10%), chlorite (3%) and minor mariposite occur throughout the sample. Pyrite (3%) is asso ciated with sericite veinlets. The minerals follow the foliation defined at 30° to C/A.
B54-1657	L18+54W 9+25S	Grey silicification (60%), seri cite (10%) and chlorite (2%) occur as veinlets. Fine-grained pyrite, chalcopyrite and argentite (4%) are associated with chlorite and sericite veinlets. A second generation of sericite veinlets cross-cut the previous veinlets at

		a low angle and are barren of sulphides.
B54-1660	L18+54W 9+25S	This sample is predominately second generation sericite veinlets, as described in the previous sample. Textures of chlorite, quartz and ankerite fragments (2mm in diameter) and minor pyrite comprise the remainder of the sample. The minerals follow the foliation defined at 30° to C/A.
B54-1663	L18+54W 9+25S	The principal minerals in the sample are quartz, ankerite and feldspars (70%). Chlorite veinlets (3%) are associated with pyrite, chalcopyrite and argentite (2%). Sericite veinlets 25% occur as second generation cross-cutting the foliation at 30° to C/A.
B54-1667	L18+54W 9+25S	The minerals in the sample are ankerite (90%), sericite (7%), quartz-ankerite (3%) and minor secondary sericite, chlorite and trace pyrite.

B54-1670	L18+54W 9+25S	Grey silicification (75%) is - intermingled with ankerite (15%) chlorite veinlets (8%) that are associated with fine grains of pyrite (2%). The minerals follow the foliation measured at 27° to C/A.
B54-1675	L18+54W 9+25S	Same description as B54-1670.
B54-1677 B54-1680	L18+54W 9+25S	Black quartz marks the contact with a polymictic conglomerate. The composition of the clasts are granitic, mafics, jasper, quartz, feldspar porphyritic. The matrix in the conglomerate is principally chlorite.

DIAMOND DRILL HOLE NUMBER B55

B55-572	L18+20W 3+50S	Chlorite (90%) dominates the mafic volcanics. Minor veinlets of quartz-carbonate and feldspar occur randomly throughout. Leucoxene (5%) occurs as disseminations in the sample. Pyrite occurs as fine disseminations.

		The Metalore Contact Zone core from this diamond drill hole was assayed and returned grades of 0.16 ounces of gold per ton across 2 feet and 0.14 ounces of gold per ton across 1 foot.
B55-577	L18+20W 3+50S	The sample is brecciated with fragments of ankerite (60%), specularite (15%), quartz (10%), chlorite (11%), hematite (4%) and trace pyrite and chalcopyrite occurring throughout.
B55-580	L18+20W 3+50S	Same description as B55-577.
B55-583	L18+20W 3+50S	Grey silicification (20%) is - associated with 15% chlorite veinlets 2% fine grains of pyrite, chalcopyrite and argentite and trace mariposite. These minerals follow the foliation at 40° to C/A. Sericite veinlets comprise the remainder of the sample.
B55-587	L18+20W 3+50S	Ankerite and feldspar (30%) are - associated with pyrite, chalco-pyrite and argentite 1%. These

		minerals follow the foliation at 33° to C/A. The remainder of the sample are veinlets of chlorite that cross-cut the sulphide zone.
B55-590	L18+20W 3+50S	The sample is principally comprised of ankerite, sericite, feldspar and muscovite that follow the foliation at 27° to C/A. A 1cm wide quartz-carbonate vein is boudinaged and is associated with chlorite (3%) and fine grains of pyrite.
B55-593	L18+20W 3+50S	Same description as B55-590.
B55-597	L18+20W 3+50S	The minerals in the sample are muscovite (80%), sericite (10%), ankerite (8%), leucoxene (2%) and trace quartz. The sample is barren of sulphides. The minerals follow the foliation at 25° to C/A.
B55-600, B55-603	L18+20W 3+50S	Same description as B55-597.
B55-607	L18+20W 3+50S	The majority of the sample is comprised of one 2.5cm wide

		quartz-carbonate vein that is mottled with ankerite, potassium feldspars and quartz. Next to the vein are sericite, leucoxene and trace pyrite. The vein is oriented at 35° to C/A.
B55-610	L18+20W 3+50S	Same description as B55-607 except 40% sericite veinlets occur in the sample.
B55-613	L18+20W 3+50S	Same description as above and the foliation is 20° to C/A.
B55-617	L18+20W 3+50S	Same description as for sample B55-597 with mariposite veining (3%) and one 0.5 cm wide quartz carbonate vein.
B55-620	L18+20W 3+50S	Same description as B55-617.
B55-623	L18+20W 3+50S	Same description as B55-597. The sample is barren of sulphides and the minerals follow the foliation at 18° to C/A.
B55-627	L18+20W 3+50S	Quartz, ankerite and feldspar (30%) occur as fragments among veinlets of chlorite (50%) and sericite (19%). Leucoxene occurs

		as fine disseminations (1%) in the sample. The sample is barren of sulphides.
B55-630	L18+20W 3+50S	Chlorite (80%) occur with boudins quartz, ankerite, feldspar, minor sericite, leuxcoene and hematite in the sample. The foliation is 27° to C/A.
B55-635	L18+20W 3+50S	Same description as B55-630.
B55-637	L18+20W 3+50S	The sample is intermingled with approximately equal proportions of sericite, quartz, ankerite, chlorite and feldspars. It is barren of sulphides.
B55-638	L18+20W 3+50S	Black quartz in the sample is cross-cut by a white quartz vein. The sample is barren of sulphides.
B55-640	L18+20W 3+50S	Polymicitc conglomerate. Same description as previous samples of the conglomerate.

DIAMOND DRILL HOLE NUMBER B56

B56-657	L0+00W 2+90S	Brecciated mafic volcanic with fragments of ankerite and quartz

		veinlets of chlorite and specularite occurring in the sample. The foliation is 27° to C/A. The Metalore Contact Zone core was assayed and returned a grade of 0.19 ounces of gold per ton across 8 feet.
B56-667, B56-677	L0+00W 2+90S	Same description as B56-657.
B56-687	L0+00W 2+90S	Same as B56-657 except ankerite increases to 60% of the sample. The foliation is 33° to C/A.
B56-697	L0+00W 2+90S	Abrupt change to chlorite domi nated mafic volcanics as described in sample B56-657.
B56-702	L0+00W 2+90S	Same description as B56-657 with the foliation at 35° to C/A.
B56-714	L0+00W 2+90S	Same description as B56-687, with the exception of an increase in quartz-carbonate veinlets follow ing the foliation defined at 55° to C/A. Pyrite is associated with chlorite veinlets in minor amounts.
B56-717	L0+00W	One half of the sample is

	2+90S	brecciated with sericite and - muscovite fragments and the other half is dominated by chlorite veinlets with associated 2% fine grains of pyrite.
B56-720	L0+00W 2+90S	The minerals in the sample are chlorite (95%) with ankerite (3%), sericite (1%) and trace pyrite.
B56-723	L0+00W 2+90S	Same description as B56-720 with one 2.5cm wide quartz vein with associated chlorite, sericite and 3% pyrite.
B56-726	L0+00W 2+90S	Three 2.5cm veins of quartz-carbonate occurring in the host rock described in B56-720.
B56-729	L0+00W 2+90S	The sample is comprised of wide quartz-carbonate veins inter mingled with 10% silicification, chlorite veinlets and associated pyrite (4%). A second generation of sericite veinlets is barren ofsulphides.
B56-732	L0+00W 2+90S	Black quartz is brecciated and occurs with a white quartz vein. Minor ankerite occurs among the

		vein.
B56-735	L0+00W 2+90S	The sample is brecciated with one 2.45cm quartz-carbonate vein as described in sample B56-723.
B56-738	L0+00W 2+90S	Same description as B56-729 with associated 4% disseminated pyrite.
B56-742	L0+00W 2+90S	Polymictic conglomerate as described from core from other diamond drill holes.

DIAMOND DRILL HOLE NUMBER B57

B57-1102	L0+00W 5+15S	Chlorite-rich mafic volcanic is with minor quartz-carbonate veinlets 1cm in width. Pyrite is associated with the wallrock of the vein and follows the foliation at 30° to C/A. The rock is cross-cut by potassium feldspar, muscovite and ankerite veinlets that comprise 70% of the sample. The Metalore Contact Zone core was assayed and returned at grade of 0.06 ounces of gold per ton across 8.1 feet.
B57-1167	L0+00W	The sample is brecciated with

	5+15S	fragments of ankerite and hematite (50%). Surrounding the frag ments are chlorite-sericite veinlets. Disseminated throughout the sample homogenously are leucoxene laths 2mm long. The sample is barren of sulphides.

DIAMOND DRILL HOLE NUMBER B58

B58-792	L2+00E 3+80S	Chlorite dominates this mafic volcanic with minor amounts of quartz-carbonate microveinlets occurring randomly throughout the sample. The Metalore Contact Zone core was assayed and returned a grade of 0.07 ounces of gold per ton across 6 feet.
B58-797	L2+00E 3+80S	The sample is intermixed with sericite, ankerite and muscovite in equal proportions. Fine grains of pyrite (1%) occur in sericite veinlets. Minor hematite occurs in the sample.
B58-800	L2+00E 3+80S	There are four sets of quartz veinlets that occur in the sample.

		The oldest set are veinlets oriented at 35° to C/A. The next set are quartz-carbonate veinlets with associated chlorite veinlets oriented at 30° to C/A. Pyrite is associated with the chlorite. The next set of veinlets are oriented at 70° to C/A, and the youngest set of veinlets are 359° to C/A.
B58-803	L2+00E 3+80S	This sample is brecciated with veinlets of sericite and associ ated pyrite (1%). Overprinting these sericite veinlets are a second generation of sericite veinlets that are barren of sulphides.
B58-806	L2+00E 3+80S	Remnant breccia fragments occur in the sample; however, it is domi nated by veinlets of sericite, muscovite and ankerite that follow the foliation at 20° to C/A. Fine grains of pyrite occur with chlorite veinlets.
B58-816	L2+00E 3+80S	Ankerite and chlorite comprise 80% of the sample. One 1cm quartz-

		carbonate vein crosses the sample with minor pyrite occurring along the walls of the vein.
B58-818	L2+00E 3+80S	Quartz dominates the sample (70%) with ankerite occurring as frag ments 29% of the sample. One percent fine disseminations of pyrite occur in the sample.
B58-820	L2+00E 3+80S	Minerals that occur in the sample are ankerite, hematite, chlorite, minor sericite and one narrow veinlet of quartz. Pyrite occurs as both coarse and fine disseminations.
B58-823	L2+00E 3+80S	The major minerals in the sample are muscovite (82%), sericite (15%), leucoxene (3%) and minor amounts of chlorite. The foliation is 18° to C/A.
B58-826	L2+00E 3+80S	Three sets of quartz-carbonate veinlets occur in the sample. The oldest set of veins is 42° to C/A. The second set of quartz-carbonate veins are associated with seric- ite, chlorite, ankerite and pyrite

		and is 5° to C/A. The third set of veinlets occur at 85° to C/A.
B58-829	L2+00E 3+80S	Hematite, ankerite and quartz occur in equal proportions with chlorite veinlets and 3% pyrite occurring as fine grains in the sample. Minor sericite occurs in the sample.
B58-832	L2+00E 3+80S	Same description as B58-829.
B58-838	L2+00E 3+80S	Chlorite dominates this sample with textures of sample B58-832. The foliation is 43° to C/A.
B58-847 B58-852	L2+00E 3+80S	Same description as B58-838.
B58-857	L2+00E 3+80S	The minerals in the sample are ankerite (75%), quartz (15%), specularite and argentite (5%), sericite (3%) and 2% pyrite.
B58-862	L2+00E 3+80S	Chlorite dominates the sample with minor sericite, quartz veining with trace pyrite occurring randomly throughout the sample. A second generation of sericite veinlets overprints the previous

		sericite veinlets and are barren of sulphides.
B58-867	L2+00E 3+80S	Same description as B58-862 where the foliation is 42° to C/A.
B58-869	L2+00E 3+80S	Same description as B58-867 except 20% sericite occurs in the sample and is not associated with the 4% fine and coarse grained pyrite follows the foliation.
B58-872	L2+00E 3+80S	Same description as B58-862 with associated 1% pyrite. The foliation is at 5° to C/A.
B58-877	L2+00E 3+80S	Same description as sample B58-872 but with 40% sericite.
B58-882	L2+00E 3+80S	Chlorite(95%) dominates the sample with minor amounts of quartz ankerite veinlets (5%).
B58-887	L2+00E 3+80S	Black quartz mottled with quartz and ankerite. The sample is barren of sulphides.
B58-892	L2+00E	Polymictic conglomerate with chlorite matrix and clast compositions of granite, quartz, jasper, mafic volcanic, diorite and feld spar porphyry.